LASER DEBONDING OF CERAMIC ORTHODONTIC BRACKETS

Thesis submitted to the
Faculty of Graduate Studies
in partial fulfilment of the
requirements for the degree of
Master of Science

The University of Manitoba
Department of Preventive Dental Science
Winnipeg, Manitoba
Canada

By

Robert Maurizio Tocchio BSc., D.D.S.

April 26, 1990

ISBN 0-315-63214-3

LASER DEBONDING OF CERAMIC ORTHODONTIC BRACKETS

BY

ROBERT MAURIZIO TOCCHIO

A thesis submitted to the Faculty of Graduate Studies of the University of Manitoba in partial fulfillment of the requirements of the degree of

MASTER OF SCIENCE

TABLE OF CONTENTS

	Page
ABSTRACT	iii
ACKNOWLEDGMENT	iv
LIST OF FIGURES	v
LIST OF TABLES	vii
INTRODUCTION	1
REVIEW OF LITERATURE	3
Orthodontic Bonding	3
Ceramic Brackets	6
Lasers: Historic Review	16
Laser and Light Theory	20
Lasers and Dental Hard Tissues	24
Thermal Considerations	31
Statement of Purpose	37
MATERIALS AND METHODS	38
Spectrographic Analysis	38
Laser Debonding Experiments	40
Thermal Evaluation	48
RESULTS	51
Spectrographic Analysis Results	51
Laser Debonding Results	60
Damage Evaluation	66
Thermal Evaluation Results	71
DISCUSSIONS	74
Temperature Measurements	83
Enamel and Bracket Damage	86
Sources of Error	88
CONCLUSIONS	90
FUTURE RESEARCH	91
BIBLIOGRAPHY	95
APPENDIX 1 (Light and Laser Theory)	105
APPENDIX 2 (Basics of Spectroscopy)	122
APPENDIX 3 (Pilot Study Results)	132
APPENDIX 4 (Raw Data)	134

ABSTRACT

The introduction of ceramic orthodontic brackets has further compounded the problems associated with debonding. The increased bonds strengths obtained with ceramic brackets has resulted in an increased incidence of enamel damage. Laser light transmitted to the bracket/adhesive interface can be used to degrade the bonding resin by either thermal or photochemical processes.

The efficacy of lasers in removing brackets safely, without enamel or bracket damage, without thermal damage to the pulp and in a clinically satisfactory time was determined. The influence of various laser wavelengths (193, 248, 308 and 1060 nm) and various bracket types (Starfire, Transcend) on debonding effectiveness was also examined. Debonding times, material damage, site of bond failure and pulpal temperature rise were correlated to absorption spectra of the adhesives and bracket types.

Sapphire brackets can be debonded more quickly than Polycrystalline (PC) brackets because they allow greater light energy to reach the adhesive. Ultraviolet wavelengths are more effective for bracket removal than 1060 nm irradiation with 248 nm being most effective. These results correlate well to the absorption spectra of the adhesive. No enamel or bracket damage was observed and little or no force is required to remove the brackets. For the laser parameters used in this study, the pulpal temperature increase is acceptable with the sapphire brackets but not with the PC brackets. Laser debonding appears to be a thermal process at low pulse energy levels and an ablative process with increased pulse energies.

ACKNOWLEDGEMENT

To my research advisor, Dr. Peter Williams, Department of Rehabilitative Dental Sciences, for his knowledge, support and guidance, and the ability to temper the many ups and downs of this project.

To my external examiner, Dr. Ken Standing, Professor, Department of Physics, for his laser expertise, for advice throughout the bulk of this work and for allowing a 'dentist' to invade his lab.

To Dr. Franz Mayer, Department of Physics, for his valuable input during the early experimentation. "Cheers" to my German friend.

To Ed Kammermyer and staff, at the Ontario Lightwave and Laser Research Center, Toronto, Ontario, for numerous valuable suggestions and the outstanding facility at which the bulk of the experimentation was performed.

To Daryl, in Biostats, for guiding me through the 'Mac' and helping me deal with the graphics nightmare.

To Dr. Ed Yen, for advice and assistance along the way and for listening when the 'wall' seemed most insurmountable.

To Dr. Robert Baker, for his wealth of knowledge in clinical orthodontics. Thanks for trying to teach me what you know.

To the many people at Unitek-3M and A-Company, for their assistance and the donation of the many ceramic brackets needed for this project.

To my new, trusted and cherished friends, Arthur and Fred. The many good times we've shared are priceless and will never be forgotten. A lifetime of friendship is ours to share.

LIST OF FIGURES

Figure		Page
1.	Stress vs strain for sapphire and steel.....	9
2.	a. Chemical structure of a silane b. Bonding of silanes to surfaces.....	11
3.	Enamel 'tearout'.....	14
4.	External transmission for sapphire.....	15
5.	Properties of coherent light.....	20
6.	IR spectra of lased and nonlased enamel.....	24
7.	Absorption spectra of enamel.....	26
8.	Bracket transmission set-up; laser.....	40
9.	Mounting jig; side view.....	43
10.	Mounting jig; top view.....	43
11.	Completed sample with orientation mark.....	44
12.	Sample mounted in holding apparatus.....	44
13.	Laser debonding set-up; 248/308 nm.....	46
14.	Laser debonding set-up; 1060 nm.....	47
15.	Thermocouple set-up.....	49
16.	UV\VIS spectra of Dynabond.....	51
17.	IR spectra of Dynabond.....	52
18.	UV\VIS\NearIR spectra of Dynabond (Hitachi)..	53
19.	IR-UV spectra of Dynabond (Carey).....	54
20.	PC bracket spectra.....	54
21.	S bracket spectra.....	54
22.	Sapphire window spectra.....	55
23.	Quartz window spectra.....	56
24.	Silane spectra (on quartz).....	56

List of Figures cont'd

Figure		Page
25.	Elemental analysis; PC bracket body.....	58
26.	Elemental analysis; S bracket body.....	58
27.	Elemental analysis; PC bonding surface.....	58
28.	Elemental analysis; S bonding surface.....	58
29.	SEM: Sapphire bracket fracture surface.....	59
30.	SEM: PC bracket fracture surface.....	59
31.	Elemental analysis; PC 'amorphous layer'.....	60
32.	SEM: S bracket debonding pattern (15x).....	68
33.	SEM: S bracket debonding pattern (200x).....	68
34.	SEM: S bracket debonding pattern (500x).....	69
35.	SEM: PC bracket debonding pattern (15x).....	70
36.	SEM: PC bracket debonding pattern (500x).....	70
37.	Potential 'degradable' adhesive spectra.....	92
38.	"Sandwich" technique for bracket removal.....	92

LIST OF TABLES

Table		Page
1.	Laser transmission of brackets.....	57
2.	PC bracket removal times; 248 nm laser.....	61
3.	S bracket removal times; 248 nm laser.....	61
4.	S/PC bracket removal times; 193 nm laser.....	62
5.	PC bracket removal times; 308 nm laser.....	63
6.	S bracket removal times; 308 nm laser.....	63
7.	PC bracket removal times; 1060 nm laser.....	64
8.	S bracket removal times; 1060 nm laser.....	64
9.	Temperature measurements; PC brackets.....	71
10.	Temperature measurements; S brackets.....	72
11.	Modes of energy dissipation for molecules....	77

INTRODUCTION

The debonding of orthodontic brackets requires the removal of both bracket and residual adhesive. It may be time consuming and frequently results in some degree of enamel damage. The amount of enamel damage is a function of the forces required to remove the brackets, the bond strengths between enamel-adhesive-bracket, and the use of hand instruments (dental chisels, hatchets) and rotary instruments and abrasive pastes to remove the remaining resin. Patient demand for improved esthetics during orthodontic therapy resulted in the premature introduction of 'ceramic' brackets prior to completion of adequate research. Unfortunately, subsequent clinical experience with 'ceramic' brackets has demonstrated that the brittleness of the bracket and increased bond strengths at the bracket-adhesive interface further compounds the debonding problems seen with metal brackets. Possible solutions for safer and more predictable bracket debonding include modifying the existing procedure through bracket-adhesive manipulations, including using unfilled bonding resins and mechanical versus chemical retention or developing alternative mechanisms such as electrothermal debonding. However these solutions may result in decreased bond strength and the possibility of thermal damage, so they may not provide a satisfactory solution to the problems inherent in currently practiced debonding techniques.

Brackets made of alumina ceramic materials have the unique ability to transmit radiant energy in a wide range of wavelengths. Therefore laser energy should be able to be used to debond 'ceramic' brackets since laser light energy can be deposited directly at the bracket-adhesive interface.

This study validates the concept of laser debonding of ceramic orthodontic brackets. Debonding times, in conjunction with an assessment of enamel and bracket damage, pulp chamber temperature rise and absorption spectroscopy of the materials involved was performed. A hypothesis regarding the mechanism of laser debonding is proposed. The results of this study suggest directions for future research.

REVIEW OF LITERATURE

Review of Orthodontic Bonding

The direct-bonding of orthodontic brackets to etched enamel has become widely employed by orthodontists since being introduced more than two decades ago.[1,2,3,4] The primary concern in the development of orthodontic adhesives has been the development of adequate bond strengths between the bracket, adhesive and etched enamel surfaces. Tensile[5,6,7],, shear[8,9,10], torquing and peel tests[11,12] have been devised to evaluate the bond strengths in vitro and mimic the force systems present during active orthodontic treatment. In addition to the inherent strength of the brackets, bonding agents and enamel, other factors have been identified as having a direct influence on the strength of orthodontic bonding. Some of these are; the bracket base surface area[13], base design[4,14], base mesh size[11,13,14], thickness of resin layer[15,16], filler content[5,8], effect of sealing agents[17,18] water sorption[19], thermal cycling[20] and technique related factors.[21]

In order to ensure successful orthodontic bonding, the forces applied during treatment must not exceed the bond strengths of the tooth-adhesive-bracket complex. The force that is exerted will be composed of forces generated by the activation of the appliance and those arising from mastication. The maximum force has been estimated to be between 30 kg\cm2 to 70 kg\cm2[9,22]. Others[23] have estimated that a minimum of 9 kg is

exerted on the bracket (≈54 kg\cm2 based on 4x4 mm bracket area) during orthodontic treatment. In the study by Yamada et al[24] comparing the bond strengths of various bonding adhesives, values were never below 80 kg\cm2 and ranged to a maximum of 176 kg\cm2. Keizer et al[9] found the enamel-adhesive bond strength to be 1.21 kg\mm2 or 121 kg\cm2. It appears from these results that such bond strengths are more than sufficient to withstand various intra-oral forces and have facilitated the trend towards decreasing bracket size in recent years. Increased bond strengths will likely result in a greater frequency of enamel damage as they approach or even exceed the reported average enamel tensile strength of 100 kg\cm2[25]. Note too however, that the reported strength of enamel is only an average and does not take into account qualitative differences such as hypocalcified and altered enamel structure or the effect of crystal orientation in strength testing. Therefore, enamel damage could occur at much lower force levels.

A number of difficulties in bonding\debonding procedures have been identified. These include loss of enamel due to etching[26,27] prior to bracket placement, fracturing[26,28,29] during bracket removal, retention of resin tags which can yellow with age and discolour the tooth[26,29], corrosion of metal brackets resulting in staining at the bracket interface[30,31], a roughened enamel surface which can result in increased plaque retention subsequent to debonding procedures[28,32,33] and a softer enamel surface with lower fluoride content more disposed to

decalcification[34]. Many of these effects are accepted by the clinician[35] who feel that they are insignificant.

The most frequently observed bond failure occurs at the bracket-adhesive interface[5,7,10,36]. If the bond strengths are high, failure will more often occur intra-adhesive or at the enamel-adhesive interface[37] resulting in enamel damage or 'Tear Outs'. This type of failure is observed when the bracket-adhesive interface bond is enhanced either by etching[38] or coating the bracket base with porous metal powder[14,39]. Bond strengths were seen to improve from 66.9 kg\cm2 for untreated bases to 169 kg\cm2 for the treated bases. Since debonding occurs at the weakest link in the bracket-adhesive-tooth complex, spot weld defects on the base surfaces of metal brackets have been shown to encourage fracture at the bracket-adhesive interface in spite of high bond strengths[13].

With the increasing esthetic demand for smaller brackets and therefore smaller bonding bases, the gap between those bond strengths which are high enough to stand up to clinical treatment and yet, are still weak enough to avoid iatrogenic tooth damage, has narrowed considerably. Ideally, if brackets could be debonded safely, easily and predictably, a clinician would desire the highest possible bond strength. This high bond strength would decrease the incidence of bonding failures and improve clinical efficiency. Perhaps Sheridan[40,41] had this in mind when he introduced an electrothermal debonding device. He may simply have wanted to prevent damage during debonding in those situations

where the bond strength equalled or exceeded the enamel strength. His cordless battery operated device generates heat which is transferred to the metal bracket by a blade placed in the bracket slot. The metal bracket conducts heat efficiently while the underlying adhesive is a relatively poor conductor of heat. Thus, the adhesive at the interface can be thermally softened and the bracket can be gently lifted off the tooth. The thermal ramifications of this technique to the pulp will be addressed in a subsequent section. In this context however, Sheridan must be credited for devising an alternative mechanism for metal bracket removal. The gap between bond or enamel strength and the force required for bracket removal has been substantially widened using Sheridan's technique. After debonding, residual adhesive is removed from the tooth by conventional hand and rotary instruments both of which have the potential to damage the enamel.

Ceramic Brackets

The search for improved esthetics in orthodontic appliances has always been active. As early as 1964 Newman's[42] introduction of polycarbonate brackets provided improved esthetics. The bond strengths reported[43] were superior to those of the metallic brackets available at that time. Unfortunately, since the polymeric brackets were prone to clinical fracture and creep[44] their clinical performance was unsatisfactory[45]. Subsequent development of metal reinforced plastic brackets[46] failed to

overcome these deficiencies.

The 'ceramic' bracket has recently been introduced to orthodontics. Ceramics are a broad class of materials which, although they contain both metallic and non-metallic elements, are neither metallic nor polymeric. They are renowned for their hardness and resistance to high temperatures and chemical degradation[47]. Their major disadvantage is their lack of ductility which renders them brittle and subject to sudden and catastrophic failure. Currently all dental ceramic brackets are composed of either polycrystalline or monocrystalline aluminum oxide. The former is made by sintering aluminum oxide powder at temperatures near 1800 °C. The monocrystalline aluminum oxide[47] is commonly called a sapphire and is formed by melting aluminum oxide (T_f<2100°C) and then slowly cooling it to grow a single crystal. Both the polycrystalline and single crystal 'blanks' are milled into their final form by either diamond cutting or by ultrasonic cutting techniques.[47] Sapphire brackets are transparent while polycrystalline brackets have a translucent, ivory white to opaque appearance.

The optical properties and strength of polycrystalline ceramics are incompatible. Since transparency increases with grain size and since strength decreases once the grain size increases over 30 um current ceramic brackets are formed by fusing aluminum oxide particles of 0.3 um. to produce brackets with grain size of 20-30 um.[47]

The tensile strength of sapphire is significantly greater

than that of annealed or cast stainless steel alloy (1800-2600 MPa psi vs. 350 MPa)[48]. In contrast Polycrystalline brackets actually may be slightly weaker than metals in tension[47]. The tensile strength for metal is a bulk related phenomenon and because of the metal's ductility, it is virtually independent of small surface defects. In contrast, the brittle material alumina is highly dependent on surface defects. Sapphire brackets possessing high tensile strengths, have very low transverse strengths and cannot withstand impact loading[47]. Surface defects such as cracks act as centers of stress concentration. In brittle materials, the crack remains sharp since there is no plastic deformation occurring to enable blunting. As such, stress concentration of several orders of magnitude can develop at the tip of the crack. Once the stress exceeds a critical level the crack will begin to self propagate and result in spontaneous failure.[49]

The measure of a material's ability to resist fracture is known as fracture toughness. Figure 1[48] is a plot of stress versus strain for sapphire and stainless steel. While the tensile strength of sapphire is much greater than steel, the % elongation (elastic and plastic deformation to failure) is 1% and 20% respectively. Since energy is defined as force times distance the area under a stress\strain curve gives an indication of the material's toughness before fracture. It is apparent, from Fig 1, that significantly less energy is required to fracture sapphire than for stainless steel.

Figure 1.[48]

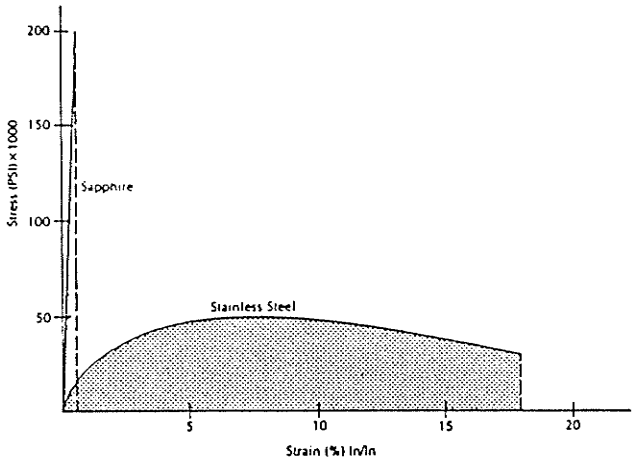

Fig. 1 Stress-Strain curves for sapphire and stainless steel. The height of the curve shows force loading, or strength. The horizontal axis shows strain, or distortion, under that load. Dashed vertical lines indicate failure (fracture) under load. The area under the curve is a rough indication of fracture toughness, or the total energy loading required to cause failure.

The units used to measure fracture toughness are the stress in Mega-Pascals (mega-Newtons/M^2) and the strain in meters. The length of the surface crack enters into the formula as the square root meter[48]. Values of fracture toughness[48] for stainless steel, polycrystalline alumina and sapphire are; 80-95 MPa√M, 3.0-5.3 MPa√M, and 2.4-4.5 MPa√M. Note that even though the tensile strength of polycrystalline alumina is much less than sapphire it is a tougher material and can resist fractures better than sapphire.

For the clinician, low fracture toughness of ceramic brackets can drastically reduce the load required for fracture. Although the hardness of ceramics is 2-3 times greater[47] than stainless steel, surface defects introduced during manufacture orduring regular appointments can dramatically reduce their strength. A clinician must inform the patient of possible 'spontaneous' bracket fracture and the possibility of ingesting sharp ceramic particles.

The hardness of ceramics can be detrimental if grinding is required to remove a fractured bracket from a tooth. Although diamond is the hardest substance known to man, and diamond cutting instruments are commonly used in dentistry, cutting alumina with a diamond instrument will still be clinically time consuming. Therefore every effort should be made to prevent fracture of ceramic brackets by minimizing the deleterious forces exerted during treatment and during debonding procedures.

Another problem has been identified by investigators[50,51,52] who have reported rapid and dramatic abrasion of enamel caused by ceramic orthodontic brackets. Although thoughtful and judicious bracket placement by the orthodontist should decrease such occurrences, the clinician should remember that using brackets of such hardness and in the case of the polycrystalline brackets, surface roughness, results in enamel wear. Kusy[53] has suggested glazing or chemically treating the bracket surface to decrease roughness and reduce the coefficient of friction.

Alumina oxide cannot be directly bonded to the acrylic materials used for orthodontic bonding. Until recently bonding of ceramic brackets was achieved through the presence of undercuts of various designs on the bracket bonding surface. Bond strengths of these brackets are comparable or less than those of metal brackets[54,55]. Buzzita et al.[55] argued that filled adhesives were less able to flow into the retentive areas of the bracket base thus explaining the higher bond strengths obtained with unfilled resin adhesives. Odgaard and Segner[56] postulated that

during curing of adhesives, the resin will contract and give rise to internal stress around the sharp corners of the grooved base. As a result the ultimate bond strength will be reduced. Iwamoto et al.[57] demonstrated that bond strengths would decrease as mechanical retention (# of grooves) was increased. The bond failure site of these brackets remains predominantly at the bracket-adhesive interface and within the adhesive[56].

More recently chemical bonding of adhesive to the bracket base has been achieved by treating the aluminum oxide base with a silane coupling agent. This technology was pioneered by Bowen[58] who foresaw the advantages of using filler particles which would couple to the resin matrix to produce a reinforced (composite) polymer network. The most common coupling agent in use is a methacrylate terminated silane, γ-methacryloxypropyl-trimethoxysilane[59], Figure 2a. This coupling agent bonds to the ceramic via the hydroxyl (usually silanol-SI-OH) groups to form a monolayer of silane with the methacrylate groups projecting from the surface, Figure 2b. These will then co-polymerize with the resin during setting.[59,60]

Figure 2 a,b.[60]

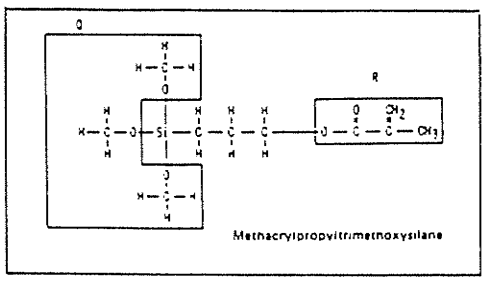

Chemical structure of commonly used silanes: Q = hydrolyzable group of silicone, e.g. alkoxy or acetoxy group R: organofunctional group selected for compatibility with the resins.

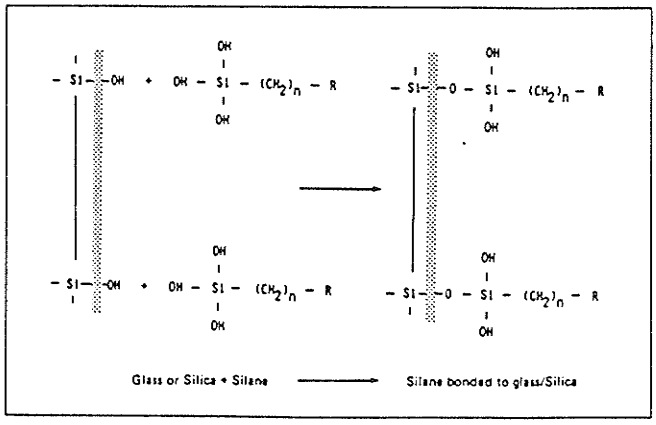

Bonding mechanism of silane to glass or silica surfaces.

The same chemical bonding mechanism has been successfully employed for bonding acrylic to porcelain. Bond strengths are reported[61,62,63] to be comparable or to exceed those for metal brackets, especially when the porcelain surface is roughened by grinding before treating with the silane primer. As bond strengths increased, so too did the incidence of porcelain fracture during debonding.[61,62,63]

While it appears that increased roughening (mechanical retention) can result in increased bond strength to porcelain, the same may not be true of silanized ceramic brackets having mechanical retention. Studies by Iwamoto et al.[57] and Slomka and Powers[37] found increased bond strengths with these silanized brackets while Newman et al[64] and Buzzitta[55] questioned the clinical effectiveness of silane application to increase the bond strength of mechanically retained ceramic brackets. Guess et al.[65] found that even though the silanization of mechanically retained ceramic brackets had no significant effect on bond strengths, fracture occurred almost exclusively at the enamel-resin interface rather than at the bracket-adhesive interface. The retention of a bracket with this design it appears, was strong enough to override any possible effects of base silanization.

A number of manufacturers have recently switched to ceramic brackets which rely exclusively on chemical bonding of the acrylic resin. Only a few published reports comparing their shear bond strengths to those of metal brackets are available.

Gwinnett[66] and Odegaard and Segner[56] have both found superior bond strengths with the chemically bonded brackets and have noted that bond failure occurs predominantly at the enamel-resin interface. High bond strengths are attributed to the chemical bonding, a lack of internal stress in the resin and lack of bracket flexure during debonding as occurs with the metal brackets[56,66]. Joseph and Rossouw[67] in a most recent report found the debonding shear force of ceramic bracket groups to be significantly higher than those of stainless steel brackets regardless of whether light or chemically cured resins were used. An average force of 28.3 MN/M^2 was required for the highest ceramic bracket group while 17.8 MN/M^2 was enough to debond the strongest metal bracket group. The site of failure for the ceramic brackets was dominantly at the enamel-adhesive interface. Enamel fractures occurred in 40% of the chemically cured resin and ceramic bracket group. Another 7% of ceramic brackets fractured during removal.

With the advent of chemically bonded ceramic brackets it seems apparent that bracket-adhesive failures are no longer found. Rather, the limiting factor in the enamel-adhesive-bracket complex has shifted to the enamel-adhesive interface. The ramifications of such a shift are vividly illustrated in the published report by Newesely and Rossiwall[52]. Utilizing X-ray SEM elemental analysis they show a high frequency of enamel tearouts in a wide range of sizes. The largest tearout found measured up to 1.5 mm in diameter, Figure 3.

Figure 3.[52]

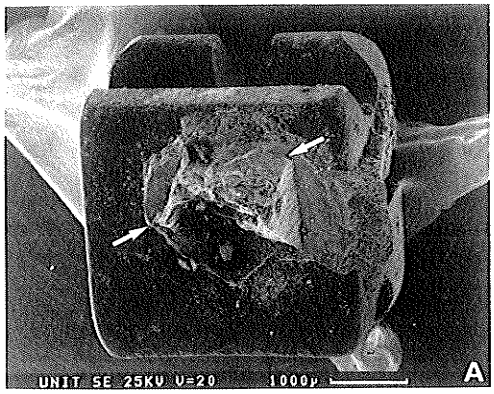

The ceramic bracket industry enthusiastically entered into the practice of orthodontics in response to the strong demand created by the bracket's optimal esthetic appeal. Unfortunately, the problems of bracket fracture, enamel abrasion and possible enamel tearouts encountered after their introduction has led many practitioners to question the efficacy of using this product. Unitek has recently converted all their chemically bonded ceramic brackets to mechanically bonded brackets by sintering silica particles to the bases. They did however, posses the technology to alter the bonding strength of the chemical ceramic bracket through direct manipulation of the number of active silane bonds[23]. Another ceramic bracket manufacturer is pursuing the possibility of utilizing the electrothermal debonding device (pers comm.) in an effort to improve the acceptability of the ceramic bracket into orthodontic practice.

Increased bond strengths should result in improved bracket retention rates and the production of smaller more esthetic brackets. Decreasing the force needed for debonding can decrease bracket fracture and eliminate lengthy clean up and provide a

controlled and less destructive bonding location. ETD (electrothermal debonding) may represent a mechanism by which the gap between bond strength and debonding force can be widened. Pulpal damage however, may be a limiting factor. The lower thermal conductivity of alumina oxide will likely result in longer debonding times and excess heating of the tooth and pulp prior to debonding.

It is apparent from the foregoing that debonding of ceramic brackets continues to be a problem for the clinician, manufacturers and patients. Ceramic brackets are formed of alumina oxide which has been shown to transmit a wide range of radiant energy, Figure 4. This special optical property may facilitate debonding through the use of lasers.

Figure 4.[68]

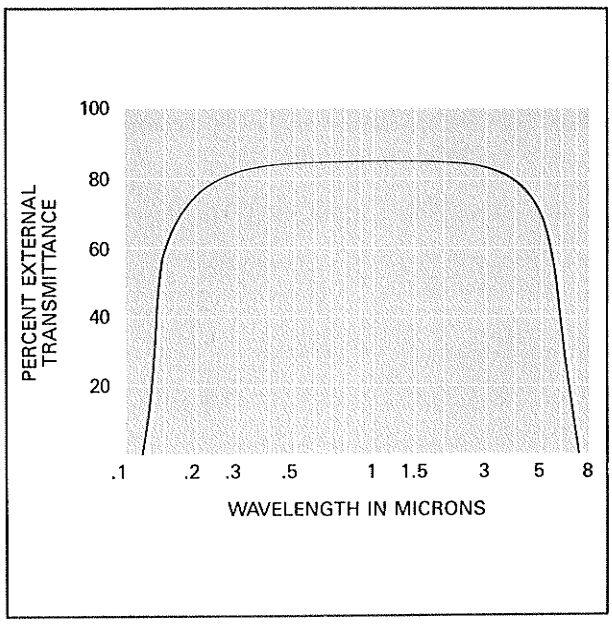

EXTERNAL TRANSMITTANCE FOR SAPPHIRE of 1mm thickness.

Lasers - Historic Review

It has been said that the laser is a solution looking for a problem, rather than a development in response to a specific need[69]. The growth in the number of laser applications has been almost exponential. Einstein discovered the theoretical background for the laser in 1917[70] but it was not until 1960 when Theodore Maimam of Hughes Aircraft, now credited as the inventor of the laser, applied the theory to create the ruby laser.[70]

Surprisingly lasers have been involved in dental research since 1963[71]. Many specific areas of laser applications in dentistry have been identified. Some of these are; surgical treatment of oral malignancies and lesions, treatment of periodontal disease, caries prevention, detection and control, endodontics, prosthodontics, biostimulation, tooth desensitization, analgesia, in-vivo welding, storage of radiographic and 3-dimensional images, etc. As existing systems are refined and new laser systems are introduced a plethora of potential applications will be conceived. As yet, there have been no reports of lasers applied specifically to the field of orthodontics.

From only three citations in the 1964 edition of the Index to Dental Literature, dental laser reports have grown to over 70 in the 1988 Index. Less than one-fifth of these citations are in English. In 1986 there were only four dental professionals listed as members of either the International or American Societies for Laser Medicine and Surgery. The emerging importance of dental

laser research warranted a World Congress on Lasers in Dentistry during 1988, in Tokyo, Japan.

Historically, Leon Goldman in 1965[72] is credited with the first in vivo report of laser application to a healthy, living human tooth. The patient reported no pain when a maxillary second molar was exposed to two direct impacts by a ruby laser (694 nm). The tooth was extracted and sent for microscopic study. Only superficial destruction of the crown occurred. Another study by Stern and Sognnaes[73,74] showed how that laser irradiation of enamel appeared to decrease enamel permeability to acidic fluids. Some[75] claimed that the ruby laser was not suitable for cavity preparation because of potential pulpal damage due to the energy levels needed to remove dental hard tissues. Further advances would have to await the introduction of newer laser instruments.

Lobene et el.[76] in 1968 were the first to use the CO2 laser for dental application. Their attempts to fuse pits and fissures as a means of caries prevention demonstrated how the mid-infrared wavelength (10.6 um) of the CO2 laser produced different thermal effects than did the ruby laser. CO2 irradiation also caused small amounts of hydroxyapatite to be converted to the more insoluble calcium orthophosphate apatite. Kantola[77] has provided a detailed description of macroscopic, microscopic and X-ray diffraction studies of CO2 irradiated enamel and dentin while Melcer[78] has demonstrated caries removal with dentin healing and reparative-dentin formation.

Laser research on dental tissues in the United States has suffered greatly during the mid to late 1970's as a result of several published reports[75,76] which minimized the potential of future research. Grant funds evaporated and potential researchers turned their efforts to other fields while the laser was gaining substantial research acceptance in many medical, bioengineering, communication and industrial applications. As a result, American laser research in dentistry has fallen well behind that in other countries. Rather than being in the forefront of dental laser application, dentistry receives most of its new laser technology second hand from the medical profession.

A large amount of literature has accumulated since the first report of the surgical (soft tissue) application of a CO2 laser[79]. Surgeons claim many advantages of surgery using a laser; a bloodless field, shorter and less traumatic procedures and less post-operative pain and edema. Unlike the CO2 laser, the light from the recently introduced Nd:YAG (Neodymium:Yttrium-Aluminum-Garnet) laser operating in the near infrared, 1.06 um, can easily be transmitted fibreoptically into a small handpiece. Applications include 'Laser Scalpels' which can perform precise bloodless cutting, removal of caries in enamel and fusing of enamel for caries prevention[80]. Recently this type of laser has been specifically manufactured and marketed to the dental profession by the American Dental Laser Corp[81]. Whether this laser possesses enough suitable characteristics to remain in the

dental laser field will depend on further research and a favorable comparison to alternative laser systems. Researchers in Japan[82] have developed a hollow, metal lined, flexible tube to transmit CO2 radiation into a handpiece. This new development may be enough to allow the CO2 laser to supercede the clinical use of the Nd:YAG laser.

A new class of lasers, the excimer laser, operating in the ultra-violet (UV) range (100-400um) was introduced to the dental field in 1987[71] following its application in the fields of ophthalmology, cardiac surgery and orthopaedics. Excimers allow extremely sharp and precise tissue cutting without thermal damage because of their ability to ablate material by photo-decomposition. These new lasers may prove valuable to the dental profession.

Laser Theory and Light Interactions with Matter

A basic knowledge of laser characteristics as well as the mechanism by which light interacts with matter are mandatory if an individual wants to interpret the results of many laser experiments.

The word LASER is an acronym for 'Light Amplification by Stimulated Emission of Radiation'. The basic differences between lasers and other light sources are the characteristics of the light emitted from a laser. They are;

1. Synchronicity (phase coherency)
2. Monochromaticity (frequency coherency)
3. Directivity (spatial coherency)
4. Excellent concentration of energy (high photon density)
5. Extremely high brightness.
6. Controllability.

The coherent properties in time and space are compared to incoherent light in Figure 5.

Figure 5.[83]

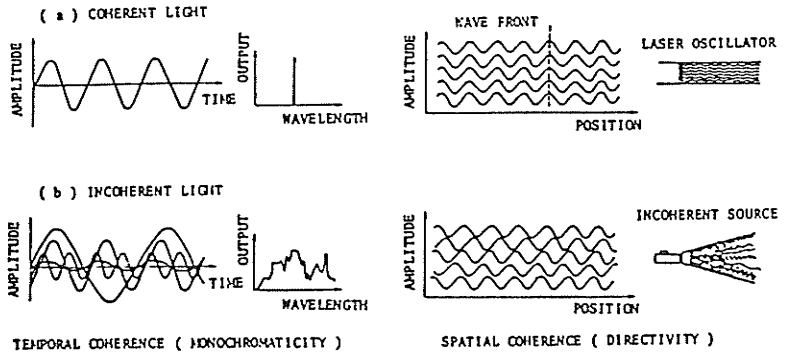

Temporal and spatial property of coherent light from a laser compared with those of incoherent light from a conventional light source

In contrast to incoherent light, light waves emitted from a laser have the same amplitude and are in phase. Conventional light sources emit light over much of the visible and infrared spectrum while for all practical purposes, the laser can be considered monochromatic, containing a beam of very narrow range wavelengths. The divergence of a laser beam is very small, about a milliradian (approximately 0.05 ° divergence). As a result of being focussed and synchronous, the output power can be concentrated to produce a small high intensity and a high energy density beam. In addition, by pulsing the laser, the energy can be released over a shorter time to give very high power pulses rather than relatively low but constant power emitted by a continuous wave (CW) laser. A more detailed discussion of the nature of light and the mechanism of laser action are found in Appendix 1.

When electromagnetic energy (light) comes into contact with matter it can either be reflected, transmitted or absorbed and then scattered or refracted within the material. The study of the interaction of light with matter is known as spectroscopy. A great deal of information can be gleaned by knowing the wavelengths of photons that an organic molecule can absorb most efficiently. The energy (E) associated with a photon is related to the frequency (f) of the light by the following formula $E=hf$, where h=Plancks constant (6.6×10^{-34} joules/sec). As the frequency increases so does the photon energy. Accordingly a photon of Ultraviolet (UV) light will have much more energy than a photon

of Infrared (IR) light. The energy absorbed by a molecule or atom can be resolved into at least four major components; translational energy, rotational energy, vibrational energy and electronic energy. The translational energy level is essentially continuous and represents the lowest energy of the molecule or atom. For each of remaining components there are certain discrete, permissible energy levels. An atom does not absorb any photons unless the photons have enough energy to bring about the transition from one energy level to another. Only those photons which carry the exact amount of energy required for transition to the next permitted level, can be absorbed. Electronic transitions require much more energy than vibrational transitions which in turn require much greater energy than rotational transitions.[84]

$$E_e >> E_v >> E_r$$

Consequently, rotational transitions are accomplished by considerably less energetic photons, and by Plancks equation, longer wavelength radiation such as microwaves. Vibrational transitions require photons in the infrared region, and electronic transitions need the more powerful photons associated with short wavelength radiation such as visible and ultraviolet radiation. In contrast, the passage of IR radiation through a material can increase the various energy levels of the atom or molecule efficiently only when radiation of the correct frequency to cause a vibrational or rotational change is absorbed. Spectroscopic study of organic compounds is therefore, in essence, an investigation of the types of waves that can be

absorbed efficiently by a compound. Spectra may thus give an indication of what lasers may best be suited for a specific purpose. (NB. further explanation of spectroscopy and light\matter interactions, with emphasis on UV and IR regions are found in Appendix 2). Spectroscopic information should indicate which laser wavelengths would be highly absorbed, allowing the desired result with as low a laser power as possible. Since low power will result in both a lower cost and lower incidence of undesired thermal effects, identification of these 'resonant' wavelengths is very desirable to maximize the laser effect.

Lasers and Dental Hard Tissues

The effect of CO2 laser irradiation on enamel and dentin tissues is well documented. The radiation is highly absorbed on the surface of enamel or dentin with low depth of penetration. Many IR spectroscopic studies have been performed on enamel and hydroxyapatite crystals[85,86].

Figure 6.[85]

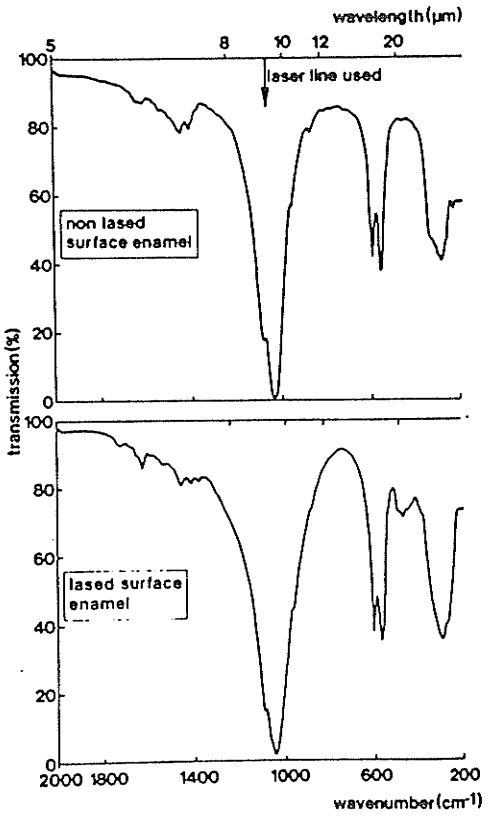

IR spectra of lased and nonlased surface human enamel in KBr pellets in the region (200-2,000 cm^{-1}). The enamel was lased with the 1,073 cm^{-1} line and a pulse energy density of 50 $J \cdot cm^{-2}$.

The spectra obtained show a very strong absorption band in the vicinity of 10.6 um., the same wavelength at which the CO2 laser operates. Many CO2 lasers are 'tunable' and can operate at several closely related wavelengths. Laser irradiation in this region of the mid-IR spectrum is strongly absorbed by the phosphate ions in the hydroxyapatite of the tooth enamel[87]. The resulting vibrational excitation results in great heat generation and surface vaporization even with low laser energy levels.

Strong surface absorption will minimize laser penetration and maximize the rate of surface heating. The latter will allow the surface to vaporize before enough time has elapsed for heat

diffusion into the tooth. Both of these will reduce adverse pulpal response. Moreover Fowler and Kurada[87] speculate that the use of selected wavelengths which coincide with specific ion absorption wavelengths of enamel will result in desired chemical reactions. For example, the selective excitation of the OH group to higher energy levels may promote Fluoride ion diffusion along the apatite channels[87]. In an artificial caries study Stern et el.[88] found that the higher absorption of enamel for 10.6 um. irradiance compared to 0.694 um (ruby laser) irradiance allowed them to use 1/15th the energy density to produce similar levels of protection of enamel against demineralization. Clearly, knowledge obtained through spectroscopic investigation of how light reacts with a material is critical to selection of the most appropriate laser for a specific purpose.

Perhaps the most dramatic example of appropriate laser selection, based on a material's properties and desired results, is that used by ophthalmic surgeons in the repair of detached retinas. Based on a lack of interaction with corneal material and a selective absorption by the retina, an Argon laser (488 green or 514.5 blue) can be used to 'spot weld' a detached retina back to its base without damaging the cornea or lens of the eye. Such a finding was not likely based on spectroscopic analyses of cornea, lens and retina but more likely on common sense. The fact that humans see colors, the visible part of the electromagnetic spectrum, indicates a significant proportion of light (in the visible range) must be transmitted through the

cornea and lens to the retina. The selective absorption of one tissue versus the selective transparency of another tissue has revolutionalized ophthalmic surgery.

While mid-infrared spectroscopic data on enamel is abundant, the literature is virtually devoid of information regarding the interaction of UV, Visible or near IR electromagnetic radiation with enamel. The effectiveness of various laser systems are often measured by comparing the energy densities needed to obtain a specific result. Morioka et el.[89] include one of the few spectra of enamel absorption in the UV to IR regions. They demonstrate that tooth enamel is virtually transparent to wavelengths between the visible and near IR spectrum. Light from Nd:YAG, ruby, and krypton lasers are essentially not absorbed by enamel. Light from carbon dioxide, carbon monoxide in the IR and krypton-fluoride, argon-fluoride and nitrogen lasers in the UV are however, remarkably more absorbed.

Figure 7.[89]

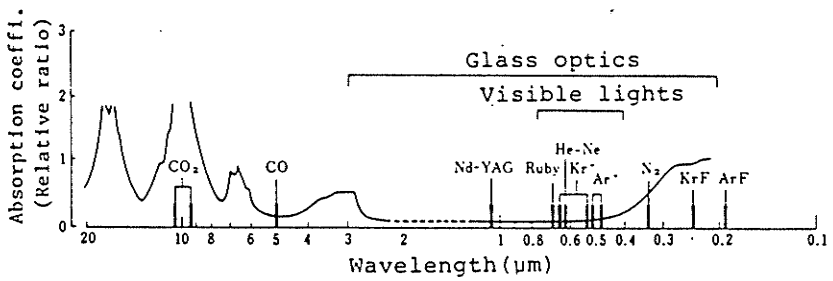

Wavelength of lasers and the absorption spectra of human tooth enamel

While it would appear that CO2 laser radiation is much more suitable for use on enamel, the Nd:YAG by American Dental Laser Corp. has become the first laser specifically marketed to the dental profession because of the relative ease with which the radiation can be fibre optically transmitted. Realizing the relatively weak absorption of Nd:YAG laser light by enamel and dentin, the manufacturers are advocating its use in conjunction with a black ink painted on the hard tissue. Results of future studies coupled with the continued emergence and refinement of laser technology may, in the future conclude that the Nd:YAG laser system was prematurely mass marketed. Boehm[90] states that up to 40% of incident radiation at wavelengths 1.25um or lower is reflected by the enamel surface.

Figure 7 demonstrates that enamel absorbs well in the UV range of the electromagnetic spectrum. When ultraviolet light interacts with matter, it affects the electronic state of atoms and thus has the ability to promote chemical reactions including dissociations, see Appendix 2. IR lasers melt and vaporize material via thermal processes. The very high melting point of human enamel (1280°C)[91] makes it nearly impossible to remove or cut enamel without significantly increasing the potential for thermal pulp damage. UV excimer lasers however, are able to photodecompose[92,93] organic and inorganic material with only limited thermal effects[93]. A highly energetic photon will induce bond cleavage producing molecular fragments and elemental compounds. Energy not consumed in bond breaking is converted into

kinetic energy by expansion of the resulting gaseous phase and the decomposition products are blown off with ultrasonic speed. Frentzen et al.[94] using a 193 ArF excimer laser demonstrated conclusively, through mass spectroscopy techniques, that enamel and dentin can be ablated. Photoablation in their study is a tissue specific process with the demineralized zones of a carious defect being ablated much more rapidly than unaffected areas. The lowest ablation rate was found in the mineralized zone on the floor of carious lesions in dentin.

Several papers demonstrating the ablative effects of 248nm KrF[95] and 308 XeCl[96] excimer laser radiation on bone have been published recently. Yow's study[96] showed a thermal damage zone of only 2-3 um in bone tissue surrounding the ablated zone. This width represents only a tenth of a diameter of a single cell and is much less than either the thermal ablation zones of 5-11 um created by the 2.9 um Erbium:YAG laser[97] or the 600 um zone created by the CO2 laser[97]. The authors also demonstrated the ablation of a bone cement composed of polymethylmethacrylate and styrene. Again the thermal damage zone of 10-40 um caused by 308 nm excimer is significantly less than the zone of 375 um caused by the Erbium:YAG[97].

Only two reports can be found describing the dental application of the 308 nm excimer laser. Pini et al.'s[98] use of the 308 excimer laser in root canal therapy demonstrated that demineralized (infected) dentin was preferentially ablated compared to sound dentin. The sound dentin acts as mechanical

guidance as the optic fibre was inserted into the canal ablating infected dentin. The rate at which the fibre proceeded was constant and slowed dramatically where much of the dentin was healthy. A smaller diameter fibre was then inserted to continue down the canal. Microscopic examination revealed a smooth clean canal of constant size corresponding to the fibre size.

Hame et al.[99] have recently studied the effect on enamel of the 308 excimer laser operating at 20 Hz and employing a 600 um fibre size. The authors measured the diameter and depth of holes created when varying the energy densities (50,70,90, mj\mm2) and exposure (500,1000,1500,3000,4000 pulses). The depth of penetration initially increased linearly with increasing number of pulses and the ablation rate increased with increasing energy density. The most rapid rate of penetration into enamel appears to occur during the first 500 pulses. Regardless of energy density, the penetration rate then drops significantly from 0.30 um\pulse to 0.05 um\pulse. The authors do not specifically offer an explanation for this finding but infer it could be related to the slight divergence of laser beam seen at higher depths. No differences were found between human and bovine enamel during lasing.

Interesting results have been found with the Erbium:YAG which is another recently released laser system. Unlike the excimer lasers which operate in the UV end of the spectrum, the Er:YAG is an infrared laser operating in the mid-IR region at 2.94 um. Unique to this laser is its strong absorption by tissue

water. A study[100], comparing the skin ablative effects of a 308 nm XeCl excimer laser and a pulsed Er:YAG laser demonstrated the Er:YAG to be very effective in tissue removal by ablation. Less thermal damage was seen with the Er:YAG relative to the 308 excimer laser. Direct comparisons between the two systems were difficult because the lasers operate at very different parameters. The XeCl excimer, with 20 nanosecond (ns) pulse width was tested between 5-50 Hz while the Er:YAG has emission duration of 250 us. Each 250 microsecond (us) pulse is composed of single energy spikes occurring at 1 us intervals. Repetition rates of only 5 Hz can be obtained with the Er:YAG. Due to strong absorption of tissue water at 2.94 um radiation the Er:YAG laser appears able to rapidly ablate tissue without thermal consequences.

As yet only two groups[101,102,103] have investigated the effects of Er:YAG irradiation of dental hard tissues. Unlike the CO2 laser which tends to melt and vaporize hydroxyapatite crystals, the Er:YAG laser is absorbed strongly by interstitial water. As the water within the surface layer of the tooth vaporizes, high pressure is generated resulting in microexplosive removal of enamel or dentin. Temperature increase is much less (16.1°C)[103] than with CO2 lasing (>1300°C)[104] and is more localized. Hibst and Keller[101] demonstrate that while the depth of cratering is in linear proportion to the number of pulses of irradiation for dentin, the depth in enamel is not directly related to pulse number. Reduced cutting rate in enamel could be

due to dentin's higher water content (enamel ≈2.5%, dentin ≈13.5%). The ablation effect of the Er:YAG has been described as threshold dependant ie; irradiation above a certain energy density will result in ablation while energy densities below this will result in heating effects. Paghdiwala[103] believes the use of a Q-switched (see Appendix) Er:YAG will increase ablation efficiency and result in even lower temperature increases.

Thermal Considerations

The acceptance of lasers into the dental profession will be based on their effectiveness and efficacy. Those lasers which can achieve similar or improved results compared to current dental procedures and prove cost and time effective will be viewed as desirable. The use of dental lasers must be shown to be biologically safe to the patient and the clinician. Lasers which can meet these criteria will likely be widely adopted by the profession.

When considering the use of dental lasers for debonding brackets, the potential thermal damage to vital pulps must be evaluated. Several investigators[105,106,107] have attempted to correlate intrapulpal temperatures, to histologic results. Lisanti and Zander[105] placed a thermocouple in a prepared buccal cavity of a vital tooth in a dog. The heat source was applied for 5 or 60 sec. giving an enamel surface temperature range from 51.6-315°C. A temperature rise at the pulpal-dentino junction (PDJ) of 1.9-24.7°C for the 5 second exposure test and 7.5-50.8°C

for the 60 second test was recorded. The thickness of dentin ranged between 0.81 mm to 1.82 mm and all cavities were subsequently filled with zinc eugenol cement. Surprisingly enough the authors report that not one pulp death was found. While elevations in pulp temperature correlated well with the severity of pulpal injury, healing occurred in every case. The stages of the recovery process are; walling off of an area of injury, then removal of necrotic tissue, followed by the replacement of damaged tissue and finally the deposition of irregular dentin opposite the irradiated tubules. Research by J.F. Cox[108] has shown that if the pulp is sealed off from the oral environment, full pulp recovery, including deposition of reparative dentin occurs even after a major insult which results in necrosis of the pulp adjacent to the site of injury.

The results reported by Zach and Cohen[106] on a similar set of experiments on the teeth of Rhesus Macaca monkeys differ dramatically from Lisanti and Zanders. The tip of a soldering gun kept at constant temperature, 275°C was applied to the enamel surface of a tooth for periods of 5-20 seconds, long enough to obtain pulp temperature increases of 2-17°C. Histologic examination showed that 15% of pulps exposed to a temperature rise of 5.6°C showed necrosis and at 11°C over 60% of teeth were necrotic. All pulps heated by 17°C became necrotic. The disparity between the above studies are certainly dramatic and elude explanation. Although there were differences; species, enamel vs.dentin, temperature measurement methods, zinc oxide filling

etc, some procedural error must exist in either study to explain such large discrepancies.

Nyborg and Brannstrom[107] have examined the reaction of the human pulp to heat. Cavity preparations were drilled into 29 sets of contralateral premolar teeth scheduled for orthodontic extraction. A temperature of 150°C was applied for 30 seconds. Dentinal thickness ranged from 0.02 mm to 1.10 mm. All cavities were restored only with amalgam. At one month histologic results showed all test teeth had sustained some pulpal injury resulting in the deposition of low differentiated predentin. Only four teeth displayed cellular changes suggesting necrosis. All teeth were asymptomatic. No measurement of intrapulpal temperatures were obtained. Such findings seem more closely related to those of Lisanti and Zander. The authors suggest that the rich blood supply of these young pulps might well have diminished greater thermal injury.

The discussion above serves to illustrate the imprecision with which thermal insult has been correlated to pulpal response. Not withstanding the foregoing imprecision, one can say with some degree of confidence, that pulpal temperature increases of up to 5.6°C (10°F) should be well tolerated and not result in irreversible damage to the pulp. Further increase however, may result in damage with subsequent repair and regeneration or result in pulpal necrosis. Ideally any pulpal effect should be avoided. In a article reviewing thermal trauma to teeth[109] it appears that pulpal temperature increase in excess of 10°F was

not found for any of the commonly performed dental procedures.

The pulpal effects of various lasers have also been investigated. Adrian et al.[75] attempted to establish energy density thresholds for pulpal response using the ruby laser. Dog teeth that were irradiated with a single laser shot were extracted 48 hours after exposure. Many teeth displayed necrosis with no surface effects. The ruby laser, they concluded, was not suitable for preparation of cavities. The authors did not however, investigate the possibility of repair and regeneration by examining teeth after a healing period. These authors went on to demonstrate a lower incidence of pulpal necrosis when teeth were exposed to similar energy densities of Nd:YAG radiation[110].

The precise mechanism by which lasers exert their effects on pulpal tissue is still very much unresolved. Shoji and Woriuchi[111] using argon, CO2 and Nd:YAG laser irradiation of whole rat teeth, demonstrated calcified tissue formation and increased alkaline phosphatase activity. Melcer et al.[112] have found similar stimulation of dentin formation after CO2 laser exposure of deep Class V lesions. Dentinogenesis occurred between 800 and 8000 J/cm2, above which they found necrosis which was unresolved three months later. Direct pulpal exposure to CO2 radiation can also result in reparative dentin formation[113,114]. The origin of the odontoblastic activity observed is not clear but could result from either repair and regeneration by cellular differentiation after thermal insult or from direct laser activation of the cell. The strong surface absorption of CO2

radiation leads one to suspect that thermal effects stimulate odontoblastic activity.

Launay et al.[115] have recently attempted to quantify the thermal effects of Nd:YAG, argon and CO2 laser on enamel, dentin and dental pulps by means of computerized infrared thermography and thermocouples. Thermal results showed a very low absorption of the Nd:YAG beam by enamel and dentin. Energy at this wavelength was transmitted to the pulp. Overheating of the pulp is in a direct ratio to the applied power. External and internal temperature rise and lack of surface alteration demonstrate how 1060 nm irradiation diffuses through hard tissues to the pulp. The small external temperature rise is consistent with absorption of a small amount of incident energy. The authors do not advocate the use of a continuous wave Nd:YAG on hard tissues without the use of a surface absorbent. The results obtained for argon laser irradiance were inconsistent and depend on whether the enamel surface is clean. An argon beam is strongly reflected back by clean enamel. According to Boehm[90] wavelengths lower than 1.25 um are reflected more than 40% by dental enamel.

Very high surface temperatures and very low pulpal temperature increases were found with CO2 irradiation of dentin or enamel. External temperatures of approximately 1230°C[115] are sufficient to melt hydroxyapatite. These temperatures are in the same order as those reported elsewhere[104]. Pulpal temperature increases were below the thresholds of 5.6°C established by Zach and Cohen.[106] Others[116] have reported similar pulpal temperatures

with single shot CO2 irradiation. A thermal threshold exists below which no overheating is noticed in the pulp chamber. Beyond this threshold, pulpal overheating grows directly with laser energy deposition[115].

It would appear from the above that the CO2 laser could be used dentally without pulpal damage. Bearing in mind however, that all of the above studies were performed with a single shot exposure. Total tooth heating during a dental procedure using a laser will likely be related to a number of factors including; total time of irradiation, repetition rate, pulse duration versus refractory time, spot size, energy density, use of coolants, wavelength of irradiation-absorption coefficient, pulpal blood flow, heat sink effects of alveolar bone and PDL etc.. Temperature measurements should be made for each dental procedure performed with the various lasers utilized in order to establish the effect on a per procedure basis.

Statement of Purpose

The main objectives of this study are to investigate the potential for debonding ceramic orthodontic brackets using various wavelength lasers;

1. Determine the efficacy of lasers in removing brackets safely, without enamel or bracket damage, without thermal damage to the pulp and in a clinically satisfactory time.

2. Examine the influence of various laser wavelengths and various bracket types on debonding effectiveness.

3. Attempt to correlate debonding times, material damage, site of bond failure and pulpal temperatures to absorption spectra.

4. Propose a mechanism for the observed results.

MATERIALS AND METHODS

I SPECTROSCOPIC ANALYSIS

A. IR and UV Absorption Spectra of Adhesives

Since the effectiveness of laser interaction with the bonding resins will be strongly dependent on the absorption of the laser radiation by the resin, an absorption spectroscopic analysis was performed. Several commercial adhesives (Challenge, System I, Monolok, Achieve and Dynabond) used for bonding orthodontic brackets, were prepared according to the manufacturer's directions. The freshly prepared adhesives were placed between two siliconized glass slides and compressed to form thin films, ranging in thickness from about 50 to 350 um. When set, the films were separated from the slides and subjected to spectroscopic analysis with a Hewlett-Packard 8452 UV\Vis Diode Array Spectrophotometer[@] with microprocessor and a Perkin-Elmer IR Spectrophotometer.[@]

Dynabond, the adhesive utilized for the laser debonding portion of the study was further analyzed using a Hitachi U2000 Double beam Spectrophotometer[*] which analyzed absorption between 190-1100 nm and the Carey 14[+] spectrophotometer which analyzed absorption between 2.5 um and 300 nm. These spectra were obtained with a silane agent (Ormco Porcelain Primer) added to the adhesive. The silane was added in order to evaluate the possibility of a synergistic absorption effect of both reactive components. A UV through visible light spectra (190-820 nm) was also obtained for Bis-GMA polymer.

@ Department of Chemistry, Univ. of Manitoba
* Department of Biochemistry, Univ. of Manitoba
+ Department of Engineering, Univ. of Manitoba

B. IR and UV Transmission Spectra of Brackets

1) As a reference standard, the spectrum from a standard grade sapphire window (2.0 cm diameter X 2.5 mm deep) was obtained (General Ruby and Sapphire Corp.), using the Hewlett-Packard Spectrophotometer.

2) To determine any differences that exist between the transmission spectra for sapphire (S) and polycrystalline alumina (PC) brackets, transmission spectra were determined, and compared to each other and to those spectra published for sapphire. Spectra were obtained using the Hewlett-Packard 8452 UV\Vis Diode Array Spectrophotometer (190-820 nm). Masking devices constructed of thick black cardboard were made to conform to each bracket type (S-A Comp, PC-Unitek) to assure that all light reaching the photodetector had passed through the bracket. Prior to obtaining bracket spectra, a reference spectrum was obtained with the masks and no bracket in place.

3) In order to determine how much light passes through the bracket to the adhesive layer, the light transmission characteristics of the brackets were determined. One sapphire and one polycrystalline bracket were placed on the edge of a moveable stage, Figure 8. The bracket surface faced the laser. The base, hanging over the edge of the stage, faced the optical power meter detector (Newport Corporation). The detector was placed as close as possible to the bracket in an effort to read all light passing through the base and to minimize loss due to scatter. A continuous wave Helium-Neon laser at 632 nm and a continuous

wave argon laser at 488 and 514.5 nm were used. The apparatus was aligned so that a light beam 1 to 1.5 mm in diameter struck the center of the bracket surface at 90°. Power readings of the incident beam and of the transmitted beam were taken. All tests were performed in darkness to eliminate the interference of ambient light. An attenuator was placed on the power meter when using the argon laser. These tests were performed at the Ontario Lightwave and Laser Research Center, in Toronto, Ontario.

Figure 8

BRACKET TRANSMISSION USING LASERS

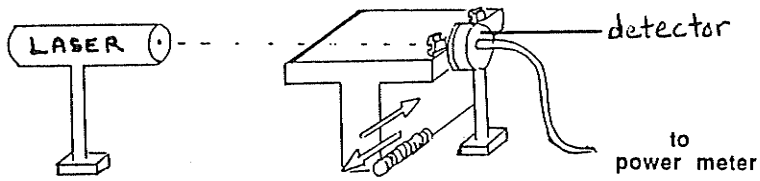

4) Bracket composition and bonding surface characteristics were examined utilizing a JXA 840 Scanning Microanalyzer. Several of each bracket type were fractured and mounted for SEM element X-Ray analysis (EDAX). All elements with higher atomic weight than Oxygen could be detected.

II Laser Debonding Experiments

A Sample Preparation

Methodology for this group of experiments had been developed as a result of a pilot study. (Appendix 3). Primary Bovine teeth were extracted and stored in room temperature water.

Before bonding, the teeth were polished with pumice powder, washed, dried, and the enamel bonding surface acid etched according to the manufacturer's directions (60 sec with 30% Phosphoric acid, thorough water wash and dried). The use of Bovine enamel as a substitute for human enamel has been justified[117,118,119]. For each wavelength to be tested (193, 248, 308, 1060 nm), 15 brackets each of Unitek (PC) and A-Comp (S) were bonded to the bovine teeth with Dynabond (Unitek) according to manufacturer's directions and stored in water until testing. In spite of the fact that a previous pilot (Appendix 3) had shown that wet versus dry storage had no significant effects on laser debonding times, all samples were kept wet in an effort to more closely mimic clinical conditions. Since the results obtained in this pilot study showed that Unitek's Dynabond gave similar results to the other adhesives tested (System 1, Achieve, Challenge) and since Unitek brackets were involved in the study, Dynabond was used for the remaining experimentation.

The bonded tooth and bracket assemblies were mounted in Coe Quick Set tray acrylic. To ensure accurate and reproducible positioning of the bracket during debonding, a mounting jig was fabricated from clear acrylic (Fig. 9). The jig had a circular recess into which would fit tightly an 18 mm diameter brass metal ring. The ring was filled with Coe Quick set tray acrylic and seated into the recess. The bracket-tooth assembly was positioned in the jig so that the bracket remained free of the tray resin and was held in place by two 0.016 SS wires running through the

bracket (Fig. 10). After the tray acrylic had partially set, an orientation mark was placed into the tray acrylic to facilitate accurate positioning into a sample holder (Fig. 11). The mounting jig was removed prior to final set of the tray acrylic. Upon complete polymerization the acrylic samples were separated from the rings, trimmed and stored in room temperature water until testing. A wooden frame was constructed to serve as a sample holder during debonding. For testing, the sample is oriented in the frame and secured into place with a set screw (Fig.12).

Figure 9 : Plastic mounting jig (side view) demonstrating fit onto brass ring.

Figure 10 : Mounting jig (top view), note Stainless Steel wires to maintain bracket-tooth orientation.

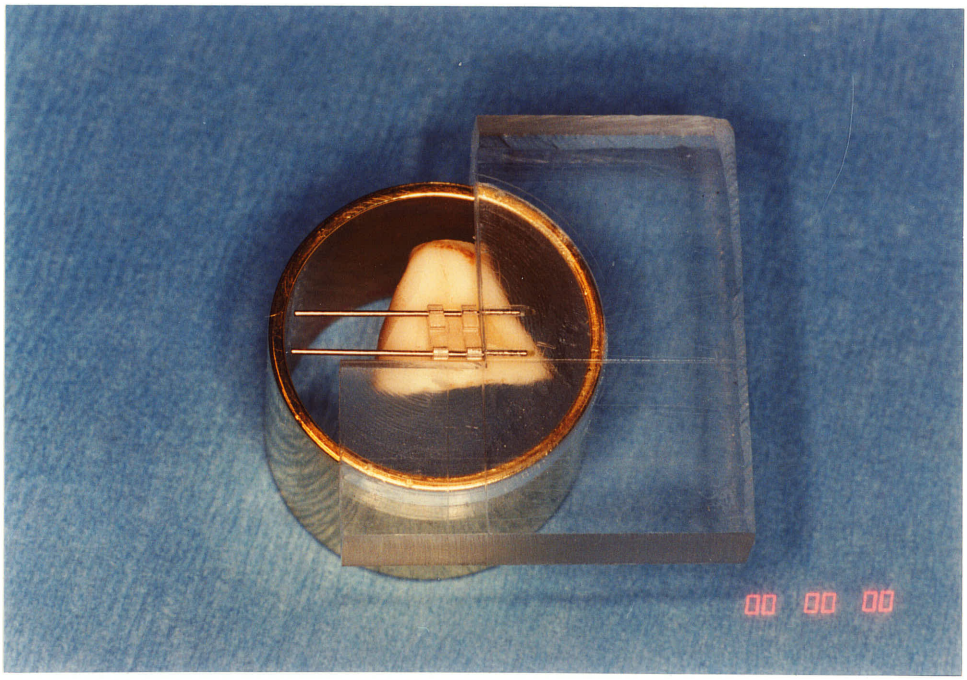

Figure 11 : Completed sample prior to separation from brass ring, note orientation mark for alignment into sample holder.

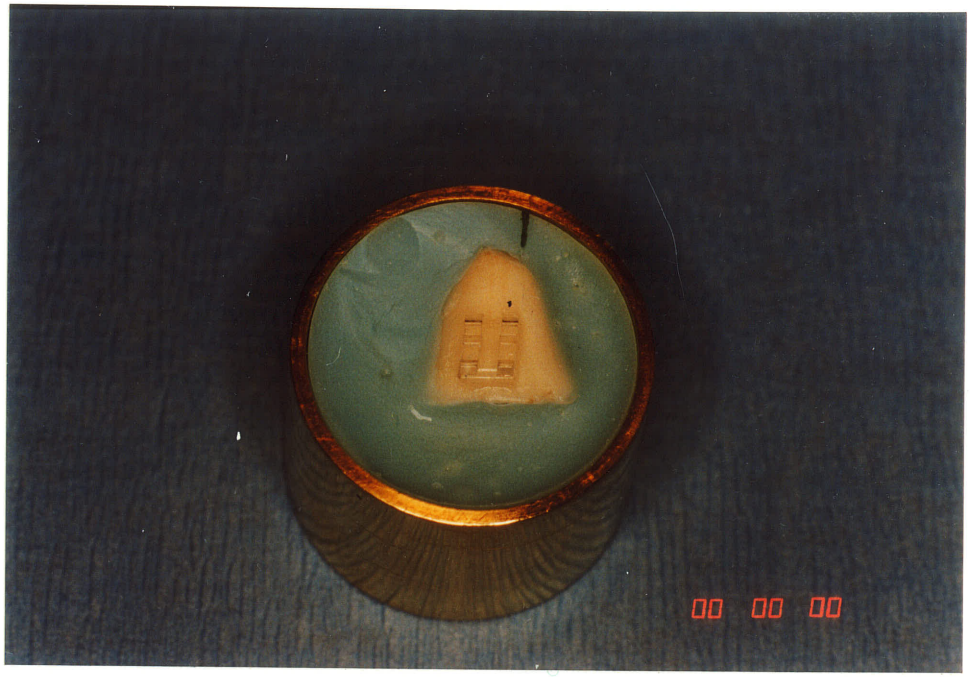

Figure 12 : Mounted sample in wooden holding apparatus, with shear force applied.

B Debonding Procedure

This portion of the experiment was performed at the Ontario Lightwave and Laser Research Center, in Toronto, Ontario. The main objectives were to examine the debonding effectiveness of various wavelengths of laser light. Fifteen PC and 15 sapphire (S) brackets were tested at wavelengths of 193, 248, 308 and 1060 nm. Samples were irradiated and the time until failure measured. A light constant shear force of 8 kg\cm^2 was applied to the brackets during debonding. This force represents only a fraction, <1/10th, of debonding values reported in the literature[24,56,66,67] . The application of a light shear force was at this time deemed to be necessary from a clinical standpoint since the viscosity of a thermally softened resin might prevent debonding. In an effort to apply a similar shear stress to both the PC and sapphire brackets, compensations for the different bracket base areas were made. Both brackets were placed on an overhead projector and magnified. Acetate tracings were made of each magnified base and the weights were compared. The PC base was 0.7176x the size of the sapphire (S) base. Based on the formula for shear stress (shear load per cross sectional area parallel to the stress) the weight applied to the PC brackets was 730.5 gms while 1018 gms was applied to the sapphire (S) brackets to give an identical shear stress.

1. Laser parameters

In order to compare the debonding effectiveness of various wavelength lasers, an identical energy density (Energy/unit area)

must be delivered at each wavelength. Since the lasers used in these experiments differed from those used in the pilot experiments, a new set of laser parameters had to be determined. Only the polycrystalline brackets were used for this determination since the sapphire brackets gave unusual results. For the PC bracket determination, a debonding time of approximately 2-4 seconds/bracket was selected as we believe such times to be within clinically acceptable limits. To achieve this debonding time for PC brackets, the energy output (Watts or Joules/s) of the Lumonics Excimer 460-SMA laser operating with KrF gas at 248 nm was focussed to give a bonding surface spot size of 3.5x3.5 mm, and was set to 49 Hz for an average power level of 4 watts. The average power density at the bonding surface was calculated as approximately 32.6 watts\cm2. This energy density was maintained as closely as possible throughout the remainder of the experiment at each wavelength tested.

The apparatus set up for irradiation at 248 and 308 nm is shown in Figure 13.

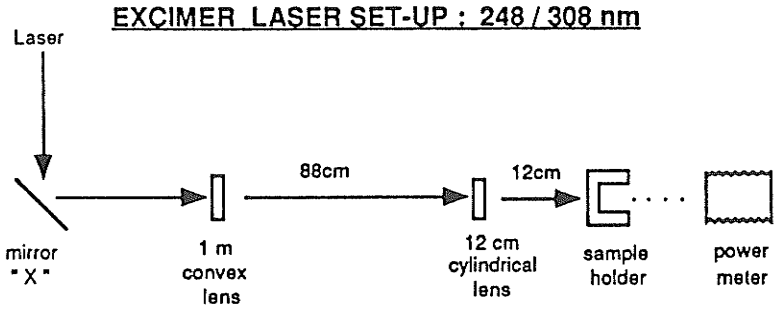

Vertical changes in the beam position were performed at the mirror ("X" in Figure 13). A one meter convex lens and a 12 cm

cylindrical lens were positioned to focus the beam to the desired spot size. Fifteen PC and 15 sapphire brackets were irradiated at 248 nm.

Several problems arose when using the ArF 193 nm laser. Since a cylindrical convex lens was not available to focus the beam horizontally at 193 nm, a 3.5 X 3.5 mm carbon mask was placed in front of the sample in an attempt to block out the unwanted portion of the beam. As this laser did not have a gas processor, ArF depletion occurred so rapidly that the laser could be operated for only thirty minutes per gas fill. At 118 Hz and 39.9 KV the maximum power obtained at the bracket after 60 sec of operation was only 1 Watt. Therefore only five of each PC and sapphire brackets were tested.

A Quantaray DCR-3 Q-switched Nd:YAG laser was used for irradiation at 1060 nm. Four watts of power was obtained and the laser was operated in the following configuration.

Figure 14.

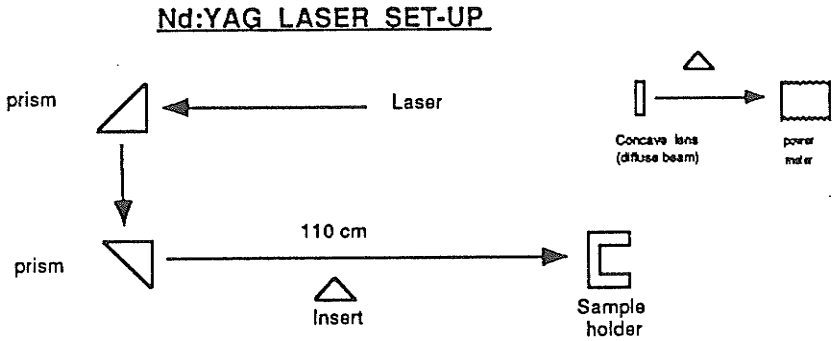

The energy distribution within the beam was irregular. A 'hot spot' of approximately 2.5-3 mm diameter was centrally located and focussed on the bracket.

A digital stopwatch was used to measure all times. A response test was carried out for timing error determination.

C Damage Evaluation

All debonded samples were collected, catalogued and inspected with a Zeiss binocular microscope at magnifications up to 40x for evidence of enamel damage and for determination of the site of fracture. A representative number of samples in each group were inspected using a JOEL-35C scanning electron microscope.

III Thermal Evaluation

A Sample preparation

In order for laser debonding to be considered efficacious the technique must not cause excessive temperature rise in the pulp. The methodology to measure pulp chamber temperature rise during laser irradiation was developed in a separate pilot project using bovine and human lower incisor teeth. Since human lower incisor teeth contain the smallest pulps of all human teeth and thinnest labial walls, laser debonding proven safe with those teeth will likely be safe with all other teeth.

For each laser wavelength and bracket type, two teeth were prepared, one Bovine with bracket and one Human with bracket. The lingual surface of the tooth was cut away until the pulpal cavity was exposed. The cavity was thoroughly cleaned and a 700 FG dental bur was used to cut a hole for the thermocouple from

the pulpal wall through the labial dentin to the enamel layer. A 1/4 round bur was then used to extend the hole until it perforated the labial enamel. The thickness of the labial wall adjacent to the hole was measured with a pair of calipers. The labial wall thickness of bovine and human incisor teeth were very similar averaging about 2.0 mm (range was 1.5 to 2.3 mm). All mesial and distal surfaces were ground parallel so the teeth could be fixed in a vice like modification of the sample holder. All teeth were etched and stored in room temperature water until final preparation.

On the day prior to testing the prepared teeth were dried and the thermocouples were installed into the teeth. A Copper/Constantan Type PT (Sensortek Inc, New Jersey) thermocouple was inserted through the lingual access to the enamel surface. A bracket (PC or S) was then bonded onto the surface as previously described and the tip of the thermocouple was pushed into contact with the bracket-adhesive interface. A second thermocouple was placed in contact with the pulpal wall. Both were secured in place with molten 'sticky wax'. All prepared samples were stored in 100% humidity overnight.

Figure 15.

CROSS SECTIONAL VIEW

OF THERMOCOUPLE SET - UP

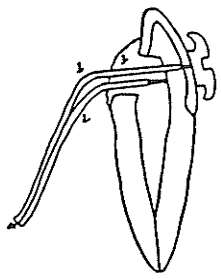

1. Interface thermocouple
2. Pulpal thermocouple
3. ' Sticky Wax '

B Experimentation

A tooth was inserted into the apparatus and aligned using very low 248 nm KrF laser power. The thermocouples were connected to the electronic digital thermometer (Bailey Model BAT 8, New Jersey). All temperature readings were converted to degrees Celsius. The initial (equilibrium) temperature was noted and the stop watch started as soon as the tooth was exposed to the laser light, using the identical parameters for power density and spot size used in the debonding study. Exposure continued for the average time of debonding as determined earlier. A reading from the bracket-adhesive interface was taken immediately after laser shut down and the measuring device was switched to read the pulpal thermocouple. Results of the pilot study demonstrated a time delay for reaching maximum temperature in the pulp as the thermal front slowly diffused through the tooth. Thus, the time at which the maximum pulp temperature is reached will occur after the digital thermometer is switched to the pulpal thermometer. Both the time to pulpal temperature maximum and the maximum temperature obtained in the pulp were recorded. Each tooth was tested five times after it had returned to the equilibrium temperature. The pilot study showed that the results of repeated tests were fairly consistent.

RESULTS

Spectra of Adhesives

The spectra obtained for the various adhesives analyzed with the Hewlett-Packard 8452 UV\Vis Spectrophotometer all appeared very similar. A typical UV\Vis spectra (Dynabond) is shown in Fig 16. The remaining spectra are found in Appendix 4.

Figure 16.

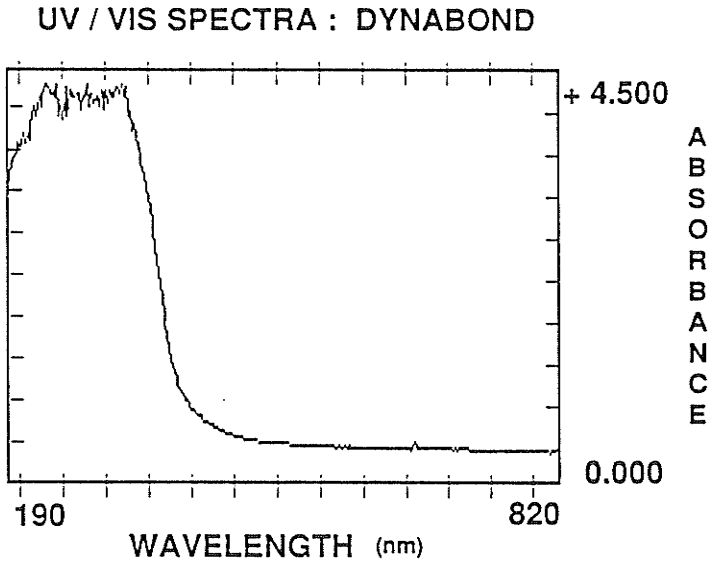

The vertical axis shows relative absorption and the horizontal axis shows the wavelength expressed in nanometers. All the adhesives strongly absorb light in the UV region of the spectrum at approximately 190-350 nm. Absorption rapidly decreases into the visible spectrum. The base line values of absorption are affected by the thickness of the film tested. Film thickness was not standardized. The adhesives had variable viscosities which, because of the method of fabrication, resulted in a variable thickness. The thinnest films, Bis-GMA and Dynabond, were clear

while other films appeared opaque. Qualitatively all the film spectra are very similar with strong UV light absorption and low visible light absorption.

A typical IR spectra of an adhesive (Dynabond) is shown in Figure 17. Again all the spectra obtained for the various adhesives tested are very similar. The remaining spectra are found in Appendix 4.

Figure 17.

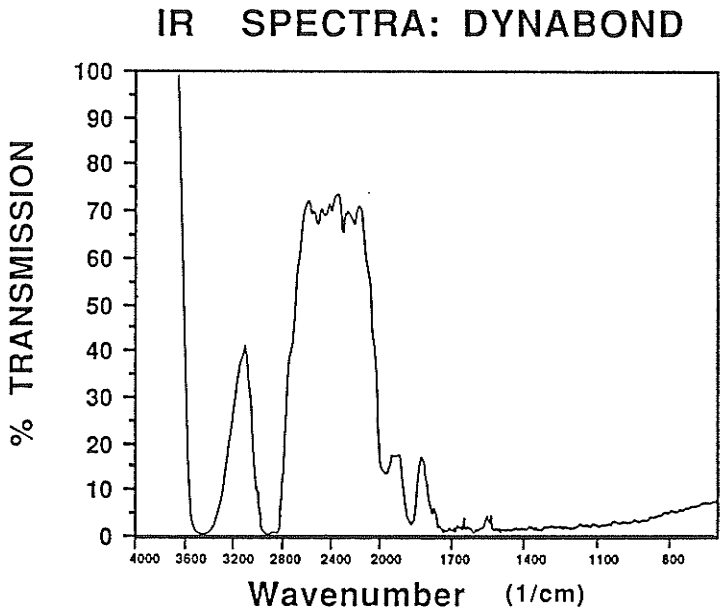

The vertical axis is expressed as the % Transmission, while the horizontal axis is expressed as the Wavenumber (cm^{-1}); the inverse of the wavelength expressed in centimeters. Strong absorption peaks occur in all samples between 3600-3400 cm^{-1} (2.7-2.9 um) and 2840-3000 cm^{-1} (3.3-3.5 um). The polymers differ slightly in the amount of transmission below 3000 cm^{-1}, while a generalized lack of transmission occurs below 1700 cm^{-1} (5.9 um).

Spectral analysis of Dynabond (Fig 18) with silane (Ormco Porcelain Primer) on the Hitachi U2000 Double Beam Spectrophotometer gave very high absorption in the UV range and low absorption throughout the visible and near infrared spectrum to 1100 nm.

Figure 18.

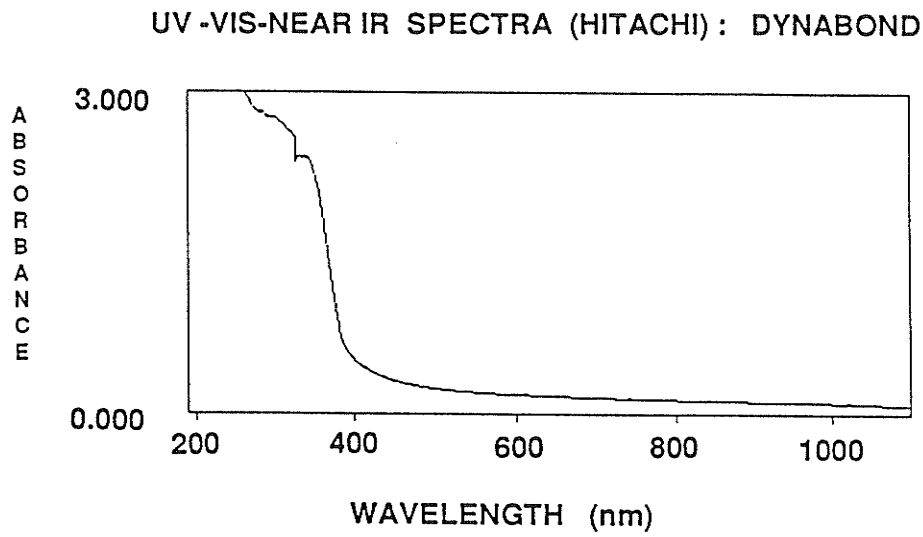

Relative to the reference beam some light energy was absorbed at 1060 nm. Whether this energy was absorbed and\or reflected by the film could not be determined. Results obtained using the Carey 14 double beam spectrophotometer, Figure 19, shows the transmission spectra obtained between 300 nm and 2.0 um. Again, a high absorption occurs in the UV. A 20% proportion of the beam is not transmitted relative to the reference beam. This energy is either absorbed and\or reflected.

Figure 19.

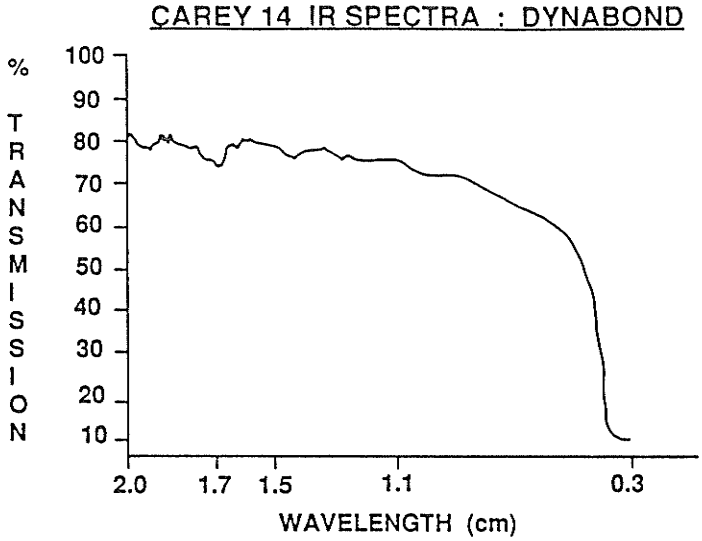

Bracket Analysis

The spectra obtained for Unitek's polycrystalline bracket, A-Company's sapphire bracket and a standard grade sapphire window (Gen. Ruby and Sapphire Co.) on the Hewlett-Packard 8452 Uv\Vis Diode Array Spectrophotometer are shown below (Fig 20,21,22). Spectra of the accompanying masking device or reference are found in Appendix 4.

Figure 20

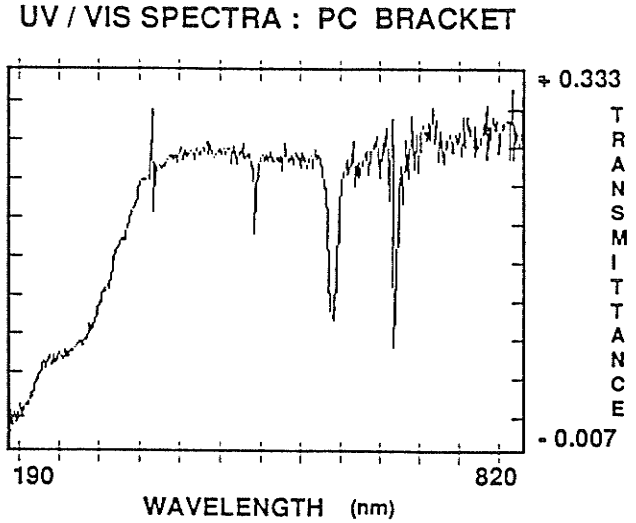

Figure 21

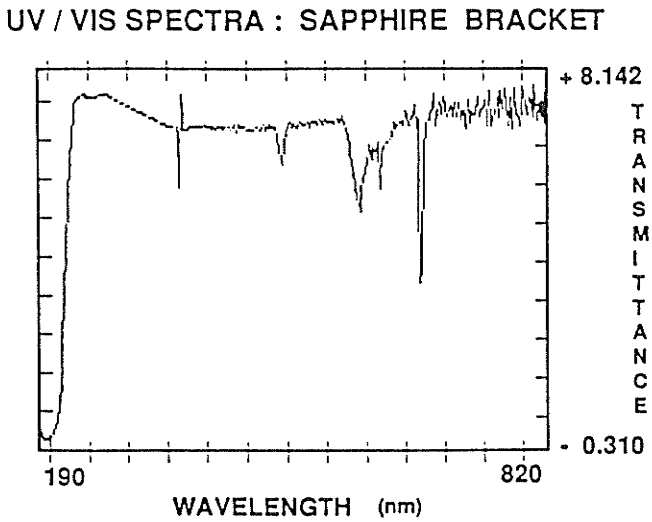

Figure 22 UV / VIS SPECTRA : SAPPHIRE WINDOW

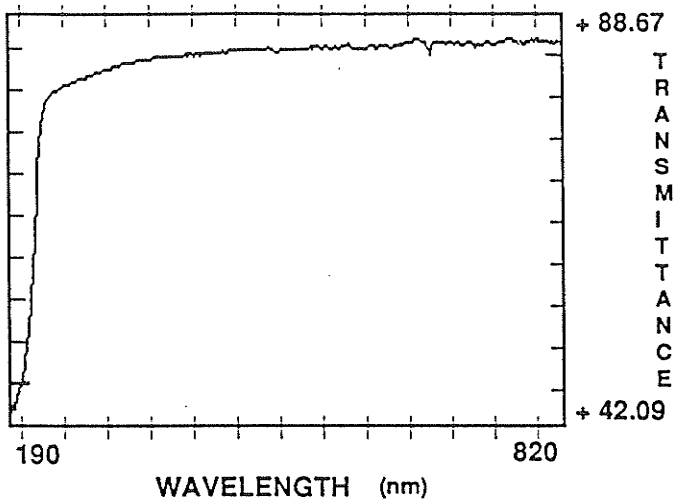

Approximately 100% transmission occurred with the masks (Append.4). In comparing the sample spectra, the most obvious difference is seen in the % transmittance. While the standard sapphire window gives a transmittance of nearly 88.7 %, which is similar to those reported in the literature[68], the maximum transmission for the sapphire (S) and polycrystalline (PC) brackets are approximately 8 % and 0.3 % respectively.

The shape of the sapphire bracket spectra is relatively similar to that of the sapphire window, showing a very strong drop in transmission starting at about 230 nm. The PC bracket displays a much more gradual drop in transmission starting at about 350 nm, with a shoulder at 225 and the lowest transmission around 200 nm. Both the PC and S bracket spectra show a number of accessory peaks not found on the spectra of the standard grade sapphire window. These peaks appear to be similar for both the PC and sapphire brackets and occur at 364, 486, 580 and 656 nm.

A scan of a quartz blank window, Fig 23, and of a common silanizing agent on the quartz blank, Fig. 24, have also been included in this section. Quartz is virtually transparent to all light between 190 and 820 nm while the silane agent appears to have slight absorption only at 225 nm and below.

Figure 23.

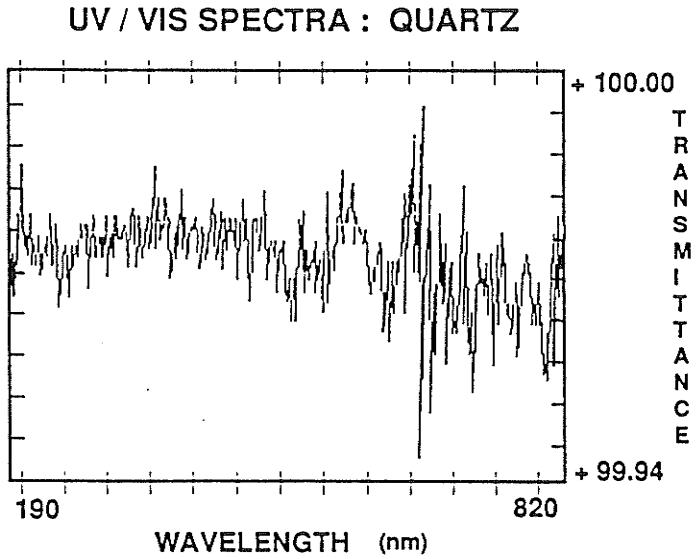

Figure 24.

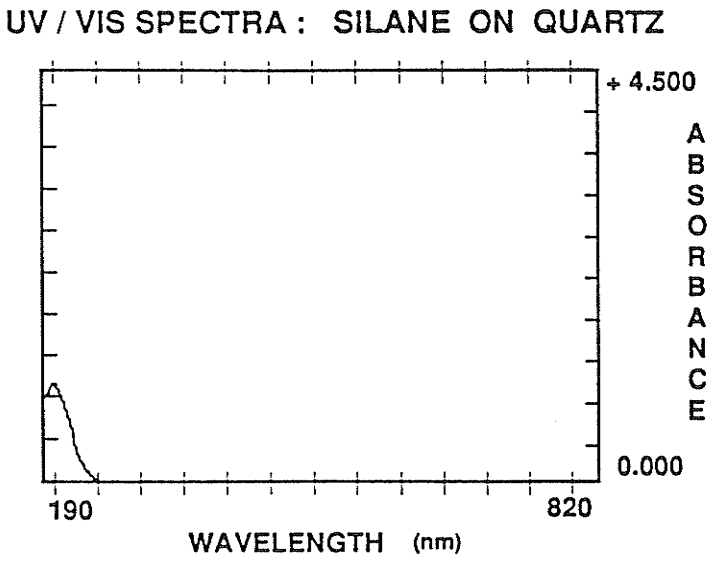

The quantification of bracket transmission utilizing lasers was carried out in an effort to support or refute the % transmissions obtained in the preceding spectral analysis and in an effort to determine what level of transmission occurs with coherent light. Transmission values obtained and calculated percentages are listed for each laser tested in Table 1.

Table 1

	Helium/Neon 632 nm	Argon 488 nm	Argon 524 nm
Incident beam	1.70 mW	22.2 mW	30.8 mW
A-Comp (S)	1.45 mW (85.3%)	15.2 mW (68.5%)	20.2 mW (65.6%)
Unitek (PC)	0.46 mW (27.1%)	2.0 mW (9.0%)	3.3 mW (10.7%)

Note that with the Helium\Neon laser, the % transmission of S approaches that obtained for the sapphire window but is less with the Argon wavelengths tested. A possible explanation for the differences might include the observed laser power drift that was found for the Argon laser. Every attempt was made to record transmission during power peaks. As well the Argon beam was 0.5 mm larger than the 1.0 mm diameter Helium\Neon beam and as such was more likely to be affected by bracket surface geometry

Results of SEM X-ray analysis of the PC and S brackets are shown in Figs. 25,26. Only elements with greater atomic weights than oxygen and present in concentrations greater than 0.1 % will

be detected by the energy dispersive X-Ray analyzer. Within the limits of the instrument detection the bulk of both brackets are composed of pure Alumina. A silicon containing compound is present on the bonding surface of both brackets, Figures 27 and 28.

Figure 25

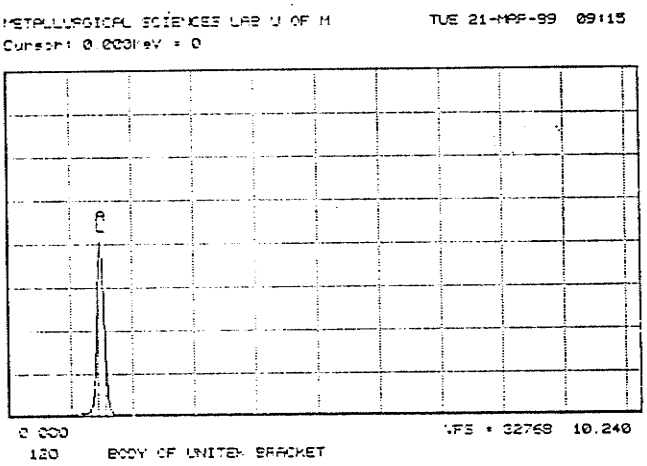

Figure 26

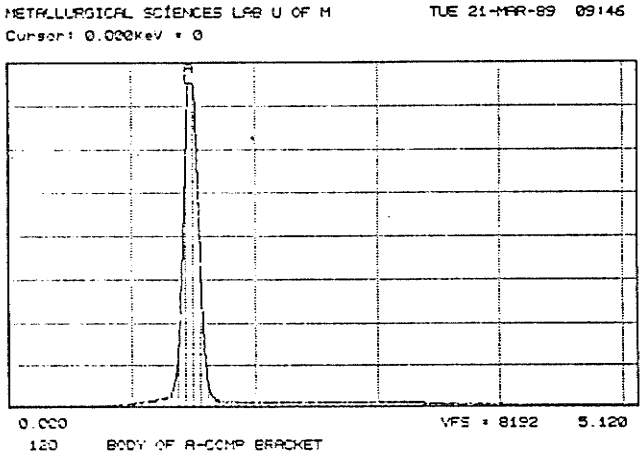

Figure 27

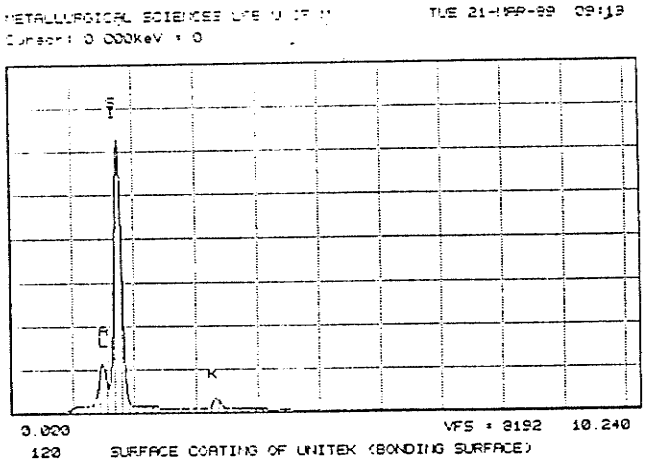

Figure 28

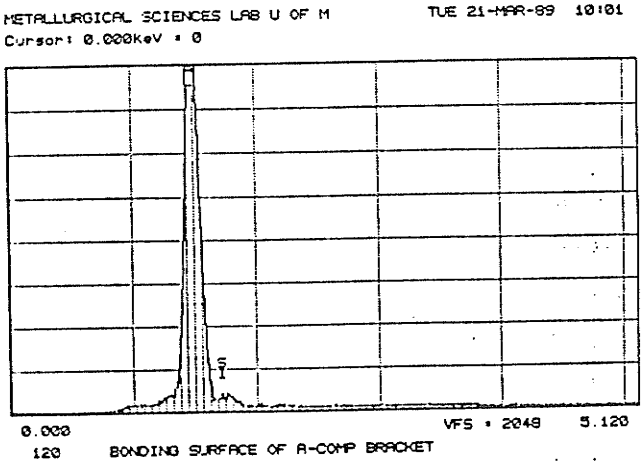

Photographs of the fracture surfaces, Figures 29 and 30, illustrate the polycrystalline nature of the Unitek bracket and the featureless, smooth surface of the monocrystalline A-Company

bracket. Individual crystal facets are clearly visible on the fracture surface of the PC bracket. A 30 um amorphous layer of

Figure 29: SEM Photograph of the Sapphire Bracket Fracture Surface

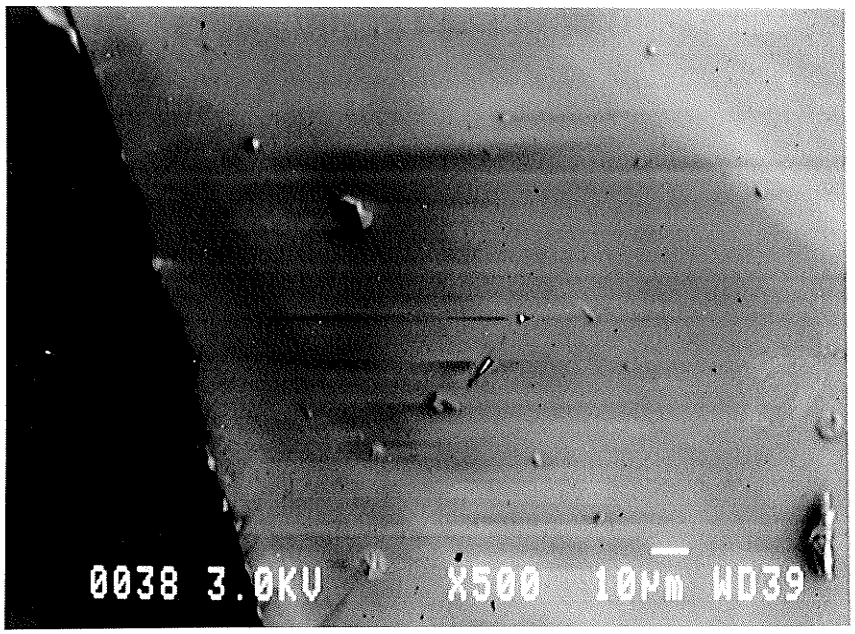

Figure 30: SEM Photograph of the Polycrystalline Bracket Fracture Surface. Note 30 um 'amorphous' layer at bonding suface interface.

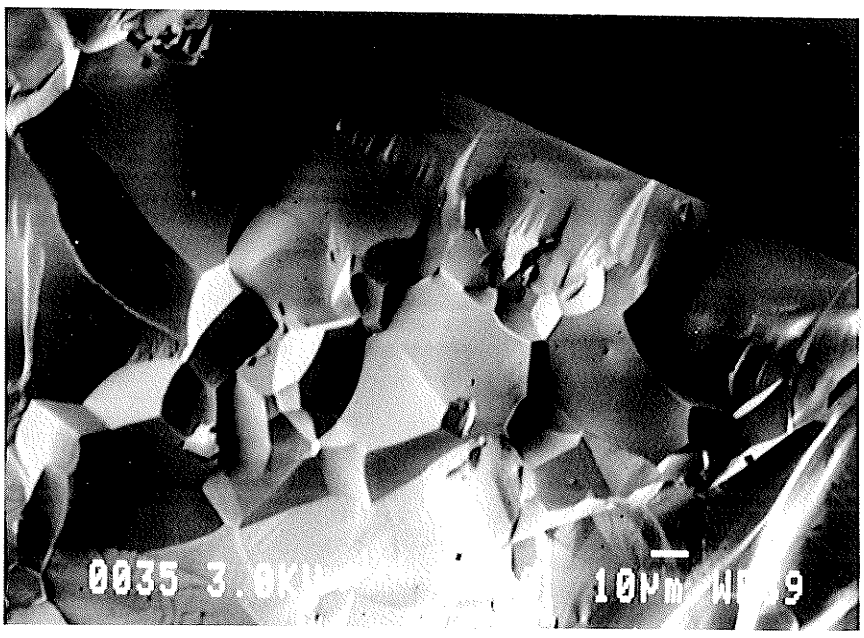

material fused to the bonding surface of this bracket can also be seen. Analysis of this layer, Figure 31, revealed a composition similar to glass with Si, NA, and K predominating.

Figure 31

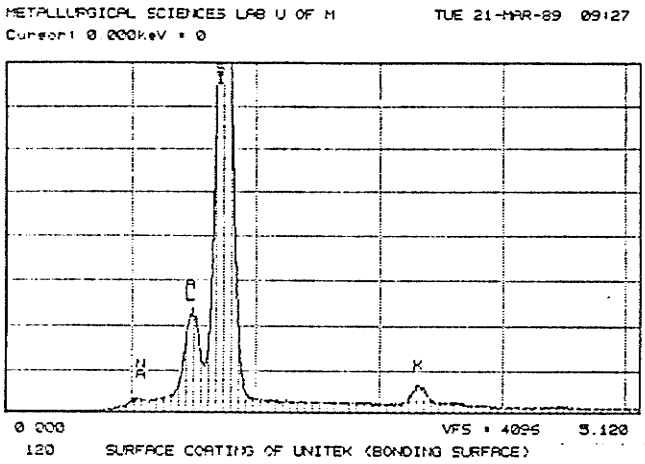

Laser Debonding

Laser parameters were initially set at 5 watts, 44 Hz and 37 Kv with a 10 ns pulse width at 248 nm (KrF). Four samples were tested with the 8 kg\cm^2 shear force applied. PC brackets were used to set the parameters because the sapphire brackets spontaneously blew off the tooth surface during irradiation and without any applied shear load. These findings were dramatically different than those seen in any of the pilot studies. Since the four PC brackets tested at 5 watts debonded in less than 2 seconds the power was dropped to 4 watts. The results for the PC brackets at 248 nm are listed in Table 2.

Table 2: PC bracket removal times (sec) using 248 nm KrF laser
Laser Parameters: 4 w, 36.5 Kv, 49 Hz, 10ns pulse

1.	3.83	9.	0.34	
2.	3.67	10.	2.75	
3.	0.69	11.	2.26	
4.	3.30	12.	2.64	
5.	3.63	13.	3.85	
6.	0.50	14.	0.48	
7.	3.94	15	2.00	
8.	0.50	Mean	3.09	SD 0.68
		(10 samples)		

Samples 3, 6, 8, and 9 were removed very quickly. These values were omitted in calculating the mean times for removal. The reasons for this omission will be discussed subsequently. An average lasing time of 3.1 seconds was required for the removal of the PC brackets at this wavelength under these parameters.

The results obtained for the S brackets are in Table 3.

Table 3: S brackets removal times using 248 nm KrF laser
Laser parameters: 4 w, 36.5 Kv, 49 Hz, 10 ns pulse

1.	0.30	+SF	9.	0.20	-SF
2.	0.29	"	10.	0.15	-SF
3.	0.42	"	11.	0.19	2.5w -SF
4.	0.17	"	12.	0.38	1.5w -SF
5.	0.22	"	13.	0.21	0.75w-SF
6.	0.15	-SF	14.	0.20	0.4w -SF
7.	0.17	-SF	15.	0.00	0.33w-SF
8.	0.17	-SF			

SF = shear force

Bracket removal times were very short, within the range of timing error calculated (Appendix 4). After the first 5 samples were debonded the shear force was removed. The next 5 samples, tested without a shear force, also gave extremely low removal

times. Thus the next 5 samples were removed with diminishing laser output power. The times for bracket removal continued to be well within the timing error measured to be 0.31 sec ± 0.15 seconds. It is possible that bracket removal could be achieved in a single pulse, but this could not be measured. The wattage was reduced by reducing the frequency from 29 Hz in sample 11 to 1 Hz in sample 15. As the samples were irradiated a crackling sound was heard as almost instantly the bracket blew forward off the tooth surface.

At 193 nm (ArF) only a limited number of samples were tested. The maximum power obtained from the laser was 1 watt at 118 Hz and 39.9 Kv. Debonding times for PC and S brackets tested are listed in Table 4.

Table 4: S and PC bracket removal times using 193 nm ArF laser
Laser parameters: 118 Hz, 39.9 Kv, 1 w, 10 ns pulse

Polycrystalline		Sapphire	
1.	26 s	1.	1.02 min
2.	44 s	2.	> 1.30 min
3.	16 s	3.	> 1.30 min
4.	53 s	4.	> 1.30 min
5.	38 s	5.	> 1.30 min
Mean	35 SD 15s	Mean	> 1.30 min

Note that only one S bracket was debonded. All other brackets were irradiated for 1.5 minutes without debonding.

At 308 nm (XeCl) 4 watts of power was obtained with 35 Kv and 36 Hz. The results are shown below in Table 5.

Table 5: PC bracket removal times (sec.) using 308 nm XeCl laser
Laser parameters: 4 w, 36 Hz, 35 Kv, 10 ns pulse

1.	5.86	9.	5.06	
2.	4.85	10.	3.93	
3.	5.35	11.	4.69	
4.	4.33	12.	0.70	
5.	0.84	13.	4.16	
6.	4.16	14.	4.57	
7.	4.53	15.	5.64	
8.	0.93	Mean	4.76	SD 0.6
		(12 samples)		

Again several samples, numbers 5, 8, and 12, gave extremely low values. These were omitted when calculating the mean. The results at 308 nm for the S brackets were very similar to those obtained at 248 nm, Table 6.

Table 6: S bracket removal times (sec.) using 308 nm XeCl laser
Laser parameters: 4 w, 36 Hz, 35 Kv, 10 ns pulse

1.	0.50	+SF	9.	0.19	-SF
2.	0.36	"	10.	0.31	-SF
3.	0.36	"	11.	0.20	2.7w -SF
4.	0.28	"	12.	0.30	2.1w -SF
5.	0.38	"	13.	0.85	1.1w -SF
6.	0.22	-SF	14.	0.92	0.6w -SF
7.	0.25	-SF	15.	8.14*	0.15w-SF
8.	0.21	-SF			

* see text for explanation

The initial five samples were tested with the shear force applied. Five more were treated without applying the shear force. Debonding times were again very short. The remaining 5 samples were tested with decreasing laser output energy. Note that the energy output was modified by adjusting the frequency, from 26 Hz in sample 10 to 1 Hz in sample 15. Sample 15* appeared to take much longer to debond, however, on closer inspection the bracket had been debonded but was still hanging in place.

Polycrystalline brackets were also removed with the 1060 nm Nd:YAG laser operating at 4 watts, 9 ns pulse width (Q-Switched) and at 17 Hz. Table 7.

Table 7: PC bracket removal times using 1060 nm Nd:YAG laser
Laser parameters: 4 w, 17 Hz, 9 ns pulse (Q-switched)

1.	21.04	9.	23.56	
2.	1.33	10.	32.06	
3.	0.62	11.	12.52	
4.	3.13	12.	35.19	
5.	21.92	13.	19.78	
6.	4.59	14.	7.83	
7.	12.44	15.	38.95	
8.	19.32	Mean	23.68	SD 9.01
		(10 samples)		

Several values, 2, 3, 4, 6, 14 were felt to be low enough as to represent a secondary or altered population as has been identified with the two previous wavelengths tested.

The results obtained with 1060 nm debonding of the sapphire brackets continued the trend seen with 248 and 308 nm. Seven brackets with or without the applied load were removed rapidly at 4 watts power. The remaining 8 brackets were tested at varying power values as seen in Table 8.

Table 8: S bracket removal times (sec.) using 1060 nm laser
Laser parameters: 4 w, 17 Hz, 9 ns pulse(Q-switched)

1.	0.48	+SF	8.	0.50	3.8w -SF
2.	0.66	"	9.	0.44	3.2w -SF
3.	0.84	"	10.	7.0 s	2.7w -SF
4.	0.50	"	11.	>1 min	2.5w -SF
5.	0.53	"	12.	>1 min	2.5w +SF
6.	0.50	-SF	13.	0.56	2.7w +SF
7.	0.50	-SF	14.	8.0 s	2.7w -SF
			15.	1.30	3.2w -SF

The power output of the Nd:YAG laser was altered in a different manner than that of the excimer wavelengths. Rather than changing the frequency, the laser energy was decreased by decreasing the voltage of the flashlamp. This decrease of voltage had a direct effect on the energy\pulse. It appears that with or without the force applied, greater than 1 minute would be required to remove the bracket at 2.5 watts. This wattage corresponds to a pulse energy of 147 millijoules. At 2.7 watts debonding time varied with the application of a shear force. If the force was applied the bracket was removed quickly. If it was not, 7 or 8 seconds was required for bracket removal. This wattage corresponds to a pulse energy of 159 millijoules. For all wattages above this value all brackets blew off instantly.

Statistical analyses (T tests) show significant differences exist between the debonding time of the sapphire and polycrystalline brackets ($p<.001$), and between the various wavelengths used for the PC brackets ($p<0.001$). Tests were not performed between the various sapphire results because debonding times were so low, and within timing error. Note that a number of samples were eliminated when calculating the mean removal times. These brackets gave unusually low debonding times and were felt to represent an altered population of brackets. It has been reported that silane on the bonding surface of the brackets can be depleted by heat, light and moisture[65,120] resulting in weaker bond strengths. The brackets obtained from Unitek were samples retrieved from various clinicians for conversion into

Transcend 2000 brackets. They did not come from the same batch number and were probably stored under variable conditions.

In order to eliminate the possibility of artificially creating significant results by elimination of some data, a non-powermetric statistical analysis was performed. The Krushal-Wallis test is based on a Median number for each group. All 45 samples (PC) were used. Results showed significant differences between all groups, similar to the results of the T tests.

Damage Evaluation

Inspection of all debonded samples with the Zeiss binocular microscope up to 40x power revealed no apparent damage to the enamel surface or bracket. The raw data characterizing each bracket failure is found in Appendix 4. The bracket-adhesive (B\A) interface dominated the site of fracture for all the PC brackets tested. While some samples (10 of 45) showed less than 10% of total surface area of enamel-adhesive (E\A) fracture only 4 of these brackets showed any appreciable E\A fracture. Three of these, samples 2, 3, 4 at 1060nm irradiation had what appeared to be very short debonding times and were considered part of the altered population of brackets. Some brackets appeared to have carbon deposits associated with the debonded surfaces. A lower incidence of carbonization was observed with the 1060 nm brackets.

The results obtained with the sapphire brackets differed substantially from those seen in previous pilot studies. Seven brackets at 248 nm exhibited complete B\A failure. All others

tested, except one at 308 nm, displayed complex failure patterns. Greater than 50 % of the bracket base area failure occurred at the B\A interface, yet all brackets demonstrated some degree of E\A or intra-adhesive (I\A) failure. A representative number of samples, 5 of each bracket type at each wavelength, were examined under SEM. Figure 32 shows the typical 'complex' debonding pattern found with the Sapphire brackets. Figure 33 is a close up of Figure 32 which demonstrates the bracket\adhesive fracture on the left, with a wall of adhesive that ends at the enamel/adhesive interface. At 500x magnification, Figure 34, the enamel rod morphology is more evident. This enamel does not however, appear similar to etched enamel. No apparent enamel damage was seen under SEM.

Figure 35 illustrates the typical appearance of the bracket/adhesive site of failure found with the PC brackets. A closer view, Figure 36, of the light area within the debonded resin face, in Fig. 35, demonstrates an unusual pattern of smooth walled clefts or bubbles. Again no apparent enamel damage could be found.

Figure 32 : SEM photograph of complex debonding pattern common to sapphire bracket samples, (15x magnification)

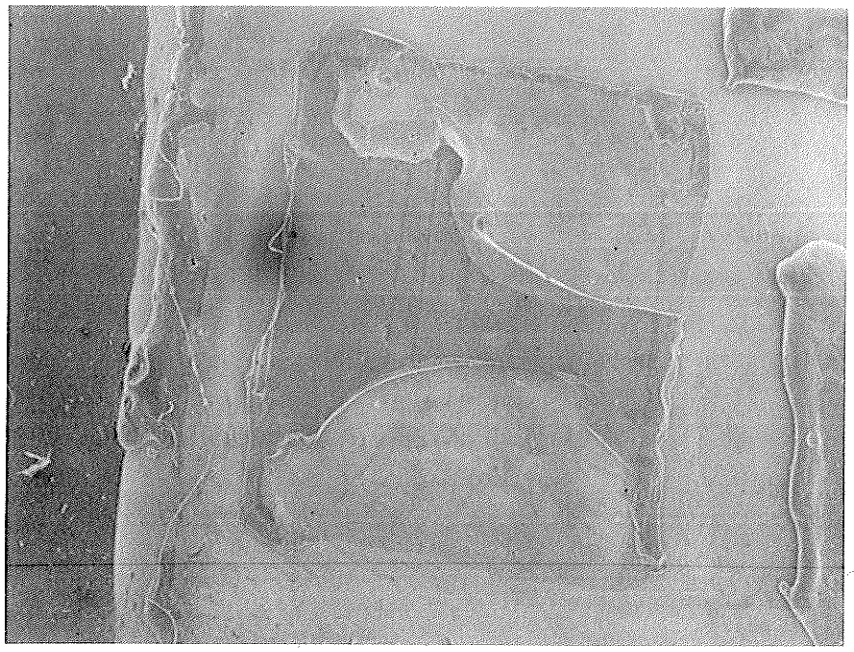

Figure 33 : SEM photograph (200x) demonstrating both bracket/adhesive (left) and enamel/adhesive interface fracture sites.

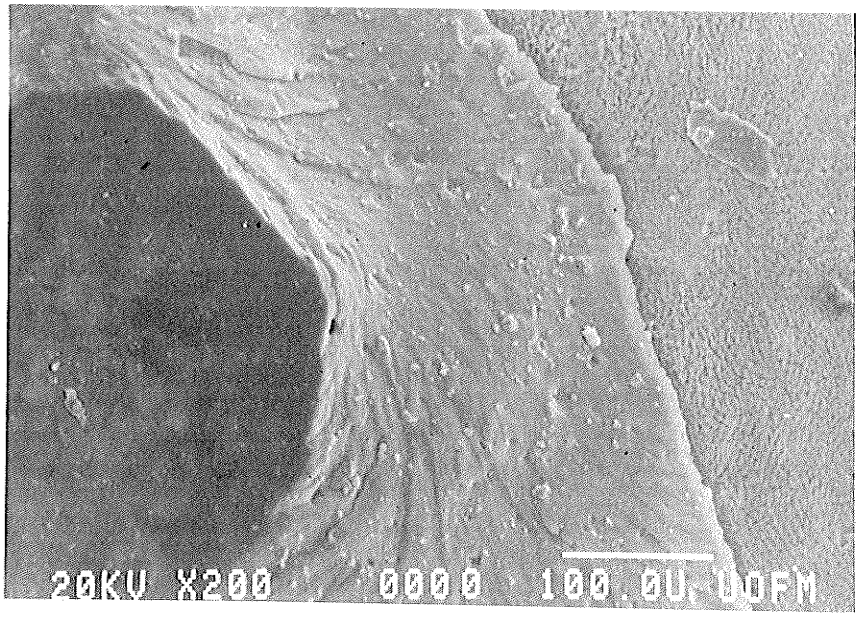

Figure 34 : SEM photograph (500x) demonstrating enamel appearance adjacent to resin wall.

Figure 35 : SEM photograph (15x) of bracket/adhesive debonding site common to Polycrystalline brackets.

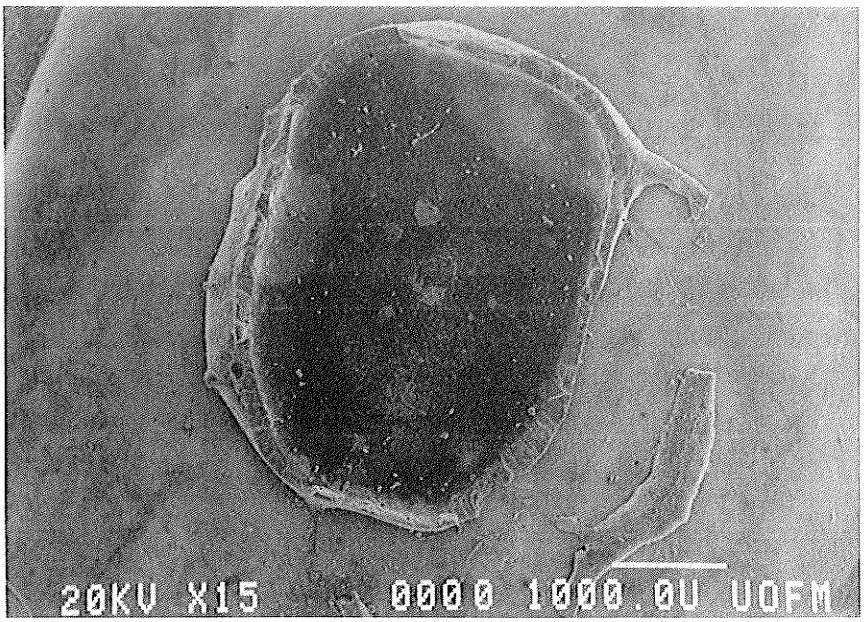

Figure 36 : SEM photograph (500x) of PC bracket debonding surface showing unusual clefting pattern.

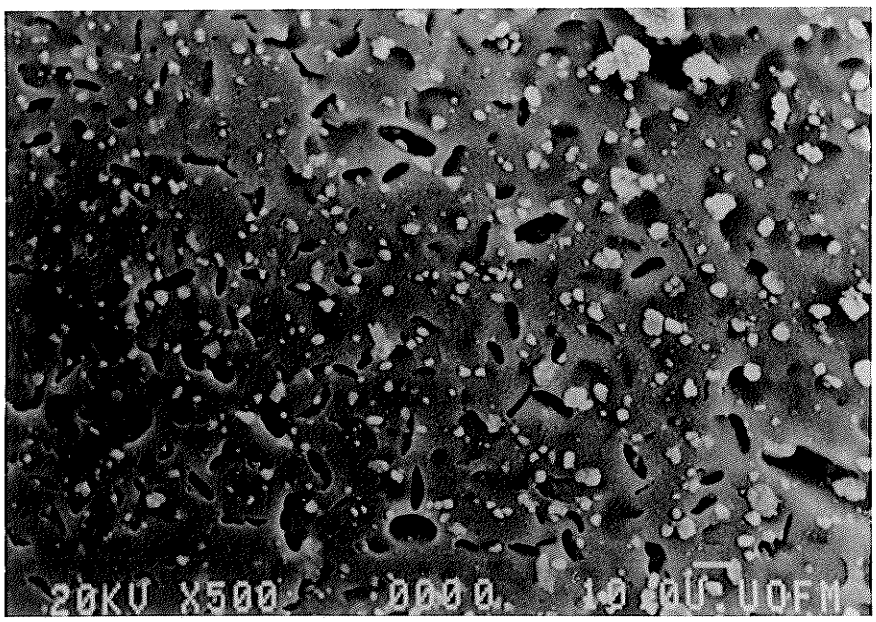

Thermal Damage

Raw data collected in this group of experiments is found in Appendix 4. The results obtained with the PC brackets is summarized in Table 9.

TABLE 9: PC BRACKET : PULPAL AND INTERFACE TEMPERATURES

		248		308		1060	
		Bovine	Human	Bovine	Human	Bovine	Human
1.	Eq. Temp.	27.0	21.8	22.2	22.3	23.3	23.1
2.	Interface T	54.3 ± 3.7	56.9 ± 5.0	72.4 ± 1.2	70.8 ± 3.8	71.5 ± 0.5	70.6 ± 0.4
3.	Increase I.	32.3	35.1	50.2	48.5	48.2	47.6
4.	Pulpal T	30.3 ± 0.9	33.6 ± 1.7	32.7 ± 0.5	41.8 ± 1.3	40.4 ± 0.8	40.4 ± 0.5
5.	Increase P.	8.3	11.8	10.5	19.5	17.1	17.3
6.	Time-Pulp	18s	10s	20.5s	21.5s	instantly	instantly
7.	Time-Exp.	3.2s	3.0s	4.7s	4.9s	20.0s	20.0s
8.	Laser Settings	4 w, 49 Hz 82 mJ\P		4 w, 36 Hz 111 mJ\P		4 w, 17 Hz 235 mJ\P	

All temperatures measured in ° C

To be considered efficacious pulpal heating cannot occur during the debonding procedure. As a result exposure times (line 7) were determined from the debonding experiments performed earlier. The interface temperature rise (line 3) was determined, as was the pulpal temperature rise (line 5). The time to pulpal maximum (line 6) shows a definite temperature lag with 248 and 308 nm irradiation with no delay when the teeth were irradiated at 1060 nm.

Temperature measurements taken at 193 nm irradiation are included in Appendix 4 but will not be considered separately. Interface and pulpal temperature increases for both bracket types are similar or slightly higher than those seen in Table 9.

The results obtained for the S brackets have been summarized in Table 10 below.

TABLE 10: SAPPHIRE BRACKET : PULPAL AND INTERFACE TEMPERATURES

		248		308		1060	
		Bovine	Human	Bovine	Human	Bovine	Human
1.	Eq. Temp.	-	22.5	21.9	21.1	22.8	23.7
2.	Interface T	-	22.8	23.3	23.9	56.7	45
3.	Increase I.	-	0.3	1.4	2.8	33.9	21.3
4.	Pulpal T	-	22.5	21.9	21.4	27.2	26.1
5.	Increase P.	-	0	0	0.3	4.4	2.4
6.	Time-Pulp	-	-	-	12s	instantly	instantly
7.	Time-Exp.	-	1 pulse	1 pulse	2 pulses	1.4s, 17 Hz	1.3s, 17Hz
8.	Laser settings	0.6 w, 120 mJ\p	0.6w, 120 mJ\p	0.15w 150 mJ\p	0.15w 150 mJ\p	3.2w 188 mJ\p	2.7w 158 mJ\p

All temperatures measured in ° C

Difficulties were encountered when attempting to measure temperatures with the Sapphire bonded teeth. No reading could be obtained with the 248 nm bovine sample as the bracket was removed during the alignment. As such, only single shot exposures were used with 248 and 308 nm and the 1060 brackets were irradiated until failure (Line 7). A minimal laser power level was used and is shown in Line 8. The Nd:YAG laser was set at two power levels near threshold. Very low temperature increases could be detected at the pulpal thermocouple. The largest increases were seen with the Nd:YAG laser although exposure times were substantially longer than with the other wavelengths and the frequency was higher at this wavelength. The pulpal thermocouple for the human tooth at 1060 nm was read first because no time delay occurred

between the surface and the pulp.

DISCUSSION

The results obtained in the study validate the use of lasers as a method of debonding 'ceramic' orthodontic brackets. Statistically significant differences exist between the two bracket types and the various wavelength lasers chosen.

Since debonding effectiveness is a result of the quality and the quantity of light which is able to pass through the bracket to act on the adhesive layer, efforts to spectroscopically characterize the brackets and adhesives were undertaken.

The transmission values obtained for the S (8%) and PC (0.3%) brackets using the H-P spectrophotometer were unexpected and well below those reported in the literature[68] for sapphire and those obtained for the sapphire window (89%). The initial impression was that the H-P spectrophotometer was an inappropriate device to investigate bracket transmission. Movement of the brackets closer to the photodetector in order to decrease scatter potential did not affect the observed transmission values. Bracket geometry may result in a large degree of surface reflection and might possibly explain such low transmission values. In an effort to clarify these findings, lasers, rather than a spectrophotometer, were employed to examine the quantity of light transmitted by the brackets. The results show substantially higher transmission percentages (60-85% for sapphire and 9-27% for polycrystalline, Table 1) than were obtained with the spectrophotometer. Some quantitative difference was evident between the He\Ne and Argon laser. Since

only a small central portion of the bracket was irradiated, the possibility of a geometric effect of the bracket on transmission values could have been minimized. In the center of the bracket the bonding surface is approximately parallel to the bracket slot and the bracket is much thinner. A large amount of scattering and refraction of the incident beam by the grain boundaries could also contribute to the low PC bracket transmission values. X-Ray SEM analysis of the fracture surfaces of each bracket type (Figs. 29,30) demonstrate the polycrystalline and monocrystalline nature of the PC and S brackets. A definitive conclusion regarding the % transmission of either PC or S brackets cannot be made with the data obtained. Further study of the transmission characteristics of the various bracket types is warranted.

The presence of a 30 um 'amorphous' layer on the PC bonding surface seems to correlate well with the transmission spectra obtained for the PC brackets. Sodium, potassium, and aluminum found in this layer (Fig 31), and a comparison of the transmission spectra of the bracket to a quartz window (Fig 23), suggest that the amorphous material is not quartz but is likely a glass substance. Reports in the literature seem to confirm this conclusion.[121] The presence of this glass layer may explain the gradual drop in PC bracket transmission starting at about 350 nm (Fig 20).

The transmission spectra of the PC and S brackets both show similar accessory absorption peaks. These peaks do not correspond

to those of a commonly used silanizing agent (Fig 24). They could represent an alternative silanizing agent to promote bonding or the presence of a non-functional organic silane. These non-functional agents are commonly used to modify bond strengths by occupying the hydroxide groups on the Alumina surface.[23]

The difference between the transmission characteristics of the PC and S brackets is demonstrated in the Debonding portion of the experiment. At all wavelengths tested, the S brackets transmitted light more effectively and were removed significantly ($p<.001$) faster than the PC brackets. Sapphire bracket removal was virtually instantaneous at 248, 308 and 1060 nm while taking between 3 to 23 sec with the PC brackets.

Thermal softening or photodegradation is very dependant on the absorption coefficient of the adhesive. Closer examination of the results obtained for the PC brackets illustrates the influence of adhesive absorption on debonding effectiveness. Debonding times for the 248, 308 and 1060 nm laser are 3.1, 4.8 and 23.0 seconds respectively. All mean times are significantly different from each one another ($p<.001$). The low times obtained with 248\308 correlate well with the high absorption displayed by the adhesive spectra in the UV range (Fig 16). The relatively low absorption at 1060 nm corresponds with a long debonding time. It is interesting to note that while the PC brackets pass more light energy to the interface at 1060 nm (Fig 20), debonding times are still substantially longer than at 248 or 308 nm. It seems the adhesive absorption of various wavelengths is more

critical for debonding effectiveness. The strongly absorbed UV wavelengths are much more energetic than IR radiation and they promote electron excitation which results in bond scission. The near-infrared radiation at 1060 nm primarily increases the vibrational energies of the molecules which is subsequently converted to heat energy and thermal softening of the adhesive. The absorption coefficient of the adhesives is important to determine what wavelengths will be absorbed most strongly. A low coefficient of absorption means that less energy will be available for heating or bond scission of the absorbing molecule.

The site of absorption and fate of the photons is very important. After absorption of a photon, a molecule exists in an excited state. Because it is not in thermal equilibrium with its surroundings, it will generally have only a short lifetime, since a number of processes can contribute to the return of the excited molecule to the equilibrium state. These processes are summarized by Guillet[122];

Table 11.

Modes of energy dissipation for electronically excited molecules.

Photophysical processes:	Conversion to thermal energy Conversion between states Energy transfer Radiative dissipation
Photochemical processes:	Free radical formation Cyclization Intramolecular rearrangement Elimination

Light absorbing molecules, called chromophores, can form free

radicals which may react within the polymer to yield new products. Such a molecule, if strategically placed within a polymer could be used to degrade the polymer upon exposure to light. Although the absorption coefficient of the adhesive is similar at 248 and 308 nm, brackets were removed significantly faster at 248 nm than at 308 nm. It is possible that molecules absorbing at 248 nm were better able to convert energy into thermal or photodegradive processes, which would decrease the strength of the adhesive. A greater number of molecules are affected by 248 nm irradiation[123] and as such this wavelength could be more effective at causing degradive processes which allow the bracket to be debonded quicker than at 308 nm. By the equation $E=h\nu$, photons of 248 nm are also much more energetic than those at 308 nm.

The results obtained while debonding the sapphire brackets were quite unexpected. During the pilot studies, S brackets took on average 3.7 seconds to be removed with a shear force applied. In this experiment however, the brackets were removed rapidly, within timing error, even without the applied shear force. With the samples tested at 248 nm the frequency of the laser was reduced until it became evident that bracket removal was possible with a single pulse of the laser. While all other sapphire brackets were removed rapidly, only one was tested with a single pulse irradiation.

Closer examination of the 1060 nm results indicated that rapid debonding may be an energy threshold dependent phenomenon.

During the pilot study the laser was operating at 400Hz, 10 ns, 8.4 w for a pulse energy of 21 millijoules. In the experiment the pulse energies were never below 75 millijoules, at 248 nm. Note that at 1060 nm as the laser power was reduced from 3.2 w to 2.7 w the time for sapphire bracket removal jumped from 1 sec to 7.0 sec. When the power was further decreased to 2.5 w, both #11 and #12 brackets (either with or without the applied shear force) (Table 8) were not removed after more than a 1 minute exposure. At 2.7 w the bracket could be removed rapidly with a shear force applied, while 8 sec was needed to remove the bracket without any applied shear force. These results seem to suggest that a 'threshold' exists. Above the threshold, brackets are removed rapidly, while below the threshold a different process is taking place resulting in much longer debonding times. For example, a 10% power increase from 2.5 to 2.7 watts was accompanied by a very large drop in debonding times from 1 min to either 0.5 sec with shear force applied or 8 sec without shear the force. Such a finding does not seem to agree with a hypothesis that laser debonding of sapphire brackets is primarily a thermal process. The decreasing mechanical properties (strength) of a polymer are well correlated to the temperature increase[124]. Adhesive temperature and strength are well correlated. A 10% increase in laser power should be correlated with an approximate 10% decrease in the debonding time. However, a dramatic change in debonding times occurred after a ten percent power increase. If the process was indeed thermal, one might expect a more linear relationship.

The existence of an ablative threshold of the adhesive may possibly explain the observed results. As the laser energy was applied, those brackets without the applied shear force spontaneously blew forward away from the tooth. A high degree of molecular excitation results when energy levels above a certain value are combined with a high substrate absorption. The rate of molecular and atomic excitation due to stimulated energy transitions is proportional to the light intensity. As such, very high rates of energy deposition into an atom or molecule, which greatly exceeds the rate of thermal relaxation, are possible. This rapid absorption of photons will allow atoms or molecules to reach their dissociation energies before heat can be generated.[125] This non-thermal process is called ablation and results in the release of small molecular or elemental fragments as a gas from material. Excess energy is converted into kinetic energy as the fragments are blown off the surface at ultrasonic speeds. During bracket debonding, the gas generated at the bracket-adhesive interface cannot escape and it is possible that pressures high enough to explosively debond the brackets from the surface of the tooth are generated at the B\A interface. As photoablation occurs as soon as the light strikes the surface, debonding times could be very short.

Below the threshold value, absorbed energy is not sufficient to achieve dissociation and the energy is converted into heat. This heat build up causes the temperature of the interface to rise until the adhesive eventually becomes soft enough to

facilitate debonding by the applied shear load. This thermal softening mechanism appears to be responsible for debonding of the PC brackets. The reduced transmittance of the PC brackets decreases the quantity of the light reaching the B\A interface. This results in sub-threshold energy values for photoablation and increased debonding times that are consistent with a thermal mechanism for debonding.

At 1060 nm irradiation a threshold of 158 millijoules (at 2.7 watts) was determined for the S brackets. This value is higher than the lowest pulse energies of 75 and 100 millijoules used at 248 or 308 nm, respectively. Threshold values were not found for either 248 or 308 nm because the frequency and not pulse energy was used to alter laser power output. The thresholds must be lower than the lowest pulse energies used in the experiment because all brackets at 248 and 308 nm were easily removed. This evidence supports the PC data which also shows that UV wavelengths are more effective than 1060 nm for debonding of brackets. In spite of a low absorption coefficient of the polymer at 1060 nm, sufficiently high deposition of energy will still result in molecular dissociation. According to Letokhov[125], it is possible to induce enough vibrational energy with IR radiation to dissociate an atom or molecule before heat develops. Note, that the 158 millijoules threshold pulse from the Q-switched Nd:YAG laser is delivered over a 9 nanosecond ($9x10^{-9}$ s.) time period. This corresponds to a very high 'peak' power output of $1.75x10^{7}$ watts (joules per second). It is evident that

a great deal of energy is rapidly delivered to the bracket-adhesive interface and could result in molecular dissociation without heat generation. The forgoing does not mean however, that these wavelengths are most effective for debonding.

The spectra obtained for Dynabond with the Carey 14 and Hitachi spectrophotometers (Figs 18,19) showed very low levels of absorption at 1060 nm. These films were tested with the addition of a silane agent to rule out any possible combined effect after the silane reacted with the adhesive. Since the central hot spot with 1060 nm was smaller than that used with 308 and 248, a large amount of energy would be concentrated in a smaller area and would effectively increase the energy density.

Debonding was also attempted using 193 nm irradiation. Although the bracket spectra infer this wavelength will not be transmitted efficiently, debonding was attempted in an effort to correlate debonding times with reduced transmittance. Unfortunately, physical problems with the laser set up reduced the power to only a 1 watt non-focussed beam at the bracket. In addition, pulse energy was only 8 millijoules compared to the 21 millijoules used in the pilots. Surprisingly the PC brackets were removed in an average time of 35 seconds. In contrast the sapphire brackets did not debond. Light energy trapped and absorbed at the grain boundaries could explain why the PC brackets were more efficient at converting the 193 nm irradiation into heat. The sapphire brackets could have reflected a large portion of the beam.

Temperature Measurements

Thermocouple results correlate well with the premise that debonding with PC brackets (Table 9) is primarily a thermal process whereas debonding with sapphire brackets (Table 10) occurs by ablation. Interface temperatures obtained with the PC brackets rose between 32.3-50.2°C with all wavelengths tested. Depending on the response time of the thermocouple and digital thermometer, and how well the thermocouple was coupled to the adhesive, the actual adhesive temperature at the B\A interface could have been much greater than recorded. Thermal softening of similar polymer adhesive occurs at temperatures of approximately 100°C[126] At such temperatures only a light applied shear load is required to cause bond failure. A separate study would be necessary to determine the softening temperatures of orthodontic bonding adhesives.

Interface temperature rise was recorded after varying times of exposures (3.0, 4.7 and 20 seconds), and all power levels were 4 watts (Table 9). A 60 % increase in exposure time between 248 and 308 nm irradiation resulted in a 50 % increase in interface temperature, whereas a 400 % increase in time between 308 and 1060 nm, resulted in no increase in the interface temperature. These results are important because they further demonstrate the variation in absorption coefficients of the adhesives in the UV and IR spectrums. The strong UV absorption by the polymer compared to the weak absorption at 1060 nm results in less time being required to obtain adequate thermal softening of

the interface adhesive in the UV range than in for 1060 nm. Thus 248 and 308 nm appear to be much more effective wavelengths to use for debonding than either 1060 or 193 nm irradiation.

It is impossible, to determine from the results of this study whether heating occurs in the bracket or at the bracket-adhesive interface. Since the interface thermocouple measurements started to drop immediately upon laser shut off, the heat generation must be occurring at or very close to the interface. If heating occurred within the bracket there should have been either a slight increase in the thermocouple reading or if steady state conditions had been reached, a slight delay before the reading fell after the laser was shut off. A separate study is required to determine the location of the thermal effects.

The interface temperatures at 248 nm are somewhat lower than those at 308 and 1060 nm (Table 9). A short exposure time of 3.1 seconds at 248 nm results in lower interface temperatures, however, this time represents the average time for bracket removal in the debonding portion of the experiment. The decrease in bond strengths resulting in bond failure could thus be a combination of ablation, photodegradation and thermal effects occurring at 248 nm.

For all the PC brackets tested, the temperature rise at the pulpal wall substantially exceeds the maximum safe rise set by Zach and Cohen.[106] For the exposure parameters used in our study, laser debonding of PC brackets would result in pulpal damage. However, the results also suggest that increased laser power

delivered in a shorter time and with increased pulse energy, would provide for removal of more PC brackets in a shorter time and with a lower temperature rise.

The thermal results with the S brackets were more difficult to obtain as the brackets had a tendency to debond after just one laser pulse exposure. If the premise regarding an ablation threshold is correct, a large amount of the laser pulse energy will go into the non-thermal photoablation process. Although some areas of the bracket adhesive complex will be exposed to sub-threshold levels and result in heat generation, the overall time of exposure is extremely low and little time is allowed for heat to build up. The maximum temperature increase of 4.4 °C obtained with 1060 nm irradiation is below the 5.6°C damage threshold established by Zach and Cohen. With the laser parameters used in this study it appears that the removal of sapphire brackets is safe and non-injurious to the pulp.

The pilot study for the thermocouple experiments (Appendix 3) demonstrated a time delay between the maximum interface temperature and the maximum pulpal temperature readings. This delay could be attributed to the slow movement of the heat front from the surface of the irradiated tooth through the enamel and dentin to the pulpal cavity. Enamel and dentin possess good insulating properties and poor thermal diffusivity.[127] Similar time delays were seen in this experiment with both 248 and 308 nm laser (Tables 9,10). Irradiation with Nd:YAG did not however, result is such time delays. The maximum pulp temperatures were

seen immediately after switching the digital thermometer from B\A interface thermocouple to the pulpal thermocouple. Higher values were obtained when the pulpal thermocouple was read first. These findings were evident despite the laser exposure time of only 20 s. with the PC brackets and approximately 1 s. with the S brackets. The literature has suggested that enamel absorption of 1060nm irradiation was quite poor. Boehm[104] suggests that up to 40 % of the incident radiation may be reflected. Lunauy[115] compared the pulpal heating of various wavelength lasers and found an increased possibility of damage with 1060 nm compared to other wavelengths. The results obtained here confirm that 1060 nm is not absorbed by the tooth but is transmitted through the tooth to the pulpal thermocouple.

Enamel and Bracket Damage

One of the purposes of exploring laser debonding of ceramic orthodontic brackets was to find a way to provide safe removal of the orthodontic bracket without enamel damage. Examination of all debonded samples using a Zeiss binocular microscope at magnifications up to 40x, revealed no apparent bracket or enamel damage. Virtually all PC brackets tested demonstrated a clean fracture surface at the B\A interface (Fig. 32). These findings support the premise that thermal debonding is the primary process occurring with the PC brackets and that softening proceeds most rapidly at the B\A interface and not within the adhesive. Light energy transmitted through the bracket would interact with the adhesive at the B\A interface increasing the temperature until

enough softening had occurred to allow the applied shear force to debond the bracket from the adhesive. The smooth clefting pattern seen on the PC debonded surface, Fig. 36, seems to suggest the resin was softened to the point where small gas bubbles were able to form. The remainder of the adhesive was left on the tooth.

While no enamel damage could be seen during the debonding of sapphire brackets, the site of fracture determination is more complex (Fig. 32). At 248 nm approximately eight brackets were removed completely at the B\A interface. The remainder of these and all those debonded at 308 and 1060 nm displayed a combination type of fracture with at least some incidence of intra-adhesive (I\A) or enamel-adhesive (E\A) failure (Fig. 33). Examination of the fracture site suggests that bracket removal was a very energetic process. Due to the partial reflection\refraction of light energy caused by bracket geometry or by variations in sample alignment or beam qualities, ablation during debonding of the S brackets might not occur over the entire B\A interface. The portion of the B\A interface that reaches the ablative threshold will decompose to yield gaseous products. If sufficient gas pressure is generated to exceed the adhesive strength of the non-affected areas, debonding would initially occur along the B\A interface. However, as debonding progressed, it would follow the path of least resistance and the site of debonding could change to I\A or E\A. Some potential for enamel damage may exist with such an energetic and uncontrolled process. However, SEM analysis at magnifications up to 1000x (Fig. 34) did not reveal any

apparent enamel damage. The enamel surface where the bracket and adhesive had been removed appeared similar to etched enamel that had retained a thin layer of resin on it. It is possible that the resin is less able to withstand the impact loading with such a rapid process and thus the resin tags penetrating the enamel surface were left behind. Use of SEM with X-ray element analysis to determine whether any enamel came off with the bracket, might prove to be a more sensitive method to evaluate enamel damage. The lowest amount of enamel exposure was found at 248nm which could indicate that at this wavelength the ablative process is more generalized over the interface area. This energy level might provide for better control of bracket removal.

Sources of Error

While the results obtained in these experiments were statistically very significant, all the procedures performed have some degree of error. The debonding studies will be affected by;

1. laser power drift
2. inaccuracies of laser power metering
3. pulse size and quality variations namely, the Gausian distribution of the 248\308 pulse, the hot spot of the 1060 nm beam and sample alignment difficulties.
4. Timing error showed that a minimum of 0.31s response needs to be factored into all timing measurements.

Error in the thermocouple portion of the study can be found in determining power readings especially when only one pulse is

used, with the sapphire brackets, because response time of the meter will affect the ultimate power measured. Direct heating of the thermocouples may have occurred. The junction of the thermocouples used have a finite length, approximately 0.25 mm. Temperatures measured will be underestimated because the measurement will be an average taken over the whole length of the thermocouple junction. If laser debonding is indeed an interface phenomenon an infinitely thin thermocouple would be required to give accurate temperature measurement. A thermocouple response time of 0.1 seconds will not be fast enough to measure the peak temperatures that occur within a single pulse. Although more sophisticated devices should be used to determine the location of the thermal heating, the devices used in this experiment are similar to those used to set pulpal damage standards and appear to be satisfactory for determining the approximate temperatures that might be generated with laser debonding. A more controlled study of laser induced pulp damage would have to include a histologic analysis of pulpal tissue. A thermometer with graphic display or memory capability might aid in eliminating the influence of human response time in temperature measurements. Sophisticated electronic storage thermometers are available that will instantaneously store the thermocouple signal.

CONCLUSIONS

Laser debonding of ceramic orthodontic brackets has been successfully achieved in this study.

1. Sapphire brackets can be debonded much easier than polycrystalline brackets as they allow greater light energy transmittance to the bracket-adhesive interface.
2. Ultraviolet wavelengths are more effective for bracket removal than 1060 nm irradiation with 248 nm being more effective than 308 nm. This finding can be correlated to the absorption spectra of the adhesive.
3. No enamel or bracket damage was observed as little or no force is needed to debond the brackets.
4. The pulpal temperature increase when debonding the sapphire brackets was within biologically established limits but too great when debonding the PC brackets.
5. Laser debonding appears to be a thermal process at low pulse energy levels and an ablative process with increased pulse energy levels. As the ablative threshold is exceeded debonding can occur during a single pulse and with a negligible temperature rise.
6. Laser debonding of the PC brackets is primarily a thermal process whereas removal of the sapphire brackets is primarily an ablative process.

Future Research

The IR spectra of the adhesives all demonstrate strong absorption at a wavenumber of 3400. This corresponds to the output of the recently introduced Er:YAG laser which operates at a wavelength of 2.94 um. Debonding with this laser should result in strong absorption by the adhesive and facilitate ablation with a low laser power. The Er:YAG laser has an advantage over the excimer laser in that it is a relatively maintenance free laser and its light is easily transmitted fibreoptically.

Debonding of the PC brackets appears to be primarily a thermal process and not a biologically efficacious one within the parameters used in the study. If the laser pulse power is increased, shorter removal times and lower temperature rises will result. A study should be performed to evaluate this effect. In addition to this experiment the applied shear force could be altered to investigate its effect on debonding times while maintaining a constant laser power. Correlation between laser power, debonding times and shear force will facilitate the establishment of safety thresholds for enamel and pulpal damage.

The ablation thresholds for the sapphire brackets at 248 and 308 nm and for the various polycrystalline brackets available should be determined.

In conjunction with polymer scientists a 'degradable' adhesive which would have target chromophores in its carbon back-bone could be developed (Figure 37). At a specific energy and frequency of irradiation, the polymer would simply

depolymerize, possibly without ablation. If such a polymer could be manufactured to depolymerize at a wavelength which would normally pass right through a regular adhesive, it could be used in a sandwich technique as shown in Figure 38.

Figure 37

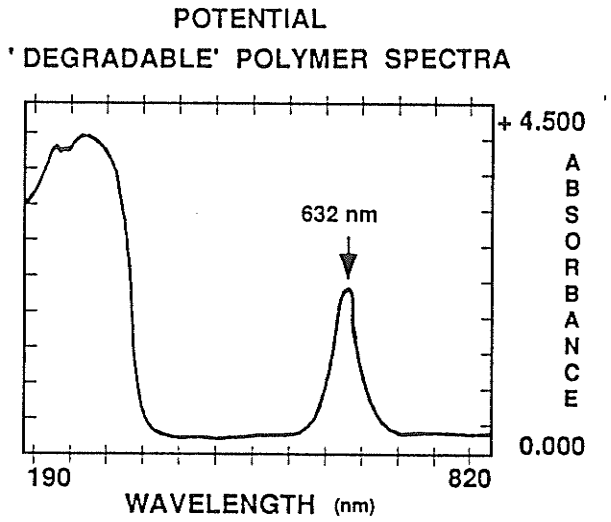

Figure 38

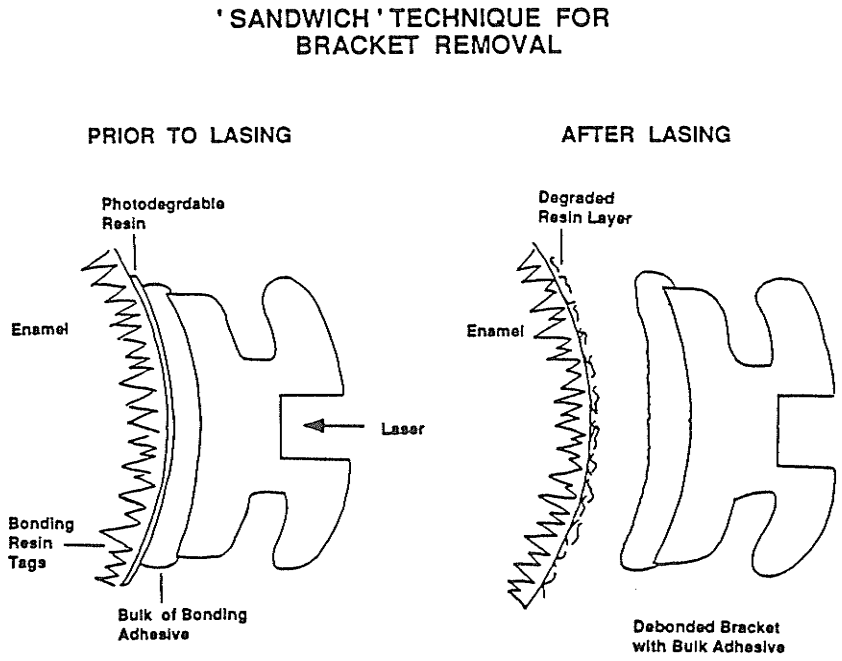

Laser debonding would include both bracket removal and removal of the bulk of the adhesive. Enamel clean up would be virtually eliminated and none of the damaging mechanical techniques currently used would be needed to remove any residual adhesive. Such a process would eliminate time consumed in current debonding and clean-up. This approach might be applied to other facets of dentistry, such as the removal of porcelain veneers or porcelain crowns. Open margins could be sealed shut and yet the crown could still be removed at a later date.

A specifically designed polymer would facilitate the use of a low cost, low power and user friendly laser operating at wavelengths that would maximize the light transmission through the prosthesis. The UV lasers utilized in this study, while apparently effective, are very large and expensive to operate. It is well documented that Ultraviolet laser radiation possesses both cytotoxic and mutagenic potential.[128] Other than the He/Ne laser, the diode lasers present possibilities for use in debonding of ceramic brackets. They operate in the visible to near infrared range of the electromagnetic spectrum, can be pulsed to give high pulse energies, can be fibreoptically transmitted, are relatively maintenance free, are easy to operate and are relatively inexpensive. There is great potential in combining this group of lasers with a specifically developed 'photodegradable' adhesive.

The laser debonding technique if developed, would allow for improved bond strength of brackets which would in turn facilitate

miniaturization. It would allow sufficiently high bond strengths to bond ceramic tubes to the molars and yet still provide for their easy removal and reorientation. This technique will ensure that ceramic brackets become an important part of orthodontic practice.

BIBLIOGRAPHY

1. Newman G. Epoxy adhesives for orthodontic attachments: progress report. Am J Orthod 1965; 51:902-12.

2. Retief D, Dreyer C, Gavron G. The direct bonding of orthodontic attachments to teeth by means of an epoxy resin adhesive. Am J Orthod 1970; 21-40.

3. Miura F, Nakagawa K, Masuhara E. New direct bonding system for plastic brackets. Am J Orthod 1971; 59:350-61.

4. Mizrahi E, Smith D. Direct attachment of orthodontic brackets to dental enamel. Br Dent J 1971; 130:392-6.

5. Reynolds I, vonFraunhofer J. Direct bonding of orthodontic attachments to teeth: the relation of adhesive bond strength to gauge mesh size. Br J Orthod 1976; 3:91-5.

6. Rogers O, Griffith J. Direct bonding of orthodontic brackets to tooth structure. Aust Dent J 1977; 22:236-7.

7. Faust J, Grego G, Fan P, Powers J. Penetration coefficient, tensile strength and bond strength of thirteen direct bonding orthodontic cements. Am J Orthod 1978; 73:512-25.

8. Moin K, Dogon I. An evaluation of shear strength measurements of unfilled and filled resin combinations. Am J Orthod 1978; 74:631-6.

9. Keizer S, Ten Cate J, Arends J. Direct bonding of orthodontic brackets. Am J Orthod 1976; 69:318-27.

10. Lopez J. Retentive shear strengths of various bonding attachment bases. Am J Orthod 1980; 77:669-78.

11. Thanos C, Munholland T, Caputo A. Adhesion of mesh-base direct-bonding brackets. Am J Orthod 1979; 75:421-30.

12. Wickwire N, Rentz D. Enamel pretreatment: a critical variable in direct bonding systems. Am J Orthod 1973; 64:499-512.

13. Maijer R, Smith D. Variables influencing the bond strength of metal orthodontic bracket bases. Am J Orthod 1981; 79:20-34.

14. Dickinson P, Powers J. Evaluation of fourteen direct-bonding orthodontic bases. Am J Orthod 1980; 78:630-39.

15. Alexandre P, Toung J, Sandrik J, Bowman D. Bond strength of three adhesives. Am J Orthod 1981; 79:653-660.

16. Evans L, Powers J. Factors affecting in vitro bond strength of no-mix orthodontic cements. Am J Orthod 1985; 87:508-512.

17. Soetopo B, Hardwick J. Mechanisms of adhesion of polymers to acid-etched enamel. J Oral Rehabil 1978; 5:69-80.

18. Prevost A, Fuller J, Peterson L. The use of an intermediate resin in the acid-etch procedure: retentive strength, microleakage, and failure mode analysis. J Dent Res 1982; 61:412-8.

19. Buonocore M, The Use of Adhesives in Dentistry. Charles Thomas, Springfield, Illonois. 1975 pg.95.

20. Jassem H, Retief D, Jamison H. Tensile and shear strengths of bonded and rebonded orthodontic attachments. Am J Orthod 1981; 79:6611-8.

21. Barkmeier W, Gwinnett J, Schaffer S. Effects of enamel etching time on bond strength and morphology. J Clin Orthod 1985; 19:36-8.

22. Reynolds I. A review of direct orthodontic bonding. Br J Orthod 1975; 2:171-8.

23. Horn S. European patent publication # 0 296 384. Dec 28, 1988. Bulletin 88\52.

24. Yamada T, Smith D, Maijer R. Tensile and shear bond strengths of orthodontic direct-bonding adhesives. Dent Mat 1988; 4:243-50.

25. Combe E. Notes on Dental Materials, 5th ed. Churchill Livingston. New York. 1986.

26. Diedrich P. Enamel alterations from bracket bonding and debonding: a study with the scanning electron microscope. Am J Orthod 1981; 79:500-522.

27. Bennett C, Schoen F, Going R. Alterations of the enamel surface following direct-bonded bracket therapy. J Pedod 1979; 3:99-113.

28. Sandison R. Tooth surface appearance after debonding. Br J Orthod 1981; 8:199-201.

29. Silverstone L. Fissure sealants, the susceptibility to dissolution of acid etched and subsequently abraded enamel in vitro. Caries Res 1977; 11:46-51.

30. Maijer R, Smith D. Corrosion of orthodontic bracket bases. Am J Orthod 1982; 81:43-48.

31. Gwinnett A. Corrosion of resin-bonded orthodontic brackets. Am J Orthod 1982; 82:441-446.

32. Gwinnett A, Ceen R. Plaque distribution on bonded orthodontic brackets: A scanning microscope study. Am J Orthod 1979; 75:667-677.

33. Gwinnett A, Gorelick L. Microscopic evaluation of enamel after debonding: clinical application. Am J Orthod 1977; 71:651-665.

34. Lehman R, Davidson D. Loss of surface enamel after acid etching procedures and its relation to fluoride content. Am J Orthod 1981; 80:73-82.

35. Council on dental materials, instruments and equipment: State of the art and science of bonding in orthodontic treatment. J Am Dent Assoc. 1982; 105:944-850.

36. Knoll M, Gwinnett A, Wolf M. Shear strengths of brackets bonded to anterior and posterior teeth. Am J Orthod 1986; 89:476-479.

37. Slomka L, Powers J. In vitro bond strength of treated direct-bonding metal bases. Am J Orthod 1985; 88:133-6.

38. Hanson G, Gibbon W, Shimizu H. Bonding bases coated with porous metal powder: a comparison with foil mesh. Am J Orthod 1983; 83:1-4.

39. Smith D, Maijer R. Improvements in bracket design. Am J Orthod 1980; 78:630-9.

40. Sheridan J, Brawley G, Hastings J. Electrothermal debonding. Part I. An in vitro study. Am J Orthod 1986; 89:21-27.

41. Sheridan J, Brawley G, Hastings J. Electrothermal debonding. Part II. An in vivo study. Am J Orthod 1986;89:141-5.

42. Newman G. Bonding plastic orthodontic attachments to tooth enamel. J New Jersey Dent Soc. 1964; 35:346-357.

43. Reynolds I, von Fraunhofer J. Direct bonding in orthodontics: A comparison of attachments. Br J Orthod 1977; 4:65-69.

44. Aird J, Durning P. Fracture of polycarbonate edgewise brackets: A clinical and SEM study. Br J Orthod 1987; 14:191-5.

45. Brandt S, Servoss J, Wolfson J. Practical methods of debonding, direct and indirect. J Clin Orthod 1975; 9:610-36.

46. Maijer R. Bonding systems in orthodontics. In : Smith D, Williams D. Biocompatibility of Dental Materials, vol II. Boca Raton, Florida: CRC Press 1982:51-76.

47. Swartz M. Ceramic brackets. J Clin Orthod 1988: 22:82-88.

48. Scott G. Fracture toughness and surface cracks - The key to understanding ceramic brackets. Angle Orthod. 1988; 1:5-8.

49. Honeycombe R. The Plastic Deformation Of Metals, 2nd ed. Edward Arnold, London, 1984.

50. Douglass J. Enamel wear caused by ceramic brackets. Am J Orthod Dentfac Orthop. 1989; 95:96-98.

51. Viazis A, Delong R, Bevis R, Douglas W, Speidel M. Enamel surface abrasion from ceramic orthodontic brackets: A special case report. Am J Orthod Dentofac Orthop 1989; 96:514-18.

52. Newesely H, Rossiwall B. Schmelzabrasionen und schmelzausrisse bei keramikbrackets. Informationen 1989; 4:577-594.

53. Kusy R. Morphology of polycrystalline alumina brackets and its relationship to fracture toughness and strength. Angle Orthod 1988; July:197-203.

54. Ferguson J, Read M, Watts D. Bond strength of an integral bracket-base combination: an In vitro study. Eur J Orthod 1984; 6:267-76.

55. Buzzitta , Hallgren S, Powers J. Bond strength of orthodontic direct-bonding cement-bracket systems as studied in vitro. Am J Orthod 1982; 81:87-92.

56. Odegaard J, Segner D. Shear bond strength of metal brackets compared with a new ceramic bracket. Am J Orthod Dentofac Orthop. 1988; 94:201-206.

57. Iwamoto H, Kawamoto T, Kinoshita Z. Bond strength of new ceramic brackets as studied in vitro (Abstract) J Dent Res 1987; 66:928.

58. Bowen R. Synthesis of a silica-resin direct filling material - progress report. J Dent Res 1958; 37:90.

59. Tyas M, Alexander S, Beech D, Brockhurst P, Cook W.Bonding-retrospect and prospect. Aust Dent J 1988; 33:364-74.

60. Roulet J. Degradation of Dental Polymers. Karger, New York, 1987, pg.19.

61. Wood D, Jordan R, Wat D, Galil K. Bonding to porcelain and gold. Am J Orthod 1986; 89:194-204.

62. Smith G, Mc Innes-ledoux P, Ledoux W, Weinberg R. Orthodontic bonding to porcelain - Bond strength and refinishing. Am J Orthod Dentofac Orthop. 1988; 94:245-251.

63. Kao E, Boltz K, Johnston W. Direct bonding of orthodontic brackets to porcelain. Am J Orthod Dentofac Orthop 1988; 94:458-68.

64. Newman S, Dressler K, Grenadier M. Direct bonding or orthodontic brackets to esthetic restorative materials using a silane. Am J Orthod 1984; 88:503-6.

65. Guess M, Watanabe L, Beck M, Crall M. The effect of silane coupling agents on the bond strength of a polycrystalline ceramic bracket. J Clin Orthod 1988; Dec:788-82.

66. Gwinnett J. A comparison of shear bond strengths of metal and ceramic brackets. Am J Orthod Dentofac Orthop. 1988; 93:346-8

67. Joseph V, Rossouw E. The shear bond strengths of stainless steel and ceramic brackets used with chemically and light activated composite resins. Am J Orthod Dentofac Orthop 1990; 97:121-5.

68. Melles Griot. Optics Guide 3. (Product Handbook) Melles Griot. 1985. Library of Congress #: 85-60624.

69. Zakariasen K, Dedrich D, Tulip. Lasers in dentistry. "Star Wars" dreaming or a future reality. CDA J 1988; 54:27-30.

70. Beesley M. Lasers and Their Applications. Taylor and Francis Ltd. London, 1976.

71. Willenborg G. Dental laser Applications: emerging to maturity. Laser Surg Med. 1989; 9:309-13.

72. Goldman L, Gray J, Goldman J, Goldman B, Meyer R. Effect of laser impacts on teeth. J Am Dent Assoc 1965; 70:601-6.

73. Stern R, Sognnaes R. Laser beam effect on dental hard tissue. J Dent Res 1964; 43:873.

74. Stern R, Sognnaes R. Laser inhibition of dental caries suggested by first tests in vivo. J AM Dent Assoc 1972; 85:1070-90.

75. Adrian J, Bernier J, Sprague W. Laser and the dental pulp. J Am Dent Assoc 1971; 83:113-17.

76. Lobene R, Bhussry R, Fine S. Interaction of carbon dioxide laser radiation with enamel and dentin. J Dent Res 1968; 47:311-17.

77. Kantola S. Laser induced effects on tooth structure: VII. X-ray diffraction study on dentin exposed to carbon dioxide laser. Acta Odontol Scand 1973; 31:381-6.

78. Melcer J, Chaumatte M, Melcer F. Treatment of dental decay by CO2 laser beam- preliminary results. Laser Surg Med 1984; 4:311-21.

79. Lenz H, Eichler J. Production of a nasoantral window with argon laser. J Maxillofac Surg 1977; 5:314-8.

80. Myers T, Myers W. The use of a laser for debridement of incipient caries. J Prost Dent 1985; 53:776-9.

81. Myers T. What lasers can do for dentistry and you. Dental Management 1989; April;26-30.

82. Atsumi . Current status and future of laser surgery and medicine in japan. In Lasers In Dentistry. Yamamoto H, Atsumi K, Kusakari H. Excerpta Medica, Amsterdam, 1989.

83. Inaba H. Essentials of laser. In Lasers In Dentistry. Yamamoto H, Atsumi K, Kusakari H. Excerpta Medica, Amsterdam, 1989.

84. Campbell I, Dwek R. Biological Spectroscopy. Benjamin/Cumming publishing Co. Inc., Don Mills Ontario, 1984.

85. Nelson D, Wefel J, Jongebloed W, Featherstone . Morphology, histology and crystallography of human dental enamel treated with pulsed low-energy infrared laser radiation. Caries Res. 1987; 21:411-26.

86. Nelson D, Williamson B. Low temperature laser raman spectroscopy of synthetic apatites and dental enamel. Aust J Chem 1982; 35:715-27.

87. Fowler B, Kuroda S. Changes in heated and in laser-irradiated human tooth enamel and their probable effects on solubility. Calcif Tissue Int 1986: 38:197-208.

88. Stern R, Vahl J, Sognnaes R. Lased enamel: ultrastructural observations of pulsed carbon dioxide laser effects. J Dent Res 1972; 51:455-60.

89. Morioka T, Tagomori S, Nara Y. Application of Nd-Yag laser and fluoride in the prevention of dental caries. In Lasers In Dentistry. Yamamoto H, Atsumi K, Kusakari H. Excerpta Medica, Amsterdam, 1989.

90. Boehm R, Baechl E, Webster J, Janke S. Laser processes in preventive dentistry. Opt Eng 1977; 16:493-6.

91. Corcia J, Moody W. Thermal analysis of human dental enamel. J Dent Res 1974 53;571

92. Srinivasan R, Leigh W. Ablative photodecomposition: action of far-ultraviolet (193 nm) laser radiation on poly (ethylene terephthalate) films.J Am Chem Soc 1982; 104:6784-5.

93. Koort J, Frentzen M. Excimer lasers: basic physics and possible applications in dental surgery. In: Lasers In Dentistry. Yamamoto H, Atsumi K, Kusakari H. Excerpta Medica, Amsterdam, 1989.

94. Frentzen M, Koort J. Caries removal and conditioning of tooth surfaces for adhesive filling techniques by using 193 nm - excimer laser - preliminary results. In: Lasers In Dentistry. Yamamoto H, Atsumi K, Kusakari H. Excerpta Medica, Amsterdam, 1989.

95. Sato K, Kohsaka Y, Fujisaka S, Ochiai S, Yamamoto H. Effects of Excimer laser irradiation on bone. In: Lasers In Dentistry. Yamamoto H, Atsumi K, Kusakari H. Excerpta Medica, Amsterdam, 1989.

96. Yow L, Nelson S, Berns M. Ablation of bone and polymethylmethacrylate by an XeCl (308 nm) excimer laser. Lasers Surg Med 1989; 9:141-7.

97. Nelson J, Yow L, Liaw L, Wright W, Andrews J, Berns M. Ablation of bone and methacrylate by a prototype mid-infrared erbium:YAG laser. Lasers Surg Med 1988; 8: 494-500.

98. Pini R, Salimbeni R, Matteo V, Barone R, Clauser C. Laser dentistry: a new application of excimer laser in root canal therapy. Lasers Surg Med 1989; 9:352-7.

99. Hame H, Ross R, Papaioannou T, Grundfest W, Johnson R. The effect of 308 nm excimer laser on tooth enamel. Laser Institute of America. ICALEO 1988. Proceedings, vol 64:184-91.

100. Kaufmann R, Hibst R. Pulsed Er:YAG and 308 nm UV-excimer laser: an in vitro and in vivo study of skin-ablative effects. Lasers Surg Med 1989; 9:132-40.

101. Hibst R, Keller U. Experimental Studies of the application of the Er:YAG laser on dental hard substances: I.Measurement of the ablation rate. Lasers Surg Med 1989; 9:338-44.

102. Keller U, Hibst R. Experimental studies of the application of the Er:YAG laser on dental hard substances: II. Light microscopic and SEM investigations. Lasers Surg Med 1989; 9:345-51.

103. Paghdiwala A. Application of the Er:YAG laser on hard dental tissues: Measurement of the temperature changes and depths of cut. Laser Institute of America. ICALEO 1988 Proceedings, vol 64:192-201.

104. Boehm R, Chen M, Blair C. Temperatures in human teeth due to laser heating. American Society of Mechanical Engineers publication # 75-WA/BIO-8, 1975.

105. Lisanti V, Zander H. Thermal injury to normal dog teeth: in vivo measurements of pulp temperature increases and their effect on the pulp tissue. J Dent Res 1952; 31:548-558.

106. Zach L, Cohen . Pulp response to externally applied heat. OS,OM & OP. 1965; 19:515-30.

107. Nyborg H, Brannstrom M. Pulp reaction to heat. J Pros Dent 1968; 19:605-19.

108. Cox J, Keall C, Keall H, Ostro E, Bergenholtz G. Biocompatability of surface-sealed dental materials against exposed pulps. JPD 1987; 57:1-8.

109. Spierings T, Peters M, Plasschaert A. Thermal trauma to teeth. Endod Dent Traumatol 1985; 1:123-9.

110. Adrian J. Pulp effects of neodynium laser. A preliminary report. Oral Surg. 1977; 44:301-5.

111. Shoji S, Horiuchi H. Histopathological changes of dental pulp after irradiation by argon, carbon-dioxide or Nd:YAG laser in rats. In: Lasers In Dentistry. Yamamoto H, Atsumi K, Kusakari H. Excerpta Medica, Amsterdam, 1989.

112. Melcer J, Chaumette M, Melcer F. Dental pulp exposed to the CO2 laser beam. Lasers Surg Med 1987; 7:347-52.

113. Melcer J, Chaumatte M, Melcer F, Zeboulon S, etc. Preliminary report on the effect of CO2 laser beam on the dental pulp of Macaca Mulatta primate and the beagle dog. J Endod 1985; 11:1-5.

114. Shoji S, Nakamura M, Horiuchi H. Histopathological changes in dental pulps irradiated by CO2 laser: a preliminary report on laser pulpotomy. J Endod. 1985; 11;379-84.

115. Launay Y, Mordon S, Cornil A, Brunetaud J, Moscheetto Y. Thermal effects of lasers on dental tissues. Lasers Surg Med. 1987; 7: 473-7.

116. Nelburger E, Misererding L. Pulp chamber warming due to CO2 laser exposure. NY State Dent J 1988; 54:25-7.

117. Nakamichi I, Iwaku M, Fusayama T. Bovine teeth as possible substitutes in the adhesion test. J Dent Res 1983; 62:1076-81.

118. Titley K, Torneck C, Smith D, Adibfar A. Adhesion of composite resin to bleached and unbleached bovine enamel. J Dent Res 1988; 67:1523-28.

119. Smith H, Casko J, Leinfelder K, Utley J. Comparison of orthodontic bracket bond stregths: human vs. bovine enamel. J Dent Res 1976; 55:B-153.

120. Lew K, Djeng S. Recycling ceramic brackets. J Clin Orthod 1990; 24:44-7.

121. Driscoll W, Vaughan W. (Editors) Handbook of Optics. McGraw Hill, New York, 1978.

122. Guillet J. Polymer Photophysics and Photochemistry. Cambridge University Press., Cambridge. 1979.

123. Rao C. Ultra-Violet and Visible Spectroscopy. Chemical Applications. Third ed., Butterworth and Co., London 1975.

124. Draughan R. Effects of temperature on mechanical properties of composite dental restorative materials. J Biomedical Mat Res 1981; 15:489-95.

125. Letokhov V. Laser-induced chemistry - basic nonlinear processes and applications. Appl Phys B 1988; 46:237-51.

126. Hayden B, Moffat W, Wulff J. The Structure and Properties of Materials. Vol III. Mechanical Behavior. John Wiley and Sons Inc., New York. 1965.

127. Minesaki Y, Muroya M, Higashi R, Shinohara et al. A method for determining thermal diffusivity of human teeth. Dent Mat J 1983; 2:204-9.

128. Kochevar I. Cytotoxicity and mutagenicity of excimer laser radiation. Laser Surg Med 1989; 9:440-5.

APPENDIX 1

The Nature of Light

Light is usually described as 'the visible part of a large range of electromagnetic radiation having corpuscular as well as wavelike properties'. Electromagnetic radiation can be considered to behave as two wavemotions at right angles to each other. One of these waves is magnetic (M) and the other is electric (E). These waves are generated by oscillating electric and magnetic dipoles and are propagated through a vacuum at $3x10^{10}$ cm/s. The energies associated with E and M are equal, but most optical effects are concerned with the electric wave.

Table 2.2 Electromagnetic radiation and the scales used

Name and (Approx.) Range of Radiation	Energy per Photon (J)	Frequency ν (Hz)	Wavelength λ (m)	Common Units of Length for Comparison
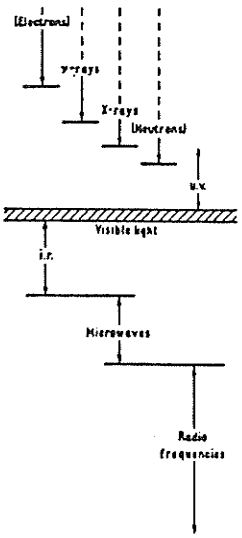	10^{-11}	10^{22}	10^{-13}	
	10^{-12}	10^{21}	10^{-12}	picometer (pm)
	10^{-13}	10^{20}	10^{-11}	
	10^{-14}	10^{19}	10^{-10}	nanometer (nm)
	10^{-15}	10^{18}	10^{-9}	
	10^{-16}	10^{17}	10^{-8}	
	10^{-17}	10^{16}	10^{-7}	micrometer (μm)
	10^{-18}	10^{15}	10^{-6}	
	10^{-19}	10^{14}	10^{-5}	
	10^{-20}	10^{13}	10^{-4}	millimeter (mm)
	10^{-21}	10^{12}	10^{-3}	
	10^{-22}	10^{11}	10^{-2}	
	10^{-23}	10^{10}	10^{-1}	meter (m)
	10^{-24}	10^{9}	1	
	10^{-25}	10^{8}	10^{1}	
	10^{-26}	10^{7}	10^{2}	kilometer (km)
	10^{-27}	10^{6}	10^{3}	
	10^{-28}	10^{5}	10^{4}	
	10^{-29}	10^{4}	10^{5}	
	10^{-30}	10^{3}		

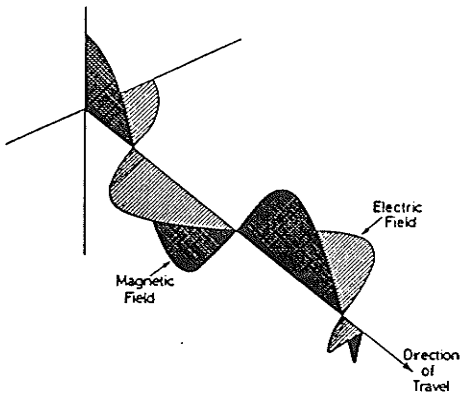

Fig. 2.3 "Snapshot" of electromagnetic wave in space. The wave moves along the "direction of travel" with a velocity of 300,000 km/sec.

Visible light is different from the rest of the electromagnetic radiation in that, only these narrow range of wavelengths and frequencies can be detected by the human eye.

The wavelike nature of the electromagnetic radiation is very much like the ripples on a pond. The frequency (ν) and wavelength (λ) of a wave are related by the equation

$$\nu = c/\lambda$$

where c is the velocity of the propagation of the wave. Frequency can also be converted directly to units of energy using the relationship $E=h\nu$, where h is Plank's constant ($h= 6.64 \times 10^{-34}$ J/s). Units of energy (Joules/mol), frequency (Hz) and wavelength (m) are all used in discussions of electromagnetic radiation. Frequency is often expressed as wavenumber to avoid using very large numbers. Wavenumber (v') is defined as the inverse of the wavelength expressed in centimeters.

The concept that radiation consists of a stream of energy packets, moving in the direction of the beam with the same velocity as that of light was introduced by Max Planck in 1900. According to the Einstein-Planck relation, in any beam of radiation of frequency ν, each photon carries (or is a bundle of) energy E, where $E=h\nu$. According to the equation the energy of a monochromatic radiation depend only on the frequency or wavelength of its waves and not on the intensity of its beam. In other words, a beam of radiation is more or less intense depending on the number of photons per unit time, per unit area but the energy per photon (ie. the quantum energy) is always the same for a definite frequency of radiation. The energy of individual photons can be calculated in any kind of radiation. The shorter the wavelength (greater the frequency) the greater

the energy of the photons and the more powerful the radiation.

Luminescence and Incandescence

Laser light is a synchronized form of the light produced by the process known as luminescence. Luminescence is the process by which certain materials can absorb energy from various sources (UV, X-rays, subatomic particles, electrical discharges and fields, chemical reactions etc) and convert this energy to produce light of a specific 'colour' or wavelength. Familiar examples of luminescence are the light produced by glow worms, fireflies, fish and by lightning. The essential feature of luminescent emission is that the material concerned does not have to be heated. In fact, heating the material usually decreases the efficiency of the light generation and eventually may stop it altogether.

Incandescence is the name given to the process of emission of light from hot bodies. Incandescence is a special form of a more general process known as thermal radiation. All bodies produce some thermal radiation even at room temperature. This radiation is generated, as with all other electromagnetic waves, by the vibration of electrically charged bodies. Heating a material from absolute zero (-273°C) causes atoms and molecules of the material to vibrate and radiate electromagnetic waves. As the temperature is increased, the amplitude and frequency of these vibrations increases; the strength of the thermal radiation increases, and shorter and shorter wavelength electromagnetic waves are produced. If the atoms are excited high enough they

will be able to radiate electromagnetic waves in the visible part of the spectrum. The material is then incandescent. Familiar examples of incandescence include the light from a burning candle, wood, coal or the light from an electric bulb. Both the colour and intensity of the thermal radiation from a material are determined by its temperature.

Light waves, whether emitted by luminescent or incandescent processes are not generated by vibrations of the molecules and atoms themselves, but by changes within the atom. The electrons that circle an atom can only occupy discrete orbits. The energy levels of electrons in orbit around the nucleus of an atom are referred to as quantum states. In any quantum state in a given atom, there is a definite energy level for the electron. The energies associated with these different orbits vary in staged levels and not continuously. In a very hot material, electrons are promoted to outer orbits through interatomic collisions. The atom does not exist very long in this excited state. As the electron reverts back to its original orbit it can give up the energy it acquired as a photon. Luminescent emission takes place without the agitation of the emitting material. In this process, atoms absorb sufficient energy directly from the exciting source to result in an excited state. There is usually very little heat produced. If a suitable material is chosen, the radiated electromagnetic waves will be in the visible spectrum.

In luminescence, the energy of the radiated wave is always less than or equal to the energy of the exciting wave. The

wavelength of the radiated wave is solely determined by the chemical nature of the material. The intensity of the exciting wave does, however, govern the intensity of the radiated wave which also depends on the characteristics of the excitation.

Many lasers are based on synchronized luminescence from atoms. Almost all solid luminescent materials consist of a so called host crystal containing a very small quantity of a substance called the activator. Balman's paint which glows violet when irradiated with ultraviolet rays was the first commercial luminescent material. It is composed of calcium sulphide with about 0.01% of a compound of bismuth. The bright red emission of a ruby is a result of the pure aluminum oxide crystal having 0.05% chromium impurity. Individual activator atoms are suspended in the center of groups of host atoms.

Emission and Absorption

Depending on the amount of absorbed energy, the outer electron of an atom can be promoted from the lowest energy level, or ground state to any of the available higher energy states of the atom. When the atom reradiates the absorbed energy, the electron may jump back in two or more steps via intermediate excited state levels. The wavelength emitted at each jump depends upon the energy lost by the atom at that jump. The light from a glowing gas consists of millions of such processes with emitted radiation over a broad spectrum. Isolate atoms produce vary narrow, but nevertheless finite, emission lines. When the excited atom is part of a gas, it may collide with other atoms and this

causes the emission lines to become broadened.

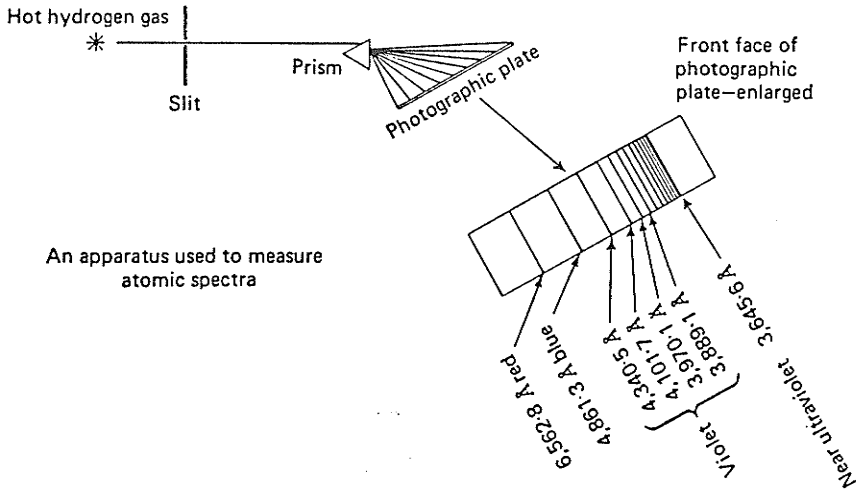

Fig. 1.10. The discontinuous nature of the emission spectrum of the excited atoms in a gas is demonstrated above

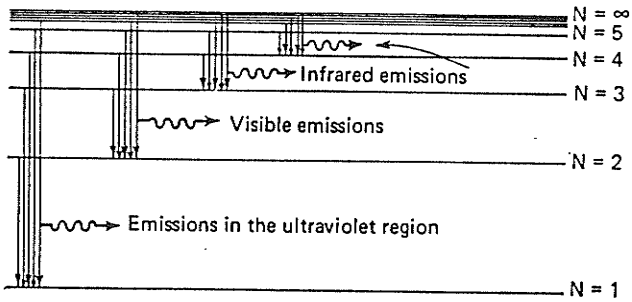

Fig. 1.11. Energy levels of hydrogen, and the wavelengths of the radiation emitted when the electron returns from an excited state to the ground state, or to an excited state of lower energy

In solids, the influence of neighboring atoms is so strong that many of the emission lines are converted into quite wide bands. Some materials like ruby, have relatively wide bands of absorption and yet narrow emission bands. Yellow/green and blue light over a band of wavelengths centered about 550 nm are readily absorbed by the chromium activator atoms in ruby. These

atoms are raised to the excited energy level marked 3 in the following Figure. Some of the absorbed energy is very quickly (10^{-12} sec.) lost and is converted to heat as the atoms drop down to the slightly lower energy level marked 2. This energy level actually consists of two closely spaced levels. Excited atoms remain in this energy level for periods ranging up to five thousands of a second and then fall back to the ground state while emitting an electromagnetic wave. At room temperature, the wavelength of the wave emitted by an atom in the upper of the two closely spaced levels is 693.9 nm while 694.3 nm is emitted from the lower of the levels. A ruby appears red because it removes yellow, blue and green light from white light and emits light in the red part of the visible spectrum.

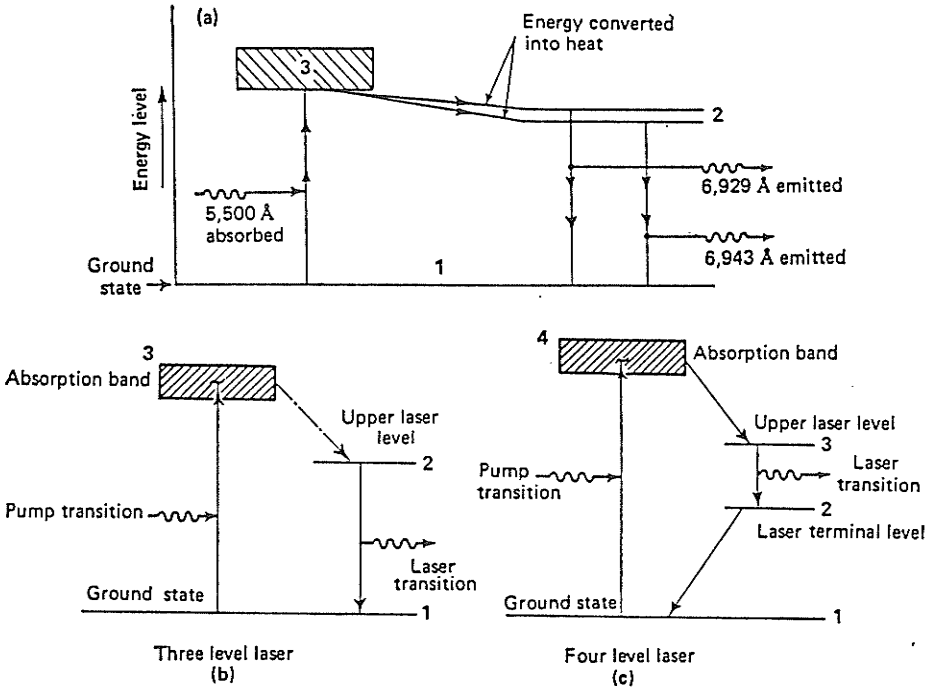

Fig. 1.12(a). Energy level diagram of ruby. Light absorbed over a broad band centred on 5,500 Å is partially converted into heat and then spontaneously radiated on narrow bands centred on 6,929 Å and 6,943 Å. (b) When the ruby is used as the active material in a laser, only one of the pair of excited state levels 2 is used. The excited state atoms do not return to the ground state spontaneously, but instead are stimulated to emit by photons. (c) In a four level system the terminal level for laser transitions is above the ground state. This has certain advantages, which are discussed in Chapter 2

Stimulated Emission

The first reference to stimulated emission of radiation was made by Einstein in 1917. He showed that the interaction of radiation and matter could be explained fully, only if the concept of stimulated emission was introduced.

Up until now it has been assumed that the excited atoms drop back to the ground state spontaneously. Most of them do, but not all. Another mechanism - stimulated emission - causes some of the atoms to return to the ground state. The stimulated emission process starts when an excited atoms drops back to the ground state and emits a photon.

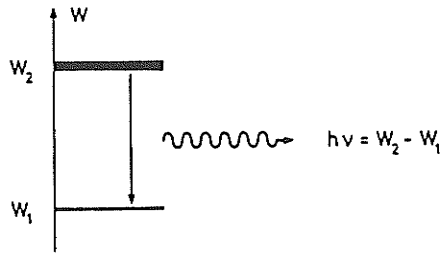

Fig. 2.2. The energy W of a two-level atom with the energy levels W_1 and W_2 of which the upper one is occupied. During the transition from level 2 to level 1 a photon of quantum energy $h\nu = W_2 - W_1$ is emitted.

If this photon strikes a neighboring excited atom it will cause it to fall back to the ground state immediately. What is important in this process of stimulated emission is that the photon emitted by the second atom will have exactly the same phase (timing) as the photon from the first atom. The two exiting photons are synchronized.

When a body is in equilibrium with an incident electromagnetic radiation field, there will always be a

proportion of atoms in the excited state. Energy will be reradiated by excited atoms at the same rate as it is absorbed from the radiation field by ground state atoms. The proportion of stimulated emissions increases with increasing wavelengths such that at 60 um wavelength the rates of spontaneous and stimulated emissions are equal. The higher the proportion of atoms in the excited states, the lower is the proportion in the ground states, and, therefore, the lower is the rate of energy absorption. Stimulated emission rates are proportional to the number of atoms in the excited state. The rate of energy absorbed can therefore, be made less than the rate at which it is emitted if the number of atoms in the excited states is greater than the number in the ground state. An electromagnetic field passing through a material in this state will be amplified.

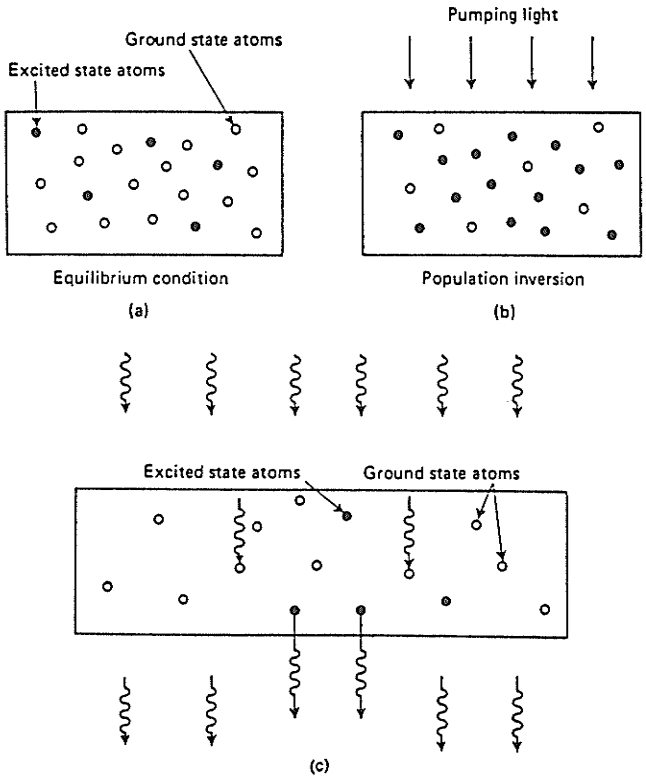

Fig. 2.1

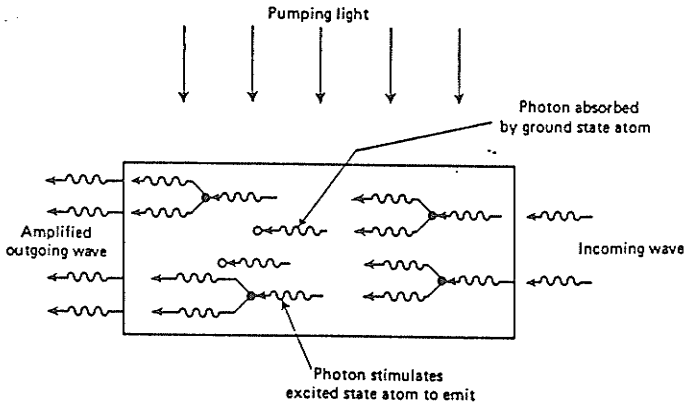

Fig. 2.1(a). Sample in equilibrium. There are many more ground state than excited state atoms. (b) Population inversion. The pumping light is absorbed by the atoms of the material and there are far more excited state than ground state atoms. (c) Sample in equilibrium with the surrounding radiation field. Some photons are absorbed by ground state atoms; but an equal number are emitted spontaneously by excited state atoms. Thus, there is as much radiation leaving the sample as entering it. (d) An electromagnetic wave passing through a sample in which there is a population inversion will be amplified

The condition where more atoms of a material exist in an excited state than in the ground state is termed a 'Population Inversion'. This is one of the fundamental processes of laser operation. The stimulated emissions that go to make up the laser beam must be built up to a high density in one direction. This build up is usually done by placing mirrors at each end of the active material.

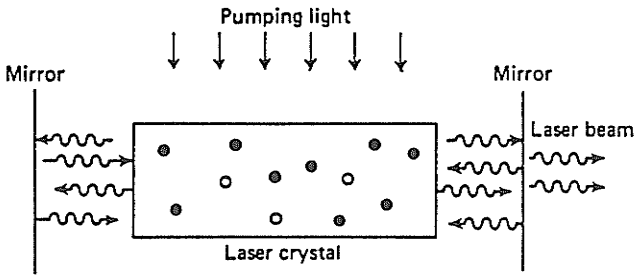

Fig. 2.2. Basic laser system

The laser process will begin shortly after development of a population inversion. An excited atom will emit a photon as it reverts to a ground state. The released photon will then strike

an excited molecule causing it to revert to ground state while it emits its photon. Further excited atoms are struck by the photons and a rapid build up in the number of synchronized photons will occur. Photons travelling parallel to the mirrored ends are reflected back into the material and induce more excited state atoms to emit. An intense beam of synchronized photons will be reflected back and forth many times. One of the mirrors can be made to be only partially reflective thus allowing part of the beam to escape.

Photons traveling at an angle to the reflecting mirrors will exit the system while other atoms will emit spontaneously. The active material, in this case ruby, will be bathed in a glow resulting from these spontaneous and off axis stimulated emissions.

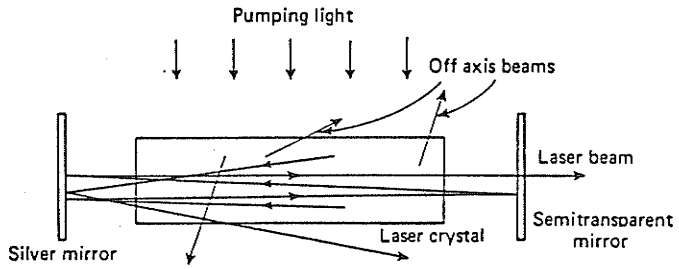

Fig. 2.3. Only photons travelling in a direction parallel or nearly parallel to the horizontal axis of the system will form part of the laser beam. Off axis photons will be amplified by stimulated emission, but they will very quickly leave the laser crystal and the amplification received will be very slight

Laser Properties

The typical properties of laser light make the laser an ideal device for many applications.

1. Laser light can have high intensities. Within laser light pulses, powers far greater than 10^{10} Watts can be achieved which would be equivalent to 10^{8}-100 watt light bulbs or more than all

the American power stations taken together. High continuous wave magnitudes can also be obtained.

2. Laser light possess a high directionality. This directivity stems from the fact that the light wave within the laser hits the mirrors at its endfaces in form of a plane wave, whereby the mirrors act as a hole giving rise to diffraction. A laser with a diameter of a few centimeters can give rise to a laser beam which, when directed to the moon, gives rise to a spot of only a few hundred meters in diameter. As such very high energy densities can be developed and ionization of atoms can easily occur. These two properties are illustrated.

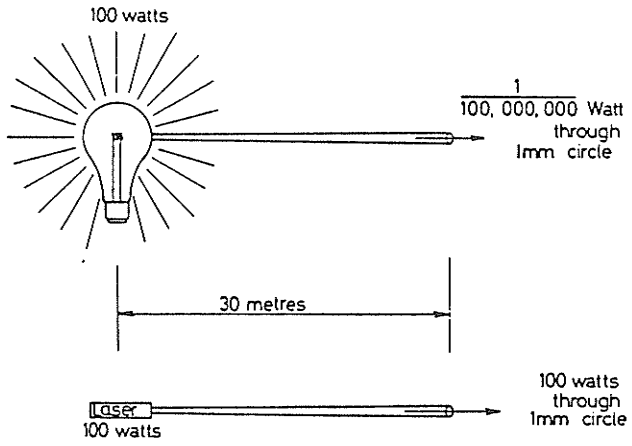

Fig. 8.4 Laser and conventional sources compared.

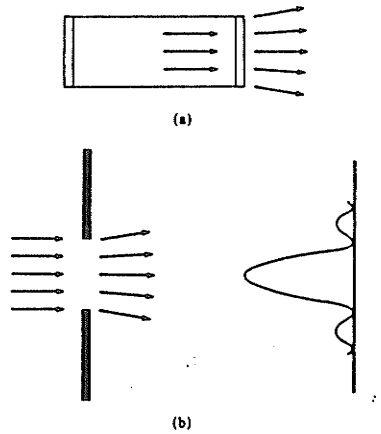

of the laser process a plane parallel wave is produced in the laser (a). The mitted beam corresponds to that of a plane wave diffracted by a slit (b).

3. The spectral purity of laser light can be extremely high. This frequency purity is achieved jointly with a high intensity of the emitted line, in contrasts to spectrographs where high frequency purity is achieved at the expense of intensity.

4. Laser light is coherent. While light of usual lamps consists of individual random wave tracks of a few meters length, laser

light wave tracks may have a length of 300,000 km.

5. Laser light can be produced in the form of ultra short pulses of 10^{-12} duration (picosecond) or even shorter eg. in the order of 10^{-15} seconds (femtoseconds).

Lasers have thresholds below which they will not operate. A plot of emitted laser power versus pumping power shows that below this threshold, emitted power is in the range of thermal light, and increases in intensity only slowly. Above the threshold, the emitted power increases rapidly.

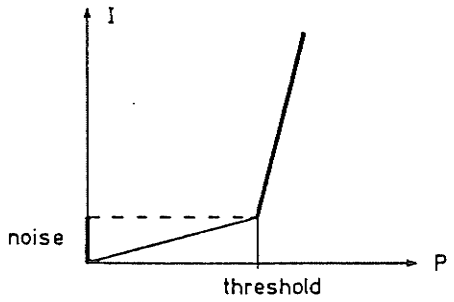

Fig. 2.6. The emitted power *I* versus pump power. Within the region of operation of the laser as a lamp the field consists of noise only and increases only slowly with increasing pump power. Above threshold the emitted intensity increases much more strongly with pump power. The intensity is taken with respect to a specific mode.

Laser Materials

Many materials have been shown to be laser active.

1. Solid State Lasers.

The first laser developed, the Ruby laser is an example of a solid state laser. The Aluminum-oxide lattice has been doped with Chromium ions as activators. Neodymium ions can be doped into yttrium-aluminum-garnet giving rise to the Nd:YAG laser which operates at 1.06 um emission.

2. Gas Lasers.

The He-Ne has laser transitions which can occur at 0.632, 1.15 and 3.39 um. Electrons of sufficiently high energies are liberated which can excite the He atoms by collisions. The excited transitions of the excited He atoms are long lived. They are able to transfer their energy to the Ne atoms during collisions.

The Carbon-dioxide laser is an example where laser action can be caused by molecular oscillations. According to the quantum theory, the different oscillations must be quantized so that discrete energy levels result. Nitrogen in the gas chamber is used to transfer energy to the CO2 molecules. Besides vibrational levels, discrete rotational levels are possible which may also participate in the laser process. Emission occurs in the mid-infrared part of the spectrum between 9.6 and 10.6 um.

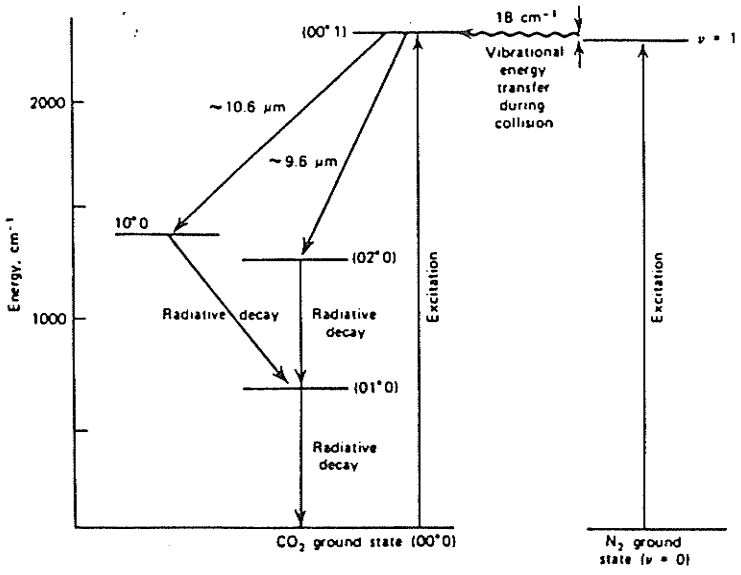

Fig. 2.21. Oscillatory states of CO_2. [C.K.N. Patel, Phys. Rev. Lett. 12, 588 (1964).]

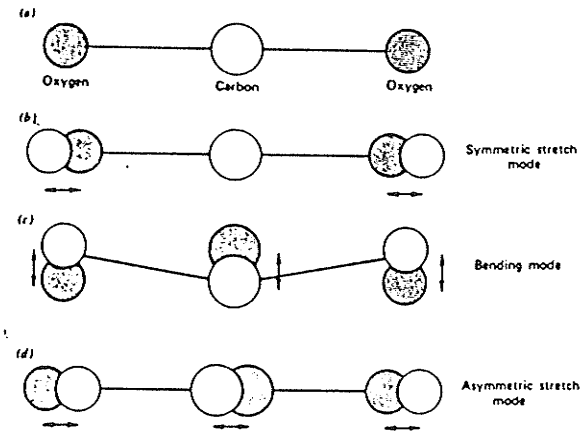

Fig. 2.20. Oscillatory states of the CO_2 molecule.

The excimer lasers represent a special form of gas laser. The wavelength of emission depends on the mixture of rare gases and halogens used, but is usually in the ultraviolet region. Having closed electronic shells in their ground state these molecules normally repel each other. As the interatomic distance of these molecules decreases the potential energy of the system greatly increases. As the closely approximated molecules are excited by a fast electrical discharge they are able to share an electron to form an 'Excimer" molecule. The lifetime of the excimer is only about 10^{-10} sec. after which it will dissociate and discharge a photon of high energy. Laser action of excimers has been found in XE, Kr, Ar, and compound of XeBr, XeF, XeCl, ArF, KrCL etc.

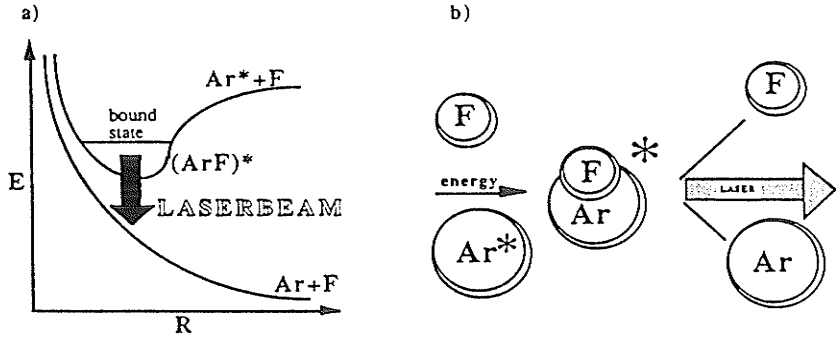

Fig. 4 Model for the excimer laser a.) Potential model of the $(ArF)^*$ excimer laser b.) Idealized picture of the confirmation of the excimer molecule $(ArF)^*$

4. Other Lasers

Lasers have been developed from many other materials. Some of these include; chemical lasers, dye lasers, semiconductor lasers, diode lasers and organic lasers.

Q-switching

The power output of many lasers can be greatly increased by a process known as Q-switching. For lasers which are normally pulsed, a single high power pulse of shorter duration can be produced while continuously operating lasers can be made to give a train of pulses. The distinction between power and energy must be appreciated. When lasers are Q-switched, they always give lower energy outputs compared with when they are not Q-switched because of the absorption and other sources of loss in the Q-switch itself. Nevertheless the instantaneous power output is very much higher because the pulse duration is shorter.

$$\text{power output (watts)} = \frac{\text{pulse energy (joules)}}{\text{pulse duration (seconds)}}$$

Q-switching involves changing the Q of the laser cavity so that feedback by mirrors is suppressed and so depletion of the population of the upper laser energy level is not permitted until its population has reached a high value. The laser is pumped with the resonator kept at very low Q; the Q of the cavity is then made to suddenly increase allowing for gain from stimulated emission to take place, with the result that the laser energy escapes in a very short, highly intense pulse. Some of the many ways of attaining Q-switched operation include, a rotating mirror method, electro-optic switching, photochemical methods and exploding film methods.

REFERENCES

1. Brown R. Lasers. A Survey of Their Performance and Applications. Business Books Ltd., London. 1969.

2. Campbell I, Dwek R. Biological Spectroscopy. Benjamin/Cummings Publishing Co. London. 1984.

3. Haken H. Light. Vol 2 Laser Light Dynamics. North-Holland Physics Pub. Amsterdam. 1985.

4. Heavens O. Lasers. Charles Scribner's Sons. New York 1971.

5. Beesley M. Lasers and Their Applications. Taylor and Francis Ltd. London. 1976.

APPENDIX 2

BASICS OF SPECTROSCOPY

I. Interaction of Electromagnetic Radiation with Matter.

The consequences of the interaction of electromagnetic waves with matter are that the waves are scattered, absorbed or emitted.

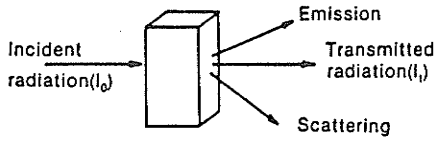

Figure 2.9 Electromagnetic radiation incident on a sample can give rise to absorption, emission, and scattering.

Scattering is usually detected by measuring the intensity of radiation at some angle to the incident wave. Reflection results when light is scattered in the direction opposite of that of the incident light. Refraction is the result of radiation scattered in the same direction as that of the incident wave. The phase of the scattered wave is different from that of the wave that passes straight through the sample. These two waves then recombine to give a wave that has apparently passed through the sample with a different velocity.

Figure 2.13 Illustration of refraction effects. (a) *Physical basis:* The transmitted and forward-scattered waves are 90° out of phase with respect to each other. This leads to an apparent change in the velocity of the superimposed waves. (b) *Macroscopic effect:* The result of the apparent change in velocity caused by the refractive index is that $\theta_1 \neq \theta_2$ in the ray diagram shown.

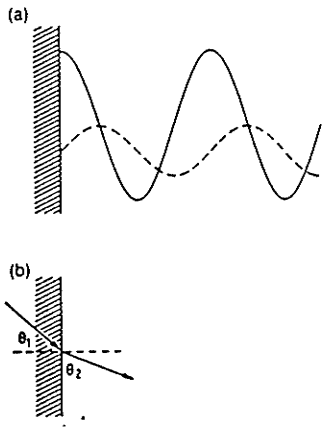

Absorption is usually measured by varying the frequency of the applied radiation and plotting the energy absorbed by a sample at each frequency. The resulting plot is called a spectrum. The frequency dependance of absorption arises because energy is absorbed by transitions induced between different energy states of the molecules in the sample. These transitions can occur only if there is a strong interaction between the incident radiation and the molecule.

There are several simple rules arising from wave mechanical treatments that help to predict whether a certain interaction will result in a transition between energy levels.

1. A fundamental rule to understand whether a transition is probable is given by;

$$\Delta E = h\nu$$

where ΔE is the separation between the energy states of interest and is the frequency of applied radiation. This equation means that absorption is most probable when the energy level separation matches the energy of the incident radiation.

2. The second rule applies to all electronic and vibrational spectra: There must be a displacement of charge induced in going from one energy state to another.

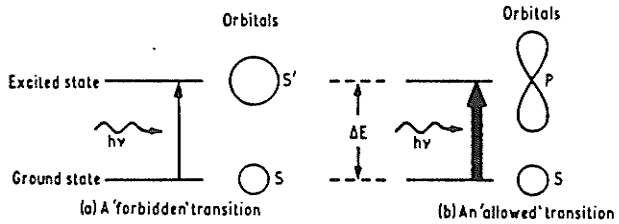

Figure 2.18 Illustration of selection rules. If the radiation applied has a frequency such that $E = h\nu$, then the transition probability between the levels will be a maximum. Another rule that applies says that there must be a charge displacement. In the figure there is no charge displacement in going between two *s*-type orbitals as shown in (a), thus the transition probability will be low—the transition is "forbidden". In (b) there is a charge displacement in going from an *s*-type to a *p*-type orbital; thus, the transition probability will be high—the transition is "allowed".

Absorption depends on the populations of energy levels. When electromagnetic radiation is applied to a sample, it is just as likely to cause transitions from an excited state to a ground state (emission) as it is to cause transitions from a ground state to an excited one. Consequently, the net absorption depends on the difference between populations of the energy concidered to be significant. Absorption spectra will also depend on the concentration of the sample.

II. Ultraviolet Spectroscopy.

Ultraviolet radiation is that part of the electromagnetic spectrum which bridges the gap between the longest-wavelength X-rays and the shortest-wavelength visible light. This ultraviolet region, which extends from 0.4 to 400 nm, is divided into the near (200-400 nm) and far (0.4-200 nm) ultraviolet regions. UV radiation is absorbed by air because of moisture and also because of electronic transitions in atmospheric oxygen, nitrogen and carbon dioxide.

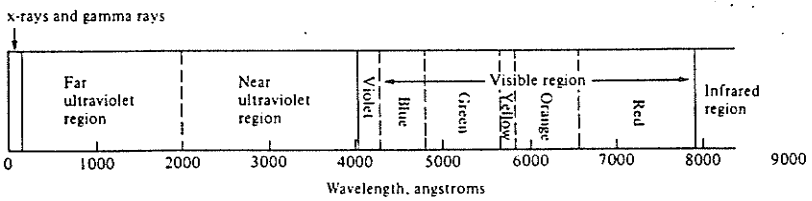

Fig. 2.1 Ultraviolet and visible regions of the electromagnetic spectrum.

Higher energy radiation is necessary to effect electronic transitions than is needed to effect rotational or vibrational transitions. Since all these transitions require fixed (quantized) amounts of energy, it is natural to expect that an

ultraviolet or visible spectrum of a compound would consist of one or more well-defined, sharp peaks, each corresponding to the transfer of an electron from one electronic level to another. The spectra however, are broad and irregular.

The peaks are often broad because each electronic state in a molecule is associated with a very large number of vibrational and rotational states. The differences between electronic energy levels E_1 and E_2 of two electronic states would be well defined, only if the nuclei of the two atoms of a diatomic molecule could be held in fixed positions, ie. only if non-rotational or non-vibrational motions in the molecule occurred simultaneously. However, vibrations and rotations of nuclei do occur constantly. Electronic states in a molecule are therefore always associated with a large number of vibrational and rotational states. The transition of an electron from one energy level to another is accompanied by simultaneous changes in vibrational and rotational states; many waves of closely spaced frequencies are thus absorbed, giving rise to a broad UV peak.

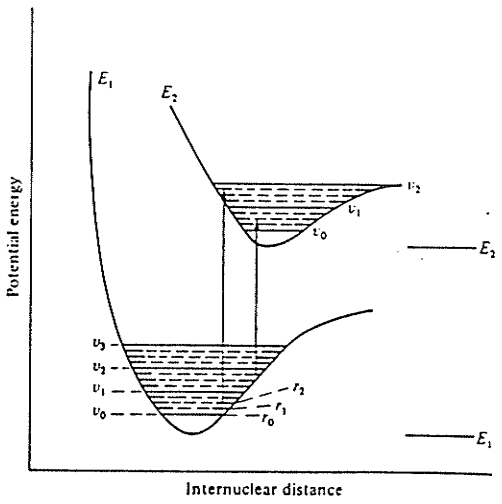

Fig. 2.3 Allowed rotational and vibrational energy levels for two different electronic states, as represented by energy curves for a light, singly bonded, diatomic molecule.

The fraction of incident radiation absorbed is proportional to the number of absorbing molecules in its path. As such, the strength of the absorption peak will be in direct relation to the number of molecules able to absorb that particular frequency of radiation.

In the early years of spectroscopy, it was recognized that some substances appear coloured because they contain functional groups which are capable of absorbing radiation of certain wavelengths when ordinary white light shines on them. For example, a substance in ordinary daylight (400-800 nm) appears blue because it has a functional group (or groups) which absorbs waves of wavelength between 570 and 590 nm (yellow light). The transmitted waves, which are now deficient in yellow light, give the effect of blue colour. Such functional groups, which confer colour on a substance, became known as chromophores. Most chromophores have unsaturated bonds such as C=C, C=O, N=N etc. Functional groups such as hydroxyl (-OH), amino ($-NH_2$), halogenic (-Cl, -Br etc) cannot confer colour on substances, but have the ability to increase the colouring power of a chromophore. Such groups became known as auxochromes.

III. Infrared Spectroscopy.

Infrared radiation extends from the visible region into the microwave region and is capable of affecting both the vibrational and rotational energy levels in molecules. The wavelength of the infrared region extend from approximately 750 nm (0.75 um) to

almost 830 um. In IR spectroscopy, only a small range is employed (between 2.5 um to about 15.4 um). This region is often referred to as the fundamental region. The shorter-wavelength region is called the near-infrared (2.5 um - 0.75 um) and the longer-wavelength region is called the far infrared (from 15.4 um to the microwave region). The units by which infrared rays are measured are somewhat confusing. Physical chemists prefer to give infrared wavelength in angstrom units and analytical chemists use microns and nanometers. Organic chemists however employ wavenumber; the inverse of the wavelength expressed in centimeters. Wavenumbers are proportional to the frequencies and therefore the energies. The higher the wavenumber the more energetic the radiation.

A simple way of relating energetics and structure is provided by the example of the potential-energy curve of a diatomic molecule. The energy of the molecule changes as the distance between its nuclei changes.

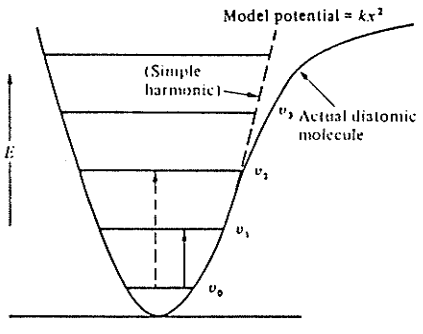

Fig. 3.6 Potential energy curves and vibrational energy levels $v_0, v_1, v_2, \ldots$, for a model and for an actual diatomic molecule. Transition of molecules from one level to the next higher level, for example, $v_0 \rightarrow v_1$ or $v_1 \rightarrow v_2$, is called *fundamental transition*, and that from one level to second- or third-higher levels, for example, $v_0 \rightarrow v_2$ or $v_1 \rightarrow v_3, v_4, \ldots$, is called *overtone transition* (terms derived from musical terminology).

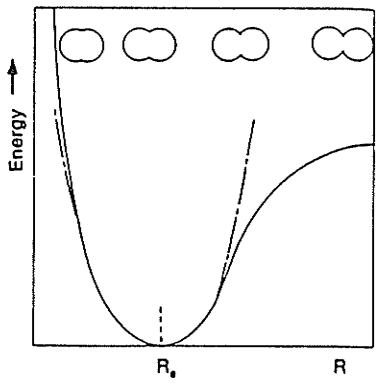

Figure 3.4 A molecular potential energy curve for a diatomic molecule. R_e is the *equilibrium bond length* of the molecule. The parabola represents the potential energy of an ideal molecule that performs simple harmonic oscillation about R_e.

At the minimum of the potential-energy curve the attraction due to various dispersive forces is balanced by the forces from charge repulsion. The stretching or contracting of the bond is then similar to the behaviour of a spring, since there is a restoring force. The vibrations of the bond can in the first instance be analyzed in terms of the molecule's undergoing simple harmonic oscillations about its equilibrium bond length.

Real molecules do not obey the laws of simple harmonic motion exactly. Quantum mechanics tells us that only certain values of the energy ar allowed. These values are represented by the horizontal lines on the Morse curve. Values of energy in between these energy levels are not permitted and the spacing between energy levels becomes smaller at higher energy values. As the energy increases, the atoms move farther from their equilibrium positions and hence enter a nonparbolic region of the Morse curve. Therefore, the vibrations can no longer be treated as simple harmonic but are described as anharmonic.

Figure 3.5 The Morse potential energy curve of a molecule. The horizontal lines represent the allowed vibrational energy levels.

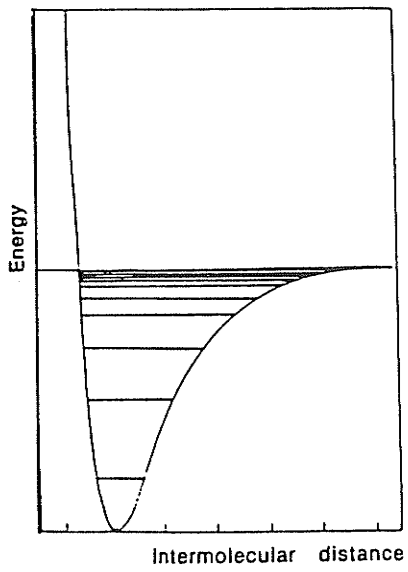

A number of factors affect infrared band frequency. The most important factors are bond elasticity and the relative masses of the bonded atoms. Others include; electrical fields, the nature size and electronegativity of neighboring atoms, hydrogen bonding, phase changes and steric effects.

For any polyatomic molecule, the number of fundamental absorption bands can be calculated from the number of its atoms and their degrees of freedom. The number of degrees of freedom is equal to the sum of the coordinates necessary to locate all the atoms of the molecule in space. Consider a molecule of N atoms. Such a molecule has 3N degrees of freedom because three Cartesian coordinates are required to locate each atom in space. However, of these atomic degrees of freedom, three describe the translation of the molecule as a whole and three describe the rotation of the molecule as a whole if the molecule is non-linear. These six degrees therefore, cannot lead to internal vibrations, and the number of remaining fundamental vibrations is thus 3N-6. In the case of a linear molecule, there are only two axes about which the molecule as a whole can rotate. The number of molecular vibrations in such case is therefore 3N-5.

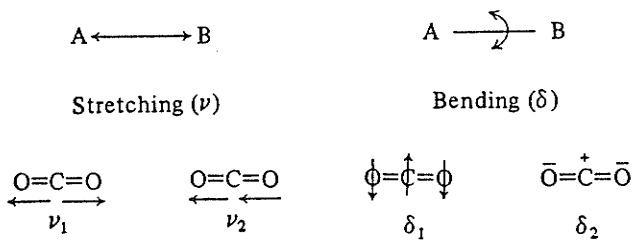

Fig. 3.7 Fundamental vibrations of carbon dioxide. Arrows indicate movement of the atoms along the bond axis, whereas + and – signify vibrations perpendicular to the plane of the paper.

The molecule carbon dioxide, being triatomic and linear gives rise to (3x3)-5=4 fundamental vibrations. Only those vibrations which alter the electric dipole will result in an irfrared absorption peak.

The figure below demonstrates various types of vibrations.

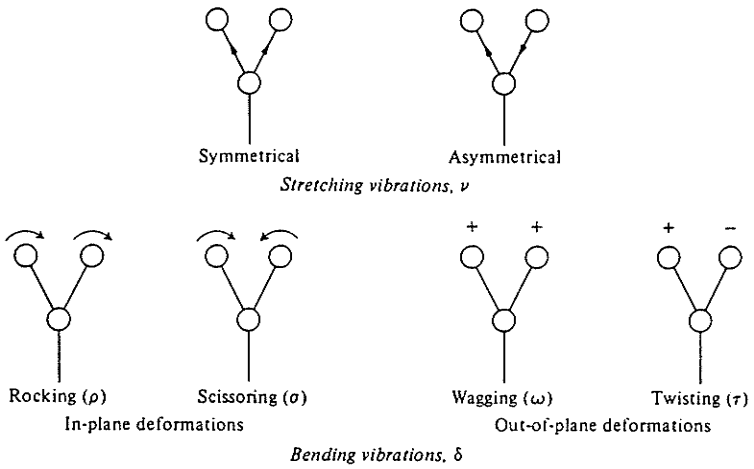

Fig. 3.8 Types of vibrations (+ and – indicate vibrations perpendicular to the plane of the paper).

Some representative characteristic IR group frequencies.

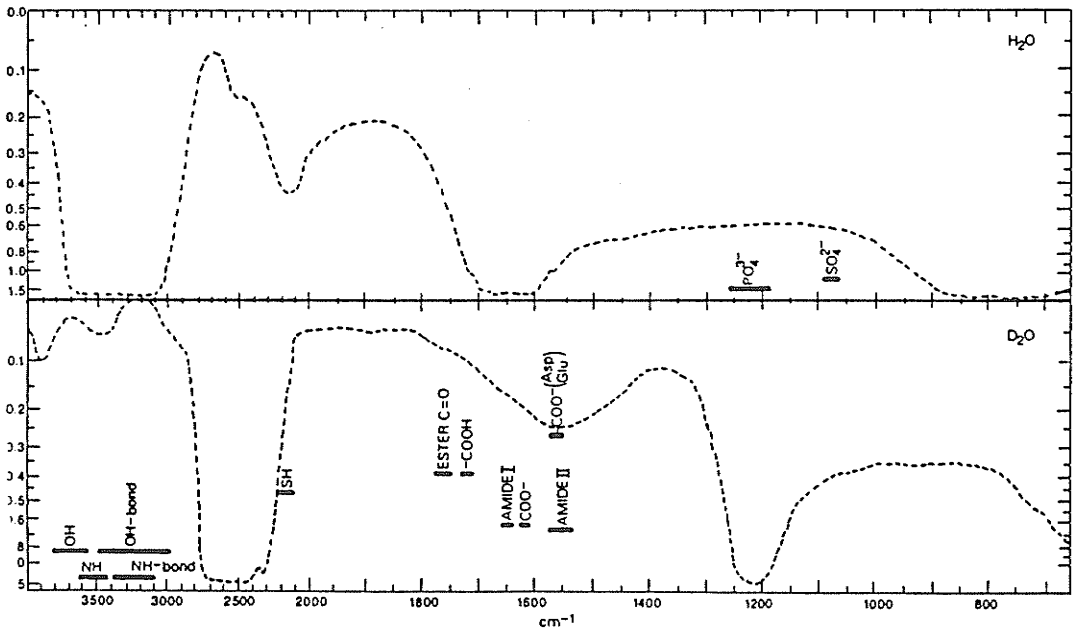

Figure 3.6 Some representative characteristic group frequencies. The infrared curves of H_2O and D_2O shown are those for the typical balance obtainable in a double beam spectrometer.

References

1. Campbell I, Dwek R. Biological Spectroscopy. Benjimen/Cummings Publishing Co. Inc., London 1984.

2. Parikh V. Absorption Spectroscopy of Organic Molecules. Addison-Wesley Publishing Co. Don Mills, Ontario, 1974.

3. Rao C. Ultra-Violet and Visible Spectroscopy. Chemical Applications. Third Ed. Butterworths & Co., 1975.

4. Kemp W. Organic Spectroscopy. John Wiley & Sons, New York, 1975.

APPENDIX 3

PILOT STUDY RESULTS

I. Laser Debonding

This pilot was performed to determine the feasibility of laser debonding; to determine the approximate laser power needed, determine the time required for debonding, evaluate any possibility of enamel damage with light applied loads.

Fifteen Starfire brackets were bonded to primary bovine teeth using the methods described in the Material and Methods section of this thesis. Debonding effectiveness was evaluated by applying a 10 N shear load to the bracket and then measuring the time to failure when the bracket was irradiated with 308 nm wavelength light from a XeCl excimer laser (Lumonics) operating at 21 mJ/pulse, 400 Hz, and 10 ns pulse width. All samples were examined under a binocular microscope at magnifications up to 25X to determine the fracture location and the presence of enamel or bracket damage. The mean time for bracket removal was 3.7 $\pm$ 0.o seconds. Bond failure occurred entirely at the bracket/adhesive interface in all but two samples and no enamel damage was detected.

II. Debonding of Various Adhesives / Wet vs Dry

This pilot was performed in order to assess laser debonding effectiveness with various commercially available adhesives and to explore what influence the storage conditions of the samples (wet or dry) had on debonding effectiveness.

For each adhesive to be tested (Dynabond, Achieve, Challenge, and System 1), ten Starfire (A-company) sapphire brackets were bonded to bovine teeth according to the manufacturer's specifications. Five samples were stored in room temperature water and 5 were stored in air.

Laser parameters for the Lumonics Excimer laser were: 308 nm (XeCl), watts at the bracket, focal spot 4x4 mm, 100 z, 33 Kv for a pulse energy of 60 millijoules.

Debonding times obtained are;

Adhesive	Dry	Wet
Dynabond	4.45 ± 0.44s	5.22 ± 0.62s
Achieve	5.02 ± 1.07s	5.86 ± 0.63s
Challenge	5.67 ± 1.63s	5.52 ± 0.96s
System 1	4.06 ± 0.54s	3.42 ± 0.55s

Wet vs Dry sample storage N.S.D ($p<0.05$)
System 1 was significantly different from all the other adhesives tested. ($p<0.05$). There were no other differences between the adhesives. Note that System 1 was the only one paste adhesive utilized. All samples were stored in water throughout the remainder of the study to more closely mimic the clinical situation even though the results obtained here do not indicate the need to do so. They were also stored in water to ovoid desiccation of the samples used for the thermal portion of the study. Dynabond was chosen as the adhesive to be used in the study because it showed less variation than did Achieve the only other adhesive tested which corresponded to one of the bracket manufacturers.

III Pulpal Temperature Assessment

The purpose of this pilot was to establish a method for determining the temperature rise occurring at the bracket/adhesive interface and in the pulp during laser debonding. Sample preparation was performed as described in the M&M section of the thesis.

The lasers setting used for this pilot were; 308 nm, 8 watts (at the laser not the bracket), 100 Hz 37 Kv. At the bracket a pulse energy of 4.65 millijoules was calculated. Note this is much lower than the energy level used in the other pilot studies.

One bovine tooth and ont human tooth with bonded sapphire brackets were tested. Each tooth was irradiated 5 times to investigate the reproducibility of temperature measurements. An exposure time of 3.7 seconds was used because it represented the average time needed to debond samples in the original pilot.

Values obtained after repeated testing were very consistent. Temperature rise was noted at both the interface and pulpal thermocouples. The rise in the pulp was much lower (less than 3°C) than that obtained at the interface. A 12-18 second time delay occurred form the interface maxima to the pulpal maxima.

APPENDIX 4

RAW DATA

Spectra obtained for various commercial adhesives and Bis-GMA.

UV / VIS SPECTRA : CHALLENGE

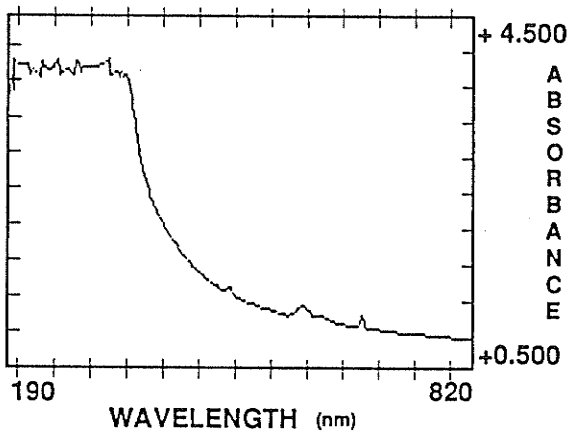

UV / VIS SPECTRA : MONOLOK

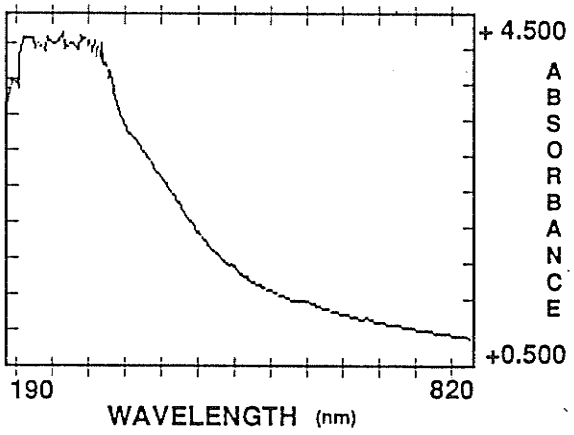

UV / VIS SPECTRA : SYSTEM 1

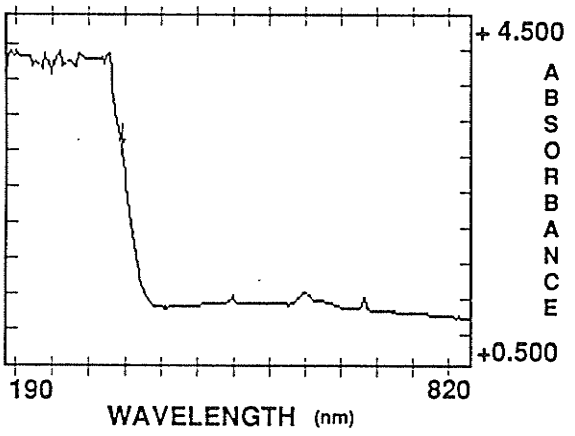

UV / VIS SPECTRA : ACHIEVE

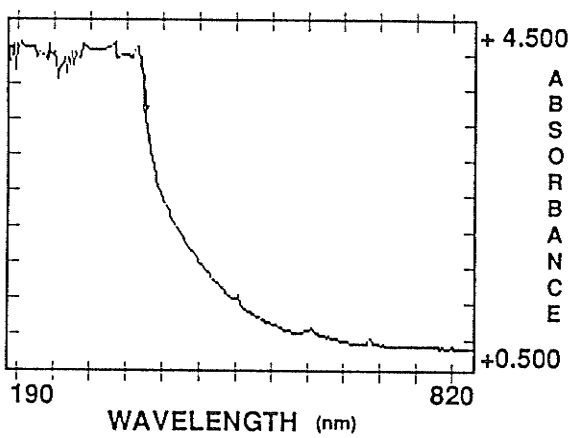

UV / VIS SPECTRA : BIS - GMA

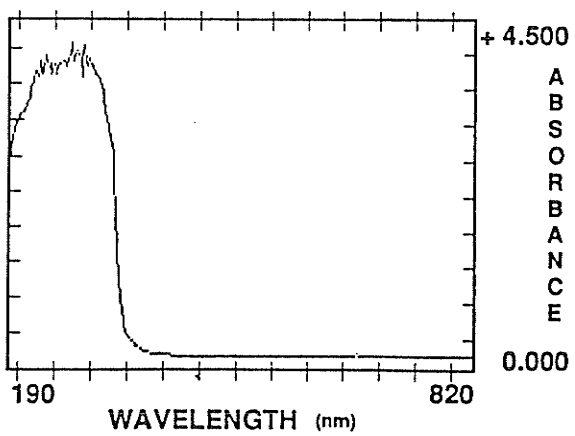

IR spectra obtained for various commercial adhesives.

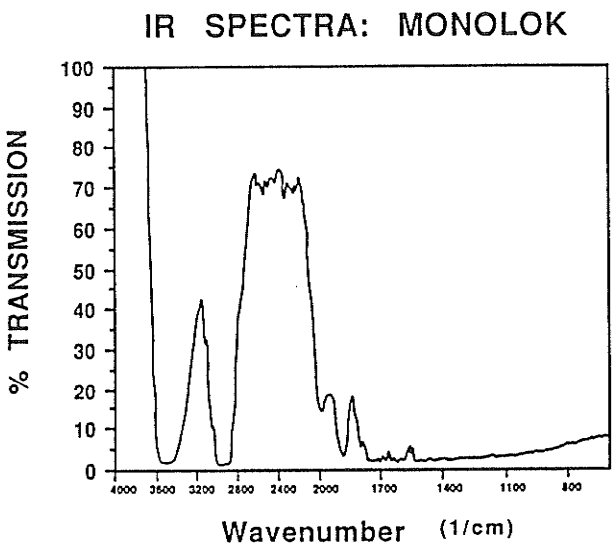

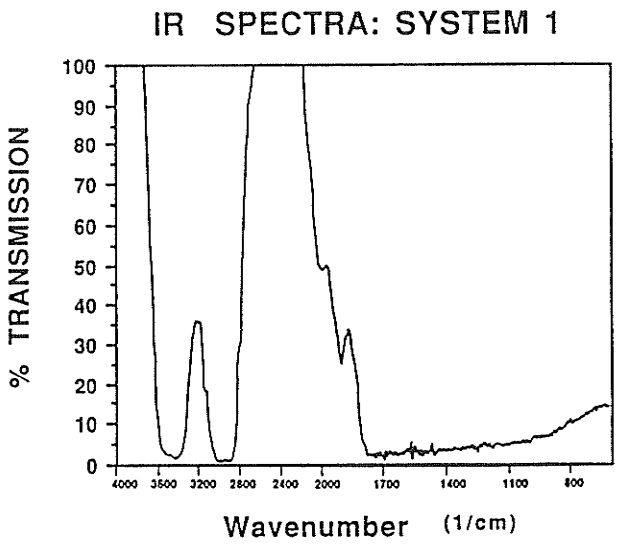

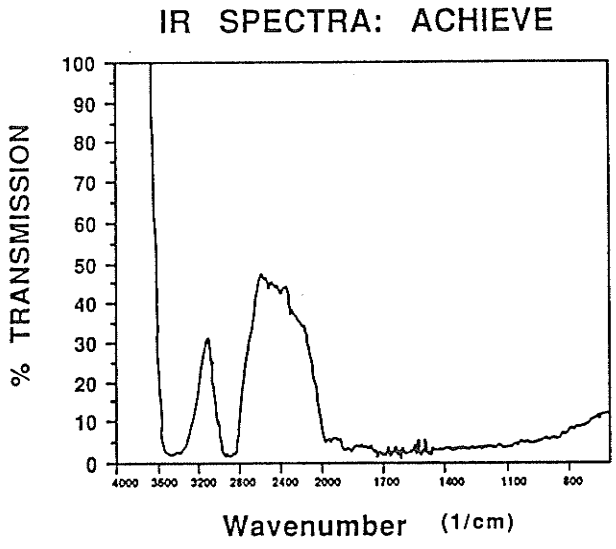

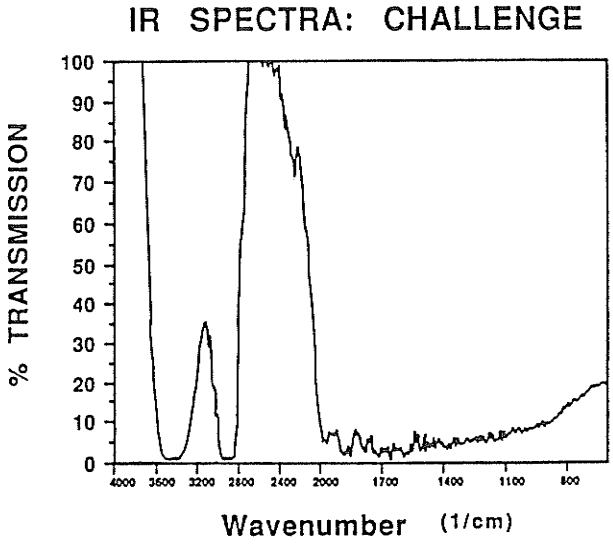

Spectra of the various masks created.

Mask for Sapphire bracket

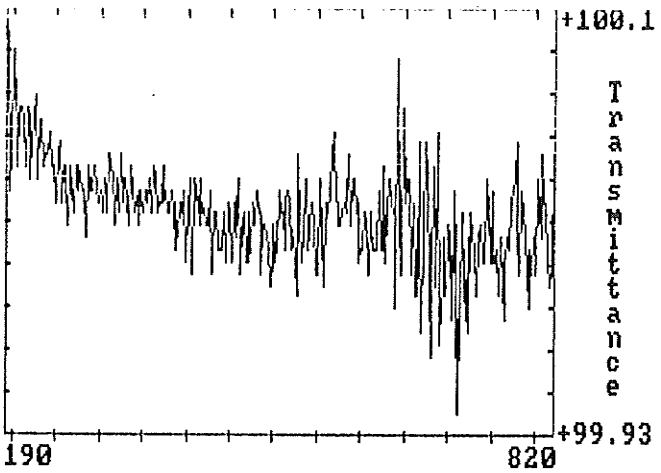

Mask for PC bracket

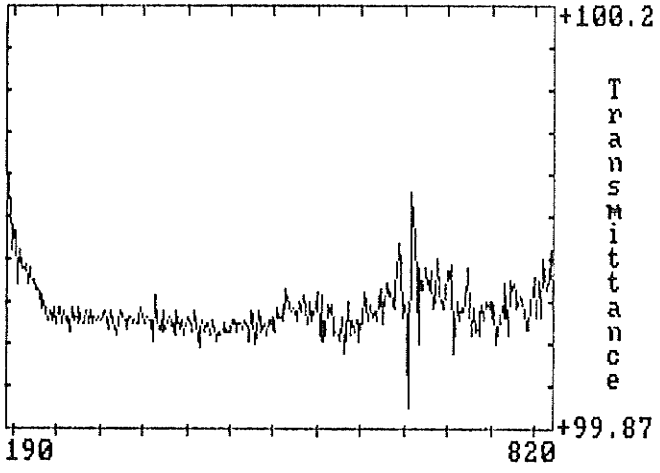

Reaction times measured with electronic stop watch in order to evaluate error in determining laser debonding times and for thermocouple experiment.

1.	0.16s	6.	0.16s	
2.	0.16s	7.	0.16s	
3.	0.12s	8.	0.15s	Mean = 15.2 s
4.	0.13s	9.	0.17s	or 0.31 s per reading
5.	0.18s	10.	0.16s	

Thermal Results with 193 nm Laser.

PC bracket/Bovine tooth

Eq. T	22.2°C
Interface	56.7
Increase at I	34.5
Pulpal	36.4
Increase at P	14.2
Exposure Time	35.0 s

S bracket/Bovine tooth

Eq. T	23.4°C
Interface	70.0
Increase at I	46.6
Pulpal	50.8
Increase at P	28.2
Exposure Time	>1.30 min

248 NM - SITE OF FRACTURE DETERMINATION

Sapphire Samples

1.  All B/A
2. 
3. 
4.  All B/A
5.  All B/A
6.  All B/A
7.  All B/A
8.  All B/A

9. 
10.  All B/A
11. 
12. 
13. 
14. 
15.  All B/A

○ = Enamel exposed
 = Intra-adhesive fracture

Polycrystalline Brackets

1. B\A with carbon
2. B\A carbon & enamel
3. B\A
4. B\A carbon
5. B\A carbon
6. B\A
7. B\A carbon
8. B\A
9. B\A enamel
10. B\A carbon
11. B\A carbon
12. B\A
13. B\A carbon
14. B\A
15. B\A enamel

Some brackets had evidence of carbon deposits (C) while others Diplayed minimal enamel/adhesive fracture.

308 NM - SITE OF FRACTURE DETERMINATION

Sapphire Samples

1. 
2. 
3. 
4. 
5. 
6. 
7. 
8. 
9. 
10. 
11. 
12. 
13. 
14.  All B/A
15. 

○ = Enamel exposure
※ = Intra-adhesive fracture

Polycrystalline Brackets

1. B\A
2. B\A C
3. B\A enamel
4. B\A
5. B\A C
6. B\A
7. B\A
8. B\A
9. B\A C
10. B\A
11. B\A
12. B\A
13. B\A
14. B\A
15. B\A C

B/A denotes Bracket-adhesive fractures.
C denotes those samples with traces of carbon deposits.

1060 NM - SITE OF FRACTURE DETERMINATION

Sapphire Samples

1. 
2. 
3. 
4. 
5. 
6. 
7. 
8. 
9. 
10. 
11.  No debonding
12.  No debonding
13. 
14. 
15. 

○ = Enamel exposure
 = Intra-adhesive fracture

Polycrystalline Brackets

1. B\A
2. B\A enamel
3. B\A enamel
4. B\A enamel
5. B\A
6. B\A
7. B\A
8. B\A
9. B\A
10. B\A
11. B\A
12. B\A
13. B\A
14. B\A
15. B\A

Three samples displayed fracture at the enamel interface. These were also the samples which came off in very short times. No carbon deposits were found with the PC bracket samples.